

Electronic Thesis and Dissertation Repository

12-14-2017 10:30 AM

Regulation of liver mitochondrial metabolism during hibernation by post-translational modification

Katherine E. Mathers, *The University of Western Ontario*

Supervisor: Staples, James F., *The University of Western Ontario*

A thesis submitted in partial fulfillment of the requirements for the Doctor of Philosophy degree in Biology

© Katherine E. Mathers 2017

Follow this and additional works at: <https://ir.lib.uwo.ca/etd>



Part of the [Biochemistry Commons](#), [Biology Commons](#), [Cellular and Molecular Physiology Commons](#), and the [Zoology Commons](#)

Recommended Citation

Mathers, Katherine E., "Regulation of liver mitochondrial metabolism during hibernation by post-translational modification" (2017). *Electronic Thesis and Dissertation Repository*. 5098.
<https://ir.lib.uwo.ca/etd/5098>

This Dissertation/Thesis is brought to you for free and open access by Scholarship@Western. It has been accepted for inclusion in Electronic Thesis and Dissertation Repository by an authorized administrator of Scholarship@Western. For more information, please contact wlsadmin@uwo.ca.

ABSTRACT

Hibernation, characterized by a seasonal reduction in metabolism and body temperature, allows animals to conserve energy when environmental conditions (e.g. temperature, food availability) are unfavourable. During hibernation, small mammals such as the 13-lined ground squirrel (*Ictidomys tridecemlineatus*) cycle between two distinct metabolic states: torpor, where metabolic rate is suppressed by >95% and body temperature falls to ~5 °C, and interbout euthermia (IBE), where metabolic rate and body temperature rapidly increase and are maintained at euthermic levels several hours. Suppression of metabolism during entrance into torpor is paralleled by rapid suppression of liver mitochondrial metabolism. In my thesis, I aimed to characterize the regulatory mechanisms that underlie this rapid and reversible mitochondrial suppression. Using high resolution respirometry and enzymatic assays, I determined that this suppression between IBE and torpor occurs at electron transport system (ETS) complexes I and II. Flux through complexes I and II is suppressed during torpor by 40% and 60%, respectively, despite no differences in protein content between the two hibernation states. I used two-dimensional differential gel electrophoresis and Blue-Native PAGE to determine if differences in post-translational modification of mitochondrial proteins parallels these metabolic changes. I found that the 75 kDa subunit of complex I is significantly more phosphorylated in torpor than IBE, and that the complex II flavoprotein subunit is significantly more phosphorylated in IBE than torpor. To investigate the potential that this differential phosphorylation mediates the observed differences in enzyme activity and mitochondrial metabolism between torpor and IBE, I attempted to manipulate phosphorylation state of complexes I and II as well as stimulate the endogenous protein kinase A (PKA) pathway within intact liver mitochondria. I found that dephosphorylation of complex I reversed suppression of its activity during torpor, and that dephosphorylation of complex II induced suppression of its activity in IBE. I was unable to stimulate the endogenous PKA within intact mitochondria, and suggest that another pathway is responsible for mediating changes in phosphorylation *in vivo*. Together, my results point to novel ETS phosphorylation sites that may contribute to metabolic regulation in general and, in particular, suppression of mitochondrial metabolism during hibernation.

Keywords: Hibernation, metabolism, post-translational modification, phosphorylation, electron transport system, metabolic suppression

CO-AUTHORSHIP STATEMENT

Chapter 2 (Regulation of mitochondrial metabolism during hibernation by reversible suppression of electron transport system enzymes) was published in *Journal of Comparative Physiology B* (2017. 187:227–234) with Sarah McFarlane, Lin Zhao, and Dr. James F. Staples as co-authors. Sarah McFarlane assisted with mitochondrial isolation and enzyme assays, and Lin Zhao contributed to experimental design and assisted with immunoblots. Dr. Staples contributed to experimental design and provided editorial input. I contributed to experimental design, performed the experiments, analysed the data, and wrote most of the manuscript. I include a copy of the reprint permission from *Journal of Comparative Physiology B* in Appendix C.

A version of Chapter 3 (Suppression of liver mitochondria during hibernation is reversed during saponin permeabilization) was published in *Biology Open* (2015. 4:858-864) and has been modified for relevance to the thesis. This manuscript was co-authored with Dr. James F. Staples, who contributed significantly to the experimental design and writing of the manuscript. I contributed to the experimental design, performed the experiments, and wrote most of the manuscript. Articles published in *Biology Open* are available for inclusion in theses/dissertations without specific permission. I include a copy of the copyright guide in Appendix C.

Chapters 4 and 5 are currently in preparation for submission to *Proceedings of the National Academy of Sciences of the United States of America* with Dr. James F. Staples as a co-author. Dr. Staples contributed significantly to the experimental design and has provided extensive editorial input on the manuscript. I contributed to the experimental design, performed the experiments, analyzed the data, and wrote the manuscript.

ACKNOWLEDGEMENTS

I would like to acknowledge the following people for their part in supporting me throughout my PhD:

First and foremost, Dr. James Staples, whose mentorship and support have been invaluable to me. I am incredibly grateful to have had the opportunity to work with and learn from you.

Drs. Norman Hüner and Christopher Guglielmo, for being supportive, creative and encouraging advisory committee members. Thank you for keeping me on track and providing the guidance that helped form my thesis into a cohesive story.

Lin Zhao, for teaching me how to do immunoblots when I knew nothing about protein, and Beth Szyszka, for much needed help with Blue-Native PAGE.

Dr. Robert Cumming, for the use of his isoelectric focuser; Dr. Tim Regnault, for the use of his gel imager; and Dr. Brent Sinclair, for the use of his microbalance.

Sharla Thompson, for animal care support. Thank you for going above and beyond to help keep the squirrels happy and healthy.

Staples lab members past and present – Amanda MacCannell, Sarah McFarlane, and Leah Hayward – thanks for making the lab fun. Thanks for going through most of this with me (especially the 2am sampling days). Thanks to Dr. Jason Brown for getting me started in the lab with surgeries and mitochondrial isolation, and thanks to Dillon Chung for some much-appreciated methodological advice.

My parents, for providing frequent and much needed emotional support.

Finally, Ethan Jackson, for being the most supportive partner I could ask for.

TABLE OF CONTENTS

ABSTRACT.....	ii
ACKNOWLEDGEMENTS.....	iv
TABLE OF CONTENTS.....	v
LIST OF FIGURES.....	x
LIST OF TABLES.....	xii
LIST OF ABBREVIATIONS AND SYMBOLS.....	xiii
LIST OF APPENDICES.....	xv

CHAPTER 1

General Introduction.....	1
1.1 Energy homeostasis and thermal strategies.....	1
1.1.1 Metabolic flexibility in endotherms.....	3
1.2 Hibernation.....	5
1.2.1 Obligate vs. facultative hibernation.....	5
1.2.2 Metabolic patterns during hibernation.....	6
1.2.3 Metabolic suppression during torpor.....	9
1.3 Mitochondrial metabolism.....	10
1.3.1 The electron transport system.....	10
1.3.2 Assessing mitochondrial metabolism.....	12
1.3.3 Mitochondrial metabolism during hibernation.....	15
1.4 Regulation of mitochondrial metabolism.....	17
1.4.1 Allosteric regulation.....	19
1.4.2 Morphological changes.....	19
1.4.3 Membrane structure.....	20
1.4.4 Respiratory supercomplexes.....	21
1.4.5 Post-translational modification.....	21
1.5 Regulation of post-translational modifications in mitochondria.....	24
1.5.1 Regulation of phosphorylation.....	24
1.5.2 Regulation of acetylation.....	25

1.6 Post-translational modification of proteins during hibernation	26
1.7 Inducing metabolic suppression: the search for a “hibernation induction trigger”	28
1.8 Thesis overview	31
1.8.1 Rationale	31
1.8.2 Objectives	31
1.9 References.....	34

CHAPTER 2

Regulation of mitochondrial metabolism during hibernation by reversible suppression of electron transport system enzymes	47
2.1 Introduction.....	47
2.2 Materials and methods	49
2.2.1 Animals	49
2.2.2 Radiotelemetry implants	50
2.2.3 Experimental groups	50
2.2.4 Isolation of mitochondria.....	51
2.2.5 Mitochondrial respiration and ETS complex flux	52
2.2.6 ETS complex activity assays	53
2.2.7 Immunoblots	54
2.2.8 Statistical analysis.....	56
2.3 Results.....	56
2.4 Discussion.....	58
2.5 Conclusions.....	64
2.6 References.....	65

CHAPTER 3

Suppression of liver mitochondria during hibernation is reversed during saponin permeabilization	68
3.1 Introduction.....	68
3.2 Materials and Methods.....	71

3.2.1 Animals	71
3.2.2 Permeabilization of Liver Tissue	72
3.2.3 Phosphatase/Deacetylase inhibitor incubations	73
3.2.4 Isolation of Mitochondria	73
3.2.5 Respirometry	73
3.2.8 Statistical analysis	76
3.3 Results	76
3.4 Discussion	80
3.5 Summary	84

CHAPTER 4

Post-translational modification of liver mitochondrial proteins during hibernation	88
4.1 Introduction	88
4.2 Materials and Methods	90
4.2.1 Animals	90
4.2.2 Mitochondrial isolation	90
4.2.3 Purification and solubilization of mitochondrial proteins	91
4.2.4 Two-dimensional differential gel electrophoresis (2D DiGE)	91
4.2.4.1 Labelling with CyDyes	92
4.2.4.2 Two-dimensional electrophoresis (2DE)	92
4.2.4.3 Image acquisition and analysis	94
4.2.5 Spot excision and digestion	94
4.2.6 Protein identification by MALDI mass spectrometry	95
4.2.7 Phosphoprotein staining of 2D gels	96
4.2.7.1 2D Electrophoresis	96
4.2.7.2 Phosphoprotein stain	96
4.2.7.3 Sypro Ruby staining for total protein	98
4.2.7.4 Image acquisition and analysis	98
4.2.8 Immunoblots for acetylated lysine	98
4.2.8.1 2D Electrophoresis	99

4.2.8.2 Protein transfer and immunodetection	99
4.2.8.3 Image acquisition and analysis	99
4.2.9 2D Blue-native PAGE.....	100
4.2.9.1 Protein solubilization	100
4.2.9.2 Native electrophoresis and SDS-PAGE.....	100
4.2.9.3 Confirming the presence of ETC complexes following 2D BN-PAGE	102
4.2.9.4 Phosphoprotein staining of BN-PAGE gels.....	102
4.2.9.5 Acetylation immunoblots from BN-PAGE gels	102
4.2.10 Q-TOF LC/MS.....	104
4.3 Results.....	105
4.3.1 2D-DiGE analysis of liver mitochondrial proteins in torpor and IBE	105
4.3.2 Phosphorylation and acetylation of liver mitochondrial proteins during torpor and IBE	108
4.3.3 Analysis of ETS proteins by BN-PAGE.....	112
4.4 Discussion.....	117
4.4.1 Differences in liver mitochondrial proteins between torpor and IBE identified following 2D-DiGE.....	117
4.4.2 Differences in ETS proteins in liver mitochondria between torpor and IBE identified following BN-PAGE	120

CHAPTER 5

Manipulating metabolism in liver mitochondria of hibernators	127
5.1 Introduction.....	127
5.2 Materials and Methods.....	130
5.2.1 Animals	130
5.2.2 Mitochondrial isolation.....	130
5.2.3 Mitochondrial respiration.....	130
5.2.4 Treatment of mitochondrial homogenates with exogenous kinases and phosphatases.....	131

5.2.4 Enzyme assays	132
5.2.6 Statistical analysis	132
5.3 Results	133
5.4 Discussion	140
5.5 Summary	144
5.6 References	145
 CHAPTER 6	
General Discussion	148
6.1 A model for mitochondrial metabolic suppression during torpor	148
6.2 The role of liver mitochondrial suppression in whole-animal metabolic suppression	153
6.3 Conclusions	155
6.4 References	156
 APPENDIX A – 13-lined ground squirrel trapping permit	
APPENDIX B – Animal Use Ethics Approval	158
APPENDIX C – Permission to reprint published materials	159
CURRICULUM VITAE	163

LIST OF FIGURES

Figure 1-1. Patterns of hibernation in the thirteen-lined ground squirrel.	7
Figure 1-2. The mammalian electron transport system (ETS).....	11
Figure 1-3. An example measurement of mitochondrial respiration in mitochondria isolated from the liver of a 13-lined ground squirrel.....	14
Figure 1-4. Succinate-fueled state 3 respiration rates in isolated liver mitochondria (measured at 37 °C) at six points of a torpor-IBE cycle.....	18
Figure 2-1. Flux through electron transport system (ETS) complexes in liver mitochondria isolated from torpid and IBE ground squirrels	57
Figure 2-2. Protein content of ETS complexes in liver mitochondria of torpid and IBE ground squirrels.	61
Figure 3-1. Representative traces showing succinate oxidation in isolated liver mitochondria (A) and permeabilized liver tissue (B) from the same animal.....	75
Figure 3-2. Succinate oxidation of permeabilized liver slices is independent of slice wet weight.	77
Figure 3-3. Succinate oxidation by isolated liver mitochondria and permeabilized liver tissue.	78
Figure 3-4. State 3 respiration rates with succinate in permeabilized liver tissue incubated with phosphatase and deacetylase inhibitors.....	81
Figure 4-1. A summary of two-dimensional differential gel electrophoresis (2D DiGE) experimental methods.	93
Figure 4-2. A summary of experimental methods used to determine total phosphorylation and acetylation of liver mitochondrial protein separated by 2D electrophoresis.	97
Figure 4-3. A summary of Blue-Native (BN) PAGE experimental methods.	101
Figure 4-4. Immunoblot of five ETS subunits in liver mitochondrial protein separated by BN-PAGE.	103
Figure 4-5. Ground squirrel liver mitochondrial proteins compared between torpor and IBE by 2D-DiGE.....	106

Figure 4-6. Total phosphorylation of liver mitochondrial protein from IBE and torpid ground squirrels.	109
Figure 4-7. Total lysine acetylation in liver mitochondrial protein from IBE (A) and torpid (B) ground squirrels.	110
Figure 4-8. 2D Blue-Native PAGE of liver mitochondrial protein from a ground squirrel in IBE.	113
Figure 4-9. Total protein phosphorylation in liver mitochondria from IBE (A) and torpid (B) ground squirrels following separation by 2D BN-PAGE.	114
Figure 4-10. Total protein acetylation in liver mitochondria from IBE (A) and torpid (B) ground squirrels following separation by 2D BN-PAGE.	115
Figure 5-1. Succinate-fueled state 3 respiration in liver mitochondria in control conditions and following incubation with H89.	134
Figure 5-2. Relative succinate-fueled respiration in liver mitochondrial following incubation with activators of the PKA pathway.	136
Figure 5-3. Maximal activity of ETS Complex I in isolated liver mitochondria following incubation with protein kinase A (PKA; Panel A) and protein phosphatase (PP; Panel B).	138
Figure 5-4. Maximal activity of ETS Complex II in isolated liver mitochondria following incubation with protein kinase A (PKA; Panel A) and protein phosphatase (PP; Panel B).	139
Figure 6-1. A model of potential mechanisms underlying reversible suppression of mitochondrial metabolism during entrance into torpor.	149
Figure 6-2. A model of potential changes in PTMs of mitochondrial electron transport system (ETS) proteins between IBE and torpor.	151

LIST OF TABLES

Table 2-1. Subunits of ETS complexes targeted by MitoProfile antibody cocktail (AbCam, ab6820).....	55
Table 2-2. Maximal activity of ETS complexes in isolated liver mitochondria.....	59
Table 2-3. Maximal activity of ETS complexes in liver tissue.....	60
Table 3-1. State 3 respiration rates of isolated mitochondria and permeabilized liver tissue.....	79
Table 4-1. Proteins identified by MALDI mass spectrometry from spots of interest in 2D-DiGE analysis comparing IBE and torpor.....	107
Table 4-2. Liver mitochondrial proteins, resolved by 2D electrophoresis, differing in phosphorylation and acetylation between IBE and torpor.....	111
Table 4-3. Electron transport system proteins, resolved by BN-PAGE, differing in phosphorylation and acetylation between IBE and torpor.....	116
Table 5-1. Succinate-fueled respiration in liver mitochondrial following incubation with activators of the PKA pathway.....	135

LIST OF ABBREVIATIONS AND SYMBOLS

8Br-cAMP	8-Bromoadenosine 3',5'-cyclic monophosphate
2D-DiGE	two-dimensional differential gel electrophoresis
2DE	two-dimensional electrophoresis
BN-PAGE	blue-native polyacrylamide gel electrophoresis
BSA	bovine serum albumin
CHAPS	(3-((3-cholamidopropyl) dimethylammonio)-1-propanesulfonate)
CoQ	coenzyme Q
DCPIP	dichlorophenolindophenol
DI	deacetylase inhibitors
DTT	dithiothreitol
EDTA	Ethylenediaminetetraacetic acid
EGTA	Triethyleneglycoldiaminetetraacetic acid
ETS	electron transport system
FADH ₂	flavin adenine dinucleotide, reduced
H89	N-[2-[[3-(4-Bromophenyl)-2-propenyl]amino]ethyl]-5-isoquinolinesulfonamide
HEPES	(4-(2-hydroxyethyl)-1-piperazineethanesulfonic acid)
HIT	hibernation induction trigger
IBE	interbout eutheria
IEF	isoelectric focusing
IPG	immobilized pH gradient
K _{cat}	enzyme active site turnover number
LDS	lithium dodecyl sulfate
LPP	lambda protein phosphatase
MALDI-TOF/TOF	matrix-assisted laser desorption/ionization-time of flight time of flight mass spectrometry
MES	2-(N-morpholino)ethanesulfonic acid
MR	metabolic rate
NAD ⁺	nicotinamide adenine dinucleotide

NADH	nicotinamide adenine dinucleotide, reduced
PAGE	polyacrylamide gel electrophoresis
PDH	pyruvate dehydrogenase
pI	isoelectric point
PI	phosphatase inhibitors
PKA	protein kinase A
PMF	proton motive force
PTM	post-translational modification
PVDF	polyvinylidene fluoride
Q-TOF LC/MS	quadruple time of flight liquid chromatography-mass spectrometry
RCR	respiratory control ratio
ROS	reactive oxygen species
SDS	sodium dodecyl sulfate
T _b	body temperature
T _{set}	thermoregulatory set point
TBST	Tris-buffered saline and Tween-20
TCA	tricarboxylic acid
TMPD	N, N', N'-tetramethyl-p-phenylenediamine
TNZ	thermal neutral zone
V _{max}	maximal enzymatic activity

LIST OF APPENDICES

APPENDIX A – 13-lined ground squirrel trapping permit	157
APPENDIX B – Animal Use Ethics Approval.....	158
APPENDIX C – Permission to reprint published materials	159

CHAPTER 1

1 General Introduction

1.1 Energy homeostasis and thermal strategies

The ability to maintain energy homeostasis is critical to organismal survival and has therefore been under strong selective pressure over evolutionary time. Many environmental factors constrain an animal's ability to transform food energy into cellular energy in the form of adenosine triphosphate (ATP), which can lead to an imbalance between energy supply and demand. For example, animals experiencing hypoxic stress are constrained by a lack of environmental oxygen which limits their ability to produce ATP through cellular respiration. The ability to obtain sufficient food energy from the environment is also a considerable challenge to homeostasis, especially in the winter, when food is typically least available. In addition to limited food availability, the colder temperatures of winter require a higher energy demand for some animals, making winter a significant metabolic challenge.

Ectothermy and endothermy are two major thermoregulatory patterns expressed by animals. In general, ectothermic animals do not rely on metabolically-derived heat to regulate body temperature, and as a result, body temperature is largely determined by environmental temperature. Ectotherms display a variety of behavioural and physiological adaptations to either regulate body temperature or adjust physiological processes to function over a range of temperatures. For example, the forest tent caterpillar (*Malacosoma disstria*) achieves a favourable body temperature for reproduction by basking in large groups (McClure et al., 2011). By relying largely on the external environment, ectothermy requires little metabolic energy to regulate body temperature. On the other hand, ectotherms are vulnerable to fluctuations in environmental

temperature, which alter the rate of temperature-dependent biological processes and have consequences for animal performance.

Endothermic animals, including birds and mammals, retain some metabolically generated heat to maintain a relatively constant core body temperature. A possible advantage of endothermy over ectothermy is the ability to maintain a favourable internal environment for biochemical functions despite fluctuations in external temperature, allowing endotherms to inhabit a wider range of environments. Despite its advantages, endothermy is energetically costly, requiring much more metabolic energy than ectothermy. For example, in a comparison of similarly sized ectotherms and endotherms (agamid lizards and mice, respectively) with the same preferred body temperature (37 °C), endotherms displayed an 8-fold higher metabolic rate (Else and Hulbert, 1981).

Most metabolic heat produced by animals originates from the mitochondrial electron transport system (ETS; reviewed in Section 1.3.1). During mitochondrial respiration, a large amount of free energy is released by the oxidation-reduction reactions that comprise the ETS. Some of that free energy is used to synthesize ATP, but as much as 60% may be released as heat (Staples, 2016). Endotherms use behavioural, morphological and physiological mechanisms to retain some of this endogenous heat to regulate body temperature. Endotherms can maintain a constant body temperature with only their basal metabolic rate over a fairly narrow range of environmental temperatures, designated the thermal neutral zone (TNZ). At temperatures below the lower limits of the TNZ, animals require a higher rate of metabolism to provide the heat necessary to maintain body temperature. This increase in heat production is accomplished in two main ways. In shivering thermogenesis, skeletal muscles contract in an uncoordinated fashion, consuming ATP. As ATP is broken down into adenosine diphosphate (ADP), flux through the ETS is stimulated, thereby producing more metabolic heat. In addition to shivering thermogenesis, some eutherian mammals can produce heat using non-shivering thermogenesis by brown adipose tissue. In brown adipose tissue mitochondria, ETS flux is uncoupled from ATP production, resulting in futile cycling of protons which produces a large quantity of heat.

Winter can be a significant energetic challenge for endotherms. Low environmental temperatures require high rates of metabolism to defend a constant body temperature, but in many habitats, food availability is lower than other seasons. This can be especially problematic for small animals, which have a higher surface area to volume ratio than larger animals, and thus lose internal heat to the environment at a faster rate. There are several strategies endotherms use to face this challenge. First, animals can remain active throughout the winter, increasing metabolic heat production with an increased metabolic rate. These animals minimize heat loss to the environment through mechanisms such as increased insulation, and many store food energy to ensure enough fuel for high winter metabolic rates. While larger endotherms can store much of this fuel in the form of body fat, a large amount of fat storage is not an option for small endotherms, who must store food energy other ways. For example, the American red squirrel (*Tamiascurius hudsonicus*) must forage from spring through autumn to amass a sufficient store of seeds to remain euthermic throughout the winter (Larivée et al., 2010). Animals can also avoid the thermal challenge of winter by leaving the area for more favourable conditions (e.g., migration). While useful for some animals, this strategy is limited to animals that can travel quickly and efficiently over large distances, such as birds, fish, and some large mammals. Finally, a strategy used by some endotherms is to reduce energy demand, which decreases the amount of energy that must be obtained from the environment.

1.1.1 Metabolic flexibility in endotherms

Reducing energy demand by decreasing metabolic rate can be an adaptive response to a variety of environmental stresses, including temperature (both cold and hot), limited food availability, and limited water. Hibernation, torpor, and estivation are examples of metabolic flexibility that occurs in such conditions, and these strategies are employed by a diverse assortment of animals. These strategies are also referred to as temporal heterothermy since decreases in metabolic rate are often accompanied by decreases in body temperature, which is a departure from typical endothermy. Heterothermy can result in significant energy savings; for example, Richardson's ground squirrels that undergo hibernation use 88% less energy over the winter compared to conspecifics that remain euthermic over the same time period (Wang, 1979). Hibernation and torpor occur in at

least ten mammalian orders (Geiser, 2004) and twelve avian families (McKechnie and Lovegrove, 2002). The presence of this metabolic flexibility in such diverse and unrelated groups is intriguing, and two opposing hypotheses may explain its evolution: 1) the common ancestor of mammals displayed metabolic flexibility (hibernation and torpor) and many lineages have lost the traits over evolutionary time, and 2) that the traits are the result of convergent evolution, having evolved repeatedly in separate lineages. In mammals, the hypothesis that hibernation and torpor evolved polyphyletically is supported by the lack of a clear common ancestor with a heterothermic phenotype. It has thus been suggested that the hibernation and torpor phenotypes evolved in mammal lineages independently as a response to environments that challenge energy homeostasis (Lovegrove, 2012). On the other hand, it has more recently been argued that since the several gene mutations required for hibernation are unlikely to occur at the same time, it is more likely that heterothermy is an ancestral trait in mammals (Malan, 2014).

Daily torpor involves a reduction in metabolic rate and body temperature that typically lasts less than 24 hours and occurs during an animal's inactive period (Geiser, 2004; Ruf and Geiser, 2015). Many endothermic species enter daily torpor in response to low ambient temperatures and short photoperiod, though torpor is often used in response to low food availability. In some animals such as the house mouse (*Mus musculus*), torpor can be induced with food restriction even when held at high (~20 °C) ambient temperature and a constant photoperiod (Brown and Staples, 2010). Social dynamics can also influence torpor use; for example, solitary striped skunks (*Mephitis mephitis*) frequently undergo daily torpor during the winter, but skunks that spend winter in communal dens rarely use torpor (Hwang et al., 2007).

Metabolic suppression can also occur in endotherms that inhabit hot and dry environments; for example, the Madagascan fat-tailed dwarf lemur (*Cheirogaleus medius*) reduces metabolism and temperature for up to seven months of a given year despite ambient temperatures of over 30 °C (Dausmann et al., 2004). The reduction of metabolism and body temperature under hot and dry conditions has been referred to as

estivation, but physiological patterns are essentially indistinguishable from hibernation during the winter.

1.2 Hibernation

It is challenging to find rigid criteria to define hibernation since the type of metabolic changes that occur can depend on many factors, such as species, body size, and ambient temperature. One current attempt to define hibernation refers to the seasonal regulated suppression of metabolic rate to less than 10% of euthermic values followed by a reduction in body temperature (Staples, 2016). By this definition, some animals that undergo seasonal heterothermy are excluded from being classified as hibernators. For example, arctic ground squirrels (*Spermophilus parryii*) that hibernate in environments where ambient temperatures frequently fall below -10 °C maintain a body temperature near -2 °C. They maintain this temperature gradient by activating thermogenesis while hibernating, resulting in metabolic rates near 50% of euthermic values (Buck and Barnes, 2000). It may therefore be useful for a definition of hibernation to exclude specific thresholds of metabolism and body temperature, and instead be defined by the pattern of metabolic changes that occur.

1.2.1 Obligate vs. facultative hibernation

Hibernation is classified as facultative or obligate. Facultative hibernation occurs only when environmental conditions (e.g. temperature, food availability) are particularly unfavourable. For example, in the black-tailed prairie dog (*Cynomys ludovicianus*), colonies in similar geographical areas display different patterns of heterothermy, with animals from some colonies remaining euthermic for the entire winter and animals from other colonies hibernating (Lehmer et al., 2006). This difference in hibernation pattern is likely influenced by local environmental conditions, as the groups of animals that underwent hibernation inhabited areas that experienced lower ambient temperatures and less rainfall during the summer compared to other areas.

Obligate hibernation, mediated by an endogenous rhythm, occurs each year regardless of environmental conditions. This remarkable circannual rhythm is exemplified by the golden mantled ground squirrel (*Callospermophilus lateralis*), in which captive populations housed at a constant temperature and photoperiod enter hibernation at approximately the same time as their wild counterparts (Pengelley et al., 1976). As the winter approaches, obligate hibernators undergo many physiological changes to prepare for a season of inactivity. In most non-food caching hibernators, body mass increases due to increased food intake to supply fat to fuel metabolism over the winter. Small animals in particular experience large increases in body fat, for example, the arctic ground squirrel increases body fat by 7-8-fold prior to hibernation, and fat comprises up to 62% of total body mass (Sheriff et al., 2013). In small hibernators such as the golden-mantled ground squirrel, the increased food intake prior to hibernation is accompanied by increases in the activities of enzymes involved in fatty acid and triglyceride synthesis in white adipose tissue (Wang et al., 1997). Many small hibernators also increase deposits of brown adipose tissue, a tissue that facilitates much of the heat production that occurs during arousal from torpor. Non-hibernating mammal species require acclimation to cold and/or short photoperiod to accumulate deposits of brown adipose tissue, but in small hibernators such as the 13-lined ground squirrel (*Ictidomys tridecemlineatus*), brown adipose tissue deposits increase prior to hibernation even when animals are held at warm ambient temperatures (22 °C) (MacCannell et al., 2017). This pattern suggests that BAT deposition in hibernators is mediated by an endogenous rhythm.

1.2.2 Metabolic patterns during hibernation

Hibernation does not simply consist of one prolonged period of reduced metabolic rate and body temperature. Throughout the hibernation season, animals undergo multiple bouts of torpor that are interrupted by brief periods where body temperature spontaneously returns to ~37 °C. In the 13-lined ground squirrel, torpor bouts last 12-14 days, and brief euthermic periods – termed interbout euthermia (IBE) – last approximately 8 hours (Figure 1-1 A). The cycle between torpor and IBE can be divided into four stages: 1) entrance, during which metabolic rate is rapidly reduced, followed by a drop in body temperature, 2) torpor, in which metabolic rate and body temperature

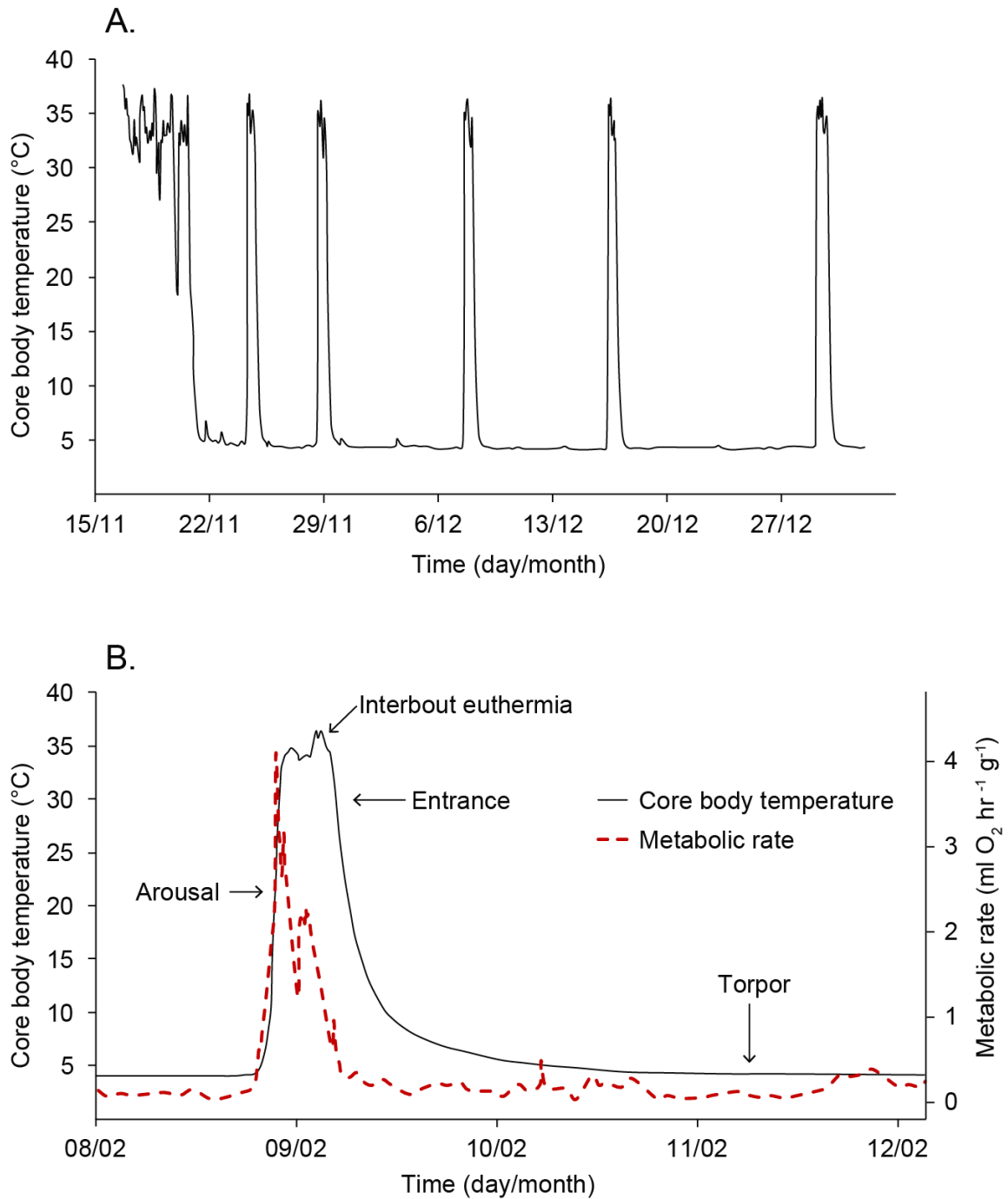


Figure 1-1. Patterns of hibernation in the thirteen-lined ground squirrel. Core body temperature of a ground squirrel undergoing torpor-arousal cycles at the beginning of a hibernation season (A), and the metabolic rate and body temperature of a ground squirrel throughout one torpor-arousal cycle (B). Modified with permission from Staples and Brown, 2008.

remain consistently low for several days, 3) arousal, where metabolic rate spontaneously and rapidly increases, followed by an increase in body temperature, and 4) IBE, where metabolic rate and body temperature remain consistently high for several hours (Figure 1-1 B). With only one known exception (the common tenrec, see below), all hibernating mammals display this pattern of metabolic suppression and arousal during hibernation.

Arousal and IBE are very energetically expensive; in species such as the arctic ground squirrel, these periods can contribute up to 86% of the total energy expended over the hibernation season (Karpovich et al., 2009). Since nearly all hibernators undergo periodic arousals despite significant energy costs, IBE likely offers a significant adaptive advantage. One potential benefit for interbout arousals is the opportunity for neuronal repair during slow wave sleep. During torpor, slow wave sleep does not occur, but during IBE, arctic ground squirrels spend much of the time in slow wave sleep (Daan et al., 1991). The significance of neurological damage during hibernation was first described by (Popov et al., 1992), who found that in Siberian ground squirrels (*Citellus undulatus*), neuronal dendrites were shorter and less branched during torpor but their structure was completely restored two hours after arousal. Subsequently, several studies have shown that neuronal synapses regress during torpor and that IBE allows reversal of this damage (reviewed in Arendt and Bullmann, 2013). Periodic arousals are also likely important for immune response. Levels of circulating lymphocytes are low during torpor but completely rebound during IBE, indicating that immune response is diminished during torpor (Bouma et al., 2011). Indeed, golden mantled ground squirrels injected with bacterial lipopolysaccharide showed no immune response during torpor, but exhibited a fever upon arousal (Prendergast et al., 2002). Periodic arousals may thus be important for a hibernator's immune system to cope with any bacterial infections that have accumulated during torpor.

Free-ranging common tenrecs (*Tenrec ecaudatus*) hibernate for up to nine months with no evidence of interbout euthermia, although their body temperatures do not decrease below 22 °C (Lovegrove et al., 2014). It is therefore possible that there is a critical

threshold body temperature in hibernators, above which periods of IBE do not provide an adaptive advantage.

1.2.3 Metabolic suppression during torpor

As a mammal enters torpor, whole-animal metabolism is reduced by up to 95% (Staples, 2016). This reduction in metabolic rate results from the three factors. First, during entrance into torpor, the thermoregulatory set point (T_{set}), around which core body temperature is regulated, progressively decreases (Heller et al., 1977). This decrease in T_{set} shifts the lower range of the TNZ to lower temperatures, reducing thermogenic metabolism, so that whole-animal metabolism falls towards basal levels. As a result of decreased thermogenic metabolism, body temperature will fall towards ambient temperature. Second, a decrease in body temperature results in a reduced metabolic rate through passive thermal effects. A decrease in temperature of 10 °C will reduce the rate of most biological reactions by two- to three-fold (the so-called Q_{10} effect), so decreased body temperature alone can account for part of the metabolic suppression that occurs during torpor. The precise contribution of these thermal effects on metabolic suppression are difficult to measure, however. Anaesthetized, non-hibernating ground squirrels, cooled exogenously, had metabolic rates approximately 15- fold higher than torpid animals at the same body temperature (Wang et al., 1990), suggesting that passive thermal effects alone can account for only a small fraction of total metabolic suppression.

In addition to decreased thermogenic metabolism and passive thermal effects, a third contribution to the metabolic suppression that occurs during entrance into torpor is active suppression of metabolism in non-thermogenic tissues. In most hibernators, metabolic rate (measured as oxygen consumption) decreases substantially before body temperature begins to fall (Staples 2016; Figure 1-1B). Along with oxygen consumption rates, heart rate also decreases prior to body temperature (MacCannell et al., submitted to J. Exp. Biol.). In non-thermogenic tissues such as liver, mitochondrial metabolism is significantly suppressed prior to decreases in body temperature, which indicates the contribution of active, regulated metabolic suppression to total metabolic suppression during torpor (Staples and Brown, 2008). The mechanisms underlying this rapid, active

metabolic suppression are currently not well understood, and have been the subject of much research.

1.3 Mitochondrial metabolism

Mitochondria, bacteria-sized organelles bound by a double membrane, exist within most eukaryotic cells. Mitochondria are believed to have originated by endosymbiosis between two prokaryotic cells approximately 2 billion years ago (reviewed by Gray et al., 1999). Most mitochondrial proteins are encoded by nuclear DNA and imported into the mitochondria, but mitochondria also contain ribosomes and DNA which, in animals, is arranged in a circular pattern, like that found in most bacteria. In mammals, this distinct mitochondrial genome encodes 13 proteins, all of which are involved in oxidative phosphorylation. Mitochondria synthesize the vast majority of ATP in cells, but are also involved in other diverse functions such as reactive oxygen species (ROS) production, cell signaling, and regulation of apoptosis.

1.3.1 The electron transport system

In eukaryotes, the majority of food energy is transformed into cellular energy within mitochondria by the process of oxidative phosphorylation, by which electron transport is linked with ATP synthesis. The mitochondrial oxidative phosphorylation system contains the electron transport system (ETS), which is composed of four multi-subunit enzymes and mobile electron carriers embedded within the inner mitochondrial membrane: NADH-dehydrogenase (complex I), succinate dehydrogenase (complex II), cytochrome bc_1 complex (complex III), cytochrome c (Cyt c), and cytochrome c oxidase (complex IV).

Electrons enter the ETS at complexes I and II with the oxidation of NADH, succinate, and $FADH_2$ (Figure 1-2). These reducing equivalents originate from different metabolic pathways including glycolysis, fatty acid oxidation, but most importantly, the tricarboxylic acid (TCA) cycle. NADH enters the ETS through complex I, whereas

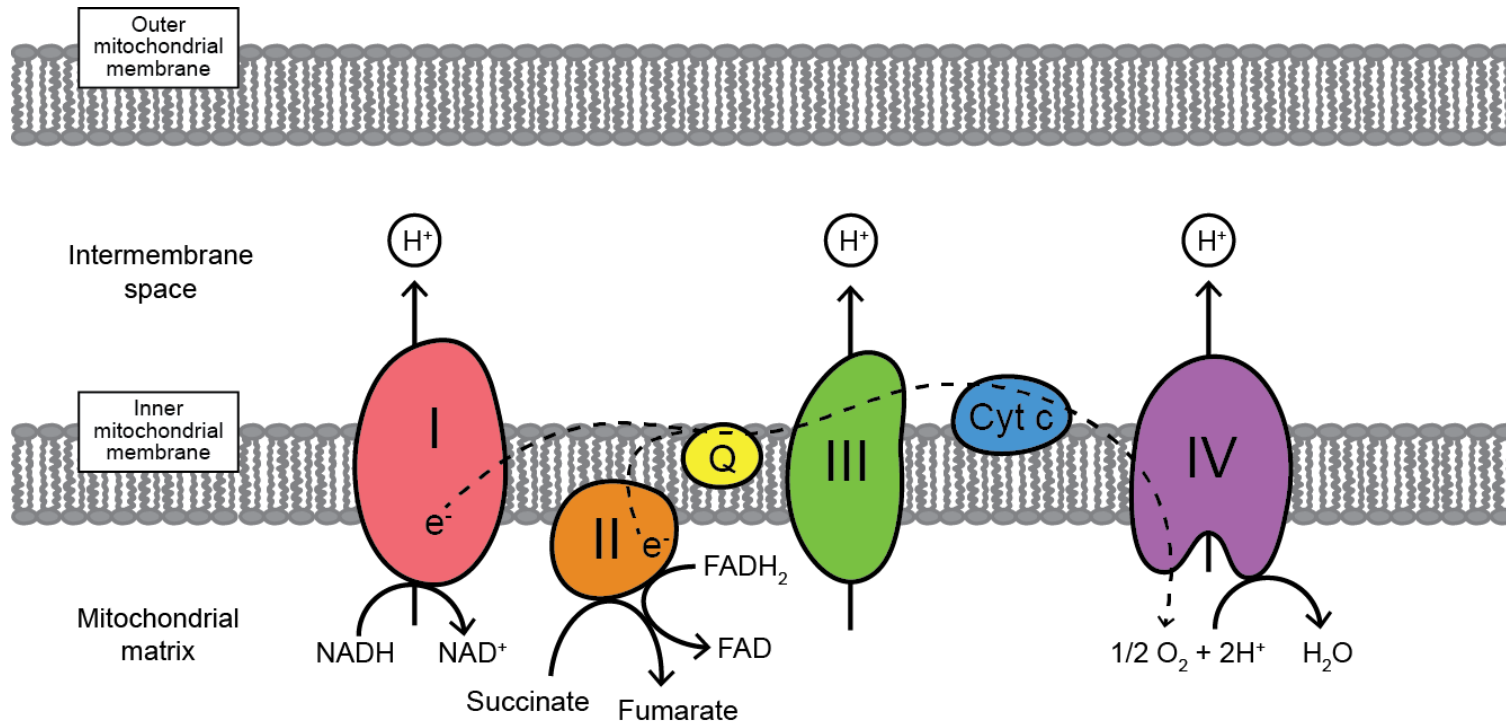


Figure 1-2. The mammalian electron transport system (ETS). Electrons enter the ETS at complexes I and II following the oxidation of succinate and reducing equivalents NADH and FADH₂. These electrons are passed to through the ETS to increasingly electronegative acceptors (indicated by dashed line), ultimately being donated to oxygen at complex IV. Some of the free energy released by the oxidation-reduction reactions at complexes I, III and IV is used to pump protons from the mitochondrial matrix to the intermembrane space, generating a proton motive force (PMF).

succinate and FADH₂ enter the ETS through complex II or other dehydrogenases such as electron-transferring flavoprotein, ubiquinone oxidoreductase, and glycerol-3-phosphate dehydrogenase. Electrons are then transferred to coenzyme Q (CoQ), and subsequently to complex III, cytochrome c, and complex IV, which utilizes oxygen as a final electron acceptor, producing H₂O. Redox reactions at ETS complexes I, III and IV result in a release of free energy that is sufficient for these complexes to transport protons across the inner mitochondrial membrane, resulting in an electrochemical gradient, the proton motive force (PMF). Ultimately, this gradient is utilized by ATP synthase (complex V), which couples the backflow of protons with phosphorylation of ADP, thereby producing ATP.

1.3.2 Assessing mitochondrial metabolism

The ability to accurately assess mitochondrial function is crucial for an understanding of energy metabolism in virtually all systems. In addition to differences in mitochondrial content, mitochondrial function and morphology varies among species, individuals, and tissue types. For example, mitochondria in mammalian skeletal muscle are interconnected into a reticulum, which minimizes metabolite diffusion differences for more efficient ATP synthesis (Glancy et al., 2015). Several different methods are used to measure the function of mitochondria, each with benefits and limitations. Historically, the maximal activities of some mitochondrial enzymes (e.g. citrate synthase, succinate dehydrogenase, and cytochrome c oxidase) have been used as a proxy for mitochondrial oxidative capacity (Lanza and Nair, 2009). While this approach has the benefit of requiring only small samples of tissue, it is unlikely that the activity of one enzyme can reflect the overall function of a complex metabolic pathway, or its regulation. Maximal capacity for ATP production is sometimes used to assess mitochondrial function at different levels of organization, as ATP is one end product of mitochondrial respiration. It is possible to use a luciferase assay to measure rates of change of ATP concentrations in tissues, cells, and isolated mitochondria. A significant limitation of this method is that ATP is generated and consumed in many pathways, so changes in ATP concentration are not simply the result of oxidative phosphorylation. Further, specialized equipment is necessary for

measuring ATP production in isolated mitochondria, which limits the tractability of this technique.

Oxygen consumption can also be used to assess mitochondrial metabolism. As conversion of O_2 to H_2O by complex IV is the final oxidation-reduction reaction of the ETS, oxygen consumption has been used to assess the function of isolated mitochondria. This process was first described Chance and Williams (1956). Although ways of describing this type of assessment vary (for example, the substrate-uncoupler-inhibitor titration protocol described by Pesta and Gnaiger (2012)), I will follow the convention described by Brand (1998). This analysis involves measuring oxygen consumption by mitochondria in three experimental conditions: 1) substrate oxidation (state 2 respiration), in which mitochondria are supplied with saturating levels of O_2 and an oxidative substrate (e.g. pyruvate or succinate), but no ADP, 2) ADP phosphorylation (state 3 respiration), in which O_2 , substrate and ADP are supplied at saturating levels, and 3) proton leak (i.e. state 4 respiration), which occurs when all ADP has been converted to ATP, but O_2 and substrate are still saturating. State 4 respiration is typically estimated by inhibiting complex V with oligomycin, preventing ATP synthesis. An example trace of oxygen consumption by isolated mitochondria in such conditions is shown in Figure 1-3. State 3 respiration rates provide particularly useful information as they represent the maximal capacity to generate ATP with a given fuel. The ratio of state 3:state 4, termed the respiratory control ratio (RCR) represents the degree of coupling between oxidation and phosphorylation and is a useful metric to describe the quality of isolated mitochondrial preparations.

Mitochondrial function is typically assessed using mitochondria that have been isolated from a tissue. The process of mitochondrial isolation aims to separate mitochondria from other cellular components while maintaining mitochondrial functionality. Typically, this is achieved by gentle homogenization of the tissue followed by centrifugation. There are several limitations to using isolated mitochondria to infer *in vivo* function. First, mitochondria exist in a 3-dimensional network within intact cells which is disrupted by the isolation process, resulting in changes in mitochondrial morphology and structure

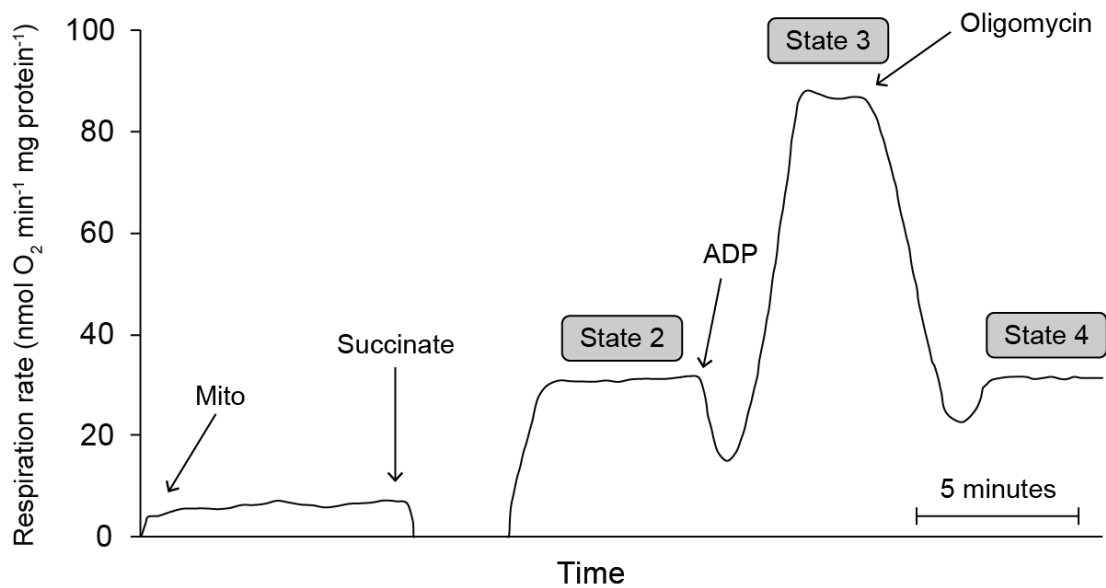


Figure 1-3. An example measurement of mitochondrial respiration in mitochondria isolated from the liver of a 13-lined ground squirrel. Following the addition of an oxidative substrate (succinate), the respiration rate increases to a stable state 2 rate. ADP is then added, increasing the rate of oxygen consumption as a state 3 rate is reached. Finally, oligomycin is added, which inhibits ATP synthase, leading to a lower, stable state 4 rate.

(Picard et al., 2011). Second, isolated mitochondria lack interactions with other cellular components (e.g. sarcoplasmic reticulum, cytoskeleton, lipid droplets) which may lead to changes in function (Saks et al., 2010). Third, some tissues contain distinct subpopulations of mitochondria, some of which are preferentially retained during isolation, potentially biasing results (Krieger et al., 1980). Finally, and perhaps most significantly, the isolation process may affect respiratory characteristics. For example, flux through complex IV is significantly higher in isolated mitochondria compared to cells and muscle fibers, suggesting that isolation of mitochondria leads to a loss of regulatory control (Picard et al., 2011). It is important to note that the consequences of these limitations likely differ depending on tissue type. For example, retaining a network structure would be more important for the function of muscle mitochondria, but less important for tissues such as liver where mitochondria are present as discrete organelles.

Recently, permeabilized tissue has been a popular alternative to isolated mitochondria for the assessment of mitochondrial function (Kuznetsov et al., 2008). This technique uses saponin, a plant-derived amphipathic glycoside, to bind cholesterol embedded within cell membranes, creating small pores but leaving the rest of the cell largely intact (Kuznetsov et al., 2008). These pores allow small molecules (e.g. pyruvate, succinate, ADP) to diffuse from the incubation media to the mitochondria. Since mitochondrial membranes have little cholesterol, mitochondria remain largely intact, and respiration can be assessed in a similar way as in isolated mitochondria. It has been argued that this method provides a better approximation of mitochondrial function *in vivo* than isolated mitochondria, but few comparisons between the two methods exist.

1.3.3 Mitochondrial metabolism during hibernation

Because of their role in energy metabolism and heat production, mitochondria in hibernators have been studied for decades. A consistent physiological characteristic of torpor is the suppression of mitochondrial metabolism in several tissues, which parallels suppression of whole-animal metabolic rate (reviewed in Staples and Brown 2008). Suppression of mitochondrial metabolism has gained much interest for its potential involvement in overall metabolic suppression. Of particular interest are the changes in

mitochondrial metabolism that occur between torpor and IBE, given the degree of metabolic change between these two states and that the transition between them occurs extremely rapidly. In liver mitochondria isolated from torpid ground squirrels, state 3 respiration is suppressed by 70% compared to IBE (Muleme et al., 2006). Other tissues show some suppression of mitochondrial metabolism but to a lesser degree; state 3 respiration is suppressed by 60% in brown adipose tissue (McFarlane et al., 2017), and 30% in skeletal (Brown et al., 2012) and cardiac muscle (Brown and Staples, 2014). The brain cortex shows no suppression of mitochondrial metabolism (Gallagher and Staples, 2013), though this result is derived from saponin-permeabilized tissue rather than isolated mitochondria.

The degree of suppression of mitochondrial metabolism in torpor depends on the conditions under which it is measured, including oxidative substrate and measurement temperature. In liver mitochondria, suppression during torpor is greatest with succinate (Muleme et al., 2006). Suppression during torpor is also evident with pyruvate and fatty acids as fuel, but to a much smaller degree. This pattern suggests that most of the mitochondrial suppression occurs at or downstream to complex II. Temperature is another important variable when considering changes in mitochondrial metabolism between torpor and IBE. Animals sampled in torpor and IBE have body temperatures of 5 and 37 °C, respectively, but it would be of little use to compare mitochondrial respiration from the two conditions at their respective temperatures since it would be impossible to distinguish active suppression from temperature effects. A more useful approach is to compare respiration between hibernation states at the same temperature. In liver mitochondria isolated from 13-lined ground squirrels, the greatest difference (approximately 70%) in state 3 rates between torpor and IBE occurs when respiration is measured *in vitro* at 37 °C. When measured at 25 °C, this difference is diminished but still significant; at 10 °C, there is no difference between torpor and IBE (Brown et al., 2012). These data suggest that suppression of mitochondrial metabolism would have a greater impact on whole-animal metabolism at higher body temperatures, e.g. the beginning of entrance into torpor.

In an attempt to determine the dynamics of mitochondrial metabolism over a torpor-arousal cycle, a study compared liver mitochondrial respiration between animals sampled at various points of this cycle, as determined by body temperature (Chung et al., 2011; Figure 1-4). As animals arouse from torpor, succinate-fueled state 3 respiration rates, measured at 37 °C, increase but only slowly, with maximal respiration rates not occurring until animals are fully aroused with a body temperature of approximately 37 °C. In contrast, respiration is rapidly suppressed early during entrance into torpor, with maximal suppression occurring by the time body temperature has decreased to only 30 °C. The mechanisms that underlie these changes in mitochondrial metabolism are unknown, but the pattern of reversible suppression over a torpor-arousal cycle offers some insight. These metabolic changes occur extremely quickly (maximal suppression between IBE and entrance into torpor occurring within hours), which likely rules out transcriptional and translational changes. In addition, initiation of protein synthesis does not occur below 18 °C during entrance into torpor, and during torpor, peptide elongation occurs slowly (van Breukelen and Martin, 2001). It is unlikely, therefore, that the synthesis of new proteins occurs during torpor or early in arousal. The mechanisms that mediate the changes in mitochondrial metabolism between torpor and IBE therefore likely cause acute changes in the function of pre-existing proteins.

1.4 Regulation of mitochondrial metabolism

The evolution of mitochondria from bacterial symbionts to the main source of ATP synthesis in most eukaryotic cells has required the coevolution of mechanisms for communication at the cellular, tissue, and organ levels to adjust ATP production to physiological demand. Chance and Williams (1955) first described the basic mechanism of respiratory control in isolated mitochondria, which states that oxidative phosphorylation is typically regulated by ADP and phosphate, substrates necessary for ATP synthesis. Rates of oxidative phosphorylation will therefore decrease as ADP is converted to ATP, and increase as ATP is utilized and ADP concentration increases. In addition to basic substrate limitation, there are several other means of acute regulatory control of mitochondrial metabolism.

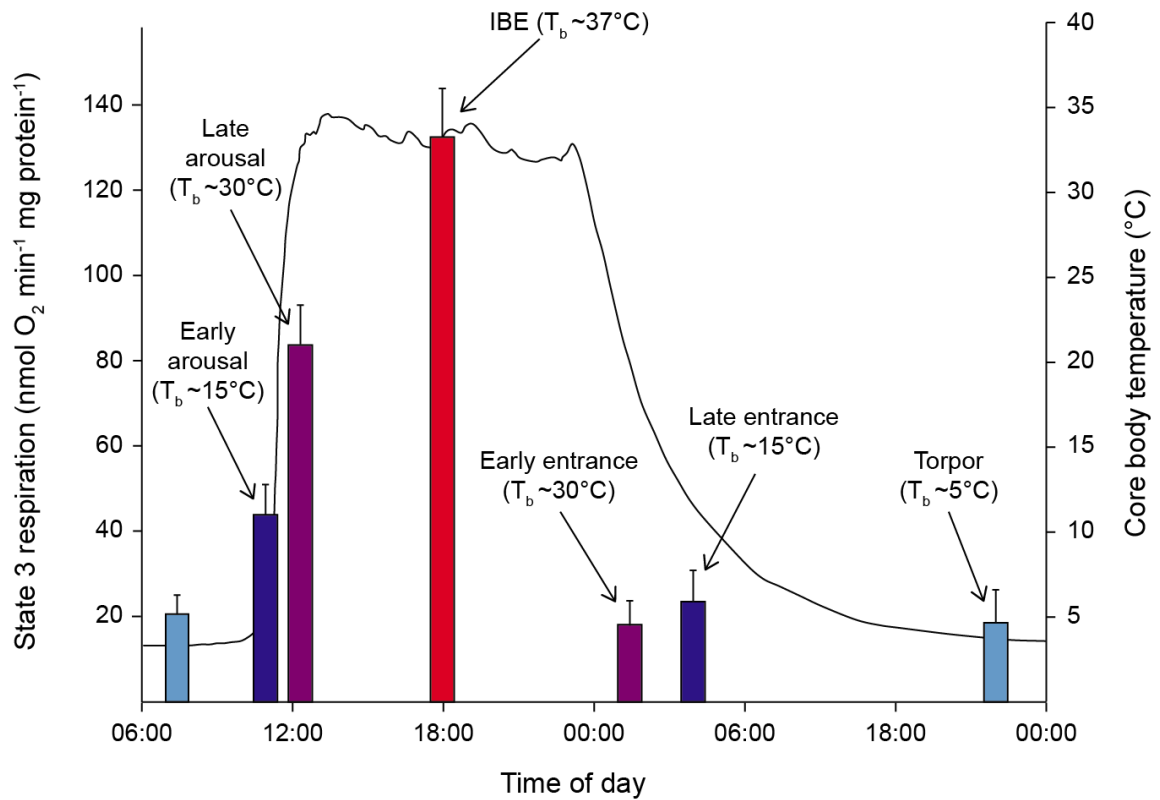


Figure 1-4. Succinate-fueled state 3 respiration rates in isolated liver mitochondria (measured at 37 °C) at six points of a torpor-IBE cycle. Bars represent average state 3 respiration rates from animals that were sampled during torpor (Body temperature (T_b)=~5 °C), early arousal (T_b=~15 °C), late arousal (T_b=~30 °C), early entrance (T_b=~30 °C), and late entrance (T_b=~15 °C), superimposed over a line showing the T_b of one ground squirrel over a typical torpor-IBE cycle. During torpor, mitochondrial respiration is low. During arousal, respiration increases gradually, reaching maximal values in IBE. In contrast, respiration is rapidly suppressed during early entrance into torpor, with maximal suppression occurring while T_b is fairly high. Modified with permission from Staples, 2016.

1.4.1 Allosteric regulation

Allosteric regulation allows fine-tuning of oxidative phosphorylation in response to products, substrates, and other signalling molecules within the intermembrane space. The best described allosteric regulators of mitochondrial metabolism are adenine nucleotides, which adjust the activity of complex IV (cytochrome c oxidase) to energy status.

Complex IV contains binding sites for both ADP and ATP, and a high ATP/ADP ratio within the mitochondrial matrix has a strong inhibitory effect on both the activity of complex IV and overall mitochondrial respiration (Arnold and Kadenbach, 1997).

Several mechanisms allow cells to adjust the inhibitory effects of ATP on mitochondrial metabolism. First, ATP inhibition depends on the phosphorylation state of complex IV (Bender and Kadenbach, 2000). A phosphorylation site on subunit 5b has been identified as necessary for this allosteric regulation (Helling et al., 2012), which provides an additional level of respiratory control. In addition, assembly of complex IV with subunit 4-2 rather than 4-1 leads to an insensitivity to ATP inhibition. Subunit 4-2 is upregulated during hypoxic stress in rodents, allowing optimization of respiratory efficiency at low oxygen concentrations (Fukuda et al., 2007).

1.4.2 Morphological changes

Mitochondria undergo several types of morphological changes which can impact the function of oxidative phosphorylation. The main morphological changes that occur are fusion (the joining of two mitochondria into one), fission (the division of one mitochondrion into two), transport (movement within a cell), and mitophagy (targeted destruction of mitochondria). Mitochondrial morphology within a given tissue is controlled by the balance of fusion and fission, which is regulated by GTPases. Increased mitochondrial fusion is associated with increased ATP production in mouse embryonic fibroblasts (Tondera et al., 2009) and rat kidney cells (Mitra et al., 2009), and disruption of fusion leads to respiratory dysfunction (Chen et al., 2005). Fusion optimizes mitochondrial function by allowing the spread of metabolites, enzymes, and gene products throughout newly connected mitochondria. Within a tissue, changes in mitochondrial morphology have been associated with energetic stress. For example, exposure to hypoxia followed by reoxygenation results in smaller mitochondria

undergoing less fusion (Liu and Hajnóczky, 2011). In the yeast *Candida glabrata*, mitochondrial fusion is associated with an increased tolerance to oxidative stress, as well as increased ATP production and lower ROS production. In hibernating long-tailed ground squirrels (*Urocitellus undulatus*), liver mitochondria from torpid animals are smaller and more resistant to swelling than mitochondria from IBE animals (Brustovetsky et al., 1993). Brown adipose tissue mitochondria in golden mantled ground squirrels also undergo morphological changes between torpor and IBE, such as increased size and surface area of cristae during IBE (Grodums, 1977), which may facilitate the rapid increases in oxidative capacity and heat production.

1.4.3 Membrane structure

Mitochondrial membrane phospholipids are critical for mitochondrial structure, protein transport, and activity of ETS proteins, and the composition of the mitochondrial membrane can have significant effects on respiratory capacity. Thermal acclimation in ectotherms often results in membrane remodeling to preserve respiratory function; for example, mitochondrial membranes in cold-acclimated fish contain higher levels of unsaturated fatty acids within phospholipids (Wodtke, 1978) and a decreased ratio of phosphatidylcholine/phosphatidylethanolamine (Hazel, 1972). In trout, this membrane remodeling is associated with a higher specific activity of complex IV (Wodtke, 1981). Changes in the phosphatidylcholine and phosphatidylethanolamine content of mitochondrial membrane phospholipids also occur as hibernating animals arouse to IBE (Armstrong et al., 2011), but the contribution to changes in metabolism is unclear. The interaction between phospholipids and proteins is especially important in the inner mitochondrial membrane, where the activity of many of the ETS complexes depends on the phospholipid composition.

Cardiolipin, a unique phospholipid that is almost exclusive to the inner mitochondrial membrane, is another important membrane component. Association with cardiolipin is necessary for the maximal activity of ETS complexes I, III, IV, and V (Paradies et al., 2014), and decreased levels of cardiolipin can have profound effects on mitochondrial metabolism. For example, in the absence of cardiolipin, complex IV functions at only 40-

50% of its maximal activity (Fry and Green, 1980). Cardiolipin is also necessary for the formation and stabilization of ETS supercomplexes (Mileykovskaya and Dowhan, 2014). Changes in cardiolipin content may contribute to regulated suppression of mitochondrial metabolism – for example in lungfish (*Protopterus dolloi*) liver mitochondria, cardiolipin content decreased ~2.3-fold during estivation which corresponded with a reduction in mitochondrial respiration (Frick et al., 2010).

1.4.4 Respiratory supercomplexes

There is now abundant evidence that ETS complexes associate together and with other proteins within the inner mitochondrial membrane, forming protein groups termed ‘supercomplexes’. Supercomplexes, found in many eukaryotic organisms, can facilitate electron transport by arranging complexes into formations similar to assembly lines, with significant effects on mitochondrial function. For example, the activity of complex I depends on the presence of complexes III and IV (Acín-Pérez et al., 2004; Li et al., 2007). Further, complexes I, III and IV are found to form different groupings of supercomplexes in many different organisms (reviewed by Dudkina et al., 2008). There is no evidence that complex II associates with other enzymes of the ETS, perhaps due to its involvement in the TCA cycle. Complex V has been found bound with phosphate and nucleotide carriers, which may improve delivery of its substrates, ATP and phosphate (Ko et al., 2003). A recent ‘plasticity model’ proposes that the mitochondrial respiratory complexes exist in combinations of individual enzymes and groups of supercomplexes in a dynamic process that can adapt to changing conditions (Porras and Bai, 2015). It has been proposed that supercomplex formation can allow cells to acutely adjust to energetic demands; for example, mammalian cells grown with limited nutrients showed increased supercomplex formation, likely to maximize respiratory capacity (Acín-Pérez and Enriquez, 2014).

1.4.5 Post-translational modification

A role for post-translational modifications (PTMs) in regulating mitochondrial metabolism has become apparent in the last decade. Over 1,000 different proteins are

found within the mammalian mitochondria. Most mitochondrial proteins are encoded by the nuclear genome and translated in the cytoplasm, where they can be modified prior to transport into the mitochondria. Several proteins encoded by mitochondrial DNA and synthesized by mitochondrial ribosomes exhibit PTMs however, suggesting that PTM events can also occur within the mitochondria. As well, several enzymes that mediate PTMs (e.g. kinases, phosphatases) are localized to mitochondria.

Oxidative phosphorylation can be regulated by phosphorylation of several ETS protein subunits. Subunit NDUFS4 of complex I was the first identified ETS protein subunit targeted by cAMP-dependent phosphorylation (Papa et al., 1996). A subsequent study found that phosphorylation of this subunit results in a 2-3-fold increase in its activity (Scacco et al., 2000). In contrast, phosphorylation of subunit NDUFB10 decreases complex I activity. Complex II is a target for phosphorylation (Salvi et al., 2005; Augereau et al., 2005; Ogura et al., 2012), but although several phosphorylation sites have been identified, the net effects of phosphorylation are complex and not fully understood. For example, phosphorylation of the flavoprotein subunit of complex II has been shown to result in both a decrease in enzyme activity (Tomitsuka et al., 2009) and an increase in activity (Nath et al., 2015), with changes in activity depending on regulatory kinases (and likely phosphorylation sites). Complex IV also contains several phosphorylation sites, some with opposing effects on enzyme activity. For example, phosphorylation of subunits I, II and IV-2 of complex IV are associated with increases in enzyme activity and mitochondrial respiration (Miyazaki et al., 2003; Acín-Pérez et al., 2009, 2011), and phosphorylation of subunit I has been found to inhibit complex IV (Lee et al., 2005). It is clear that phosphorylation of ETS proteins regulates mitochondrial metabolism in a complex way. Many of the apparently antagonistic effects of phosphorylation on enzyme activity likely result from phosphorylation of different sites. As I will discuss in more depth in the next section (1.5.1), phosphorylation is mediated by various enzymes, each of which respond to various regulatory cues.

Lysine acetylation/deacetylation is another key modification that allows many mitochondrial proteins to adjust to metabolic cues. Up to 20% of all mitochondrial

proteins can be acetylated (Kim et al., 2006), with most acetylation events corresponding with inhibition of protein function (Baeza et al., 2016). The acetylation status of mitochondrial proteins is largely modified through the action of deacetylases, which remove acetyl groups from lysine residues. Sirtuin 3 (Sirt3), an NAD-dependent deacetylase, is found within the mitochondrial matrix and is responsible for deacetylation of several key mitochondrial proteins including complexes I, II, III and V. Increased acetylation corresponds with decreased activity of complex I (Ahn et al., 2008), complex II (Cimen et al., 2010; Finley et al., 2011), and complex V (Bao et al., 2010; Wu et al., 2013). This decrease in activity may explain the decreased ATP levels observed in the heart, liver, and kidneys of Sirt3 knockout mice (Ahn et al., 2008). Complex IV contains 14 acetylation sites, most associated with stabilization of enzyme structure (Liko et al., 2016). In mouse liver mitochondria, complex IV subunit Vc showed acetylation after fasting but not before (Kim et al., 2006).

Redox reactions are central to mitochondrial metabolism, and several redox-related PTMs can affect metabolism, including S-oxidation, S-nitrosylation, and S-glutathionation. For example, nitrosylation of complex V, which occurs as nitric oxide reacts with cysteine residues, inhibits protein activity (Chang et al., 2014). Succinylation involves the addition of succinyl group to a lysine residue on a protein and is also involved in regulation of oxidative phosphorylation. Desuccinylation of complex II subunits SDHA and SDHB by Sirtuin 5 (Sirt5) decreased enzymatic complex II activity (Park et al., 2013).

While much is known about modifications to mitochondrial proteins, less is known about their effects since it can be challenging to obtain functional data for many of these modifications. Further, it is difficult to determine which biochemical feature of a protein is affected by a PTM; in addition to changes in activity, PTMs can also influence protein-protein interactions, stability, and localization.

1.5 Regulation of post-translational modifications in mitochondria

1.5.1 Regulation of phosphorylation

Phosphorylation, a common protein modification, can result in fast responses to various stimuli by influencing enzyme activity, subcellular localization, and stability.

Phosphorylation can affect mitochondrial metabolism in a complex way through direct modification of ETS proteins (Section 1.4.5), and regulation of phosphorylation can add another level of complexity.

Most studies of phosphorylation in mitochondrial proteins have focused on pathways involving 3',5'-cyclic adenosine monophosphate (cAMP). Some of the first studies on PTMs in mitochondria found that cAMP-dependent protein kinase (PKA) induces phosphorylation on serine/threonine (S/T) residues of several mitochondrial proteins (Sardanelli et al. 1995, 1996; Technikova-Dobrovo et al. 1994). cAMP, a secondary messenger involved in many signaling pathways, is generated from ATP by adenylate cyclases (ACs). Two forms of ACs occur in cells: a membrane-bound form (tmAC), thought to be restricted to plasma membranes, and a soluble form (sAC). The concentration of cAMP in any subcellular compartment depends on the balance between its synthesis by ACs and its degradation by phosphodiesterases. PKA, a downstream target of cAMP, is a tetrameric enzyme composed of two catalytic subunits and two regulatory subunits. With no cAMP present, PKA is inactive. When cAMP is present, it binds to the regulatory subunits, releasing the active catalytic subunits (reviewed by Taylor et al. 2004). As such, the activity of PKA depends on all the upstream factors that determine cAMP concentration. The source of mitochondrial cAMP and the role of PKA-mediated phosphorylation of mitochondrial proteins has been somewhat controversial. In contrast to theories that mitochondria contain endogenously-produced sAC, it was proposed that all cAMP is generated in the cytosol and imported into mitochondria (DiPilato et al., 2004). Acín-Pérez et al. (2009) later demonstrated a complete signaling cascade within rat liver mitochondria in which local sAC generates cAMP, activating PKA and resulting in functional changes to respiration and mitochondrial protein activity.

The results of this study have been contested, however, by groups that could not replicate the results (Covian et al., 2014).

Phosphorylation of tyrosine (Y) residues also occurs, although less commonly than S/T phosphorylation. Tyrosine phosphorylation is emerging as an important mechanism for regulating mitochondrial metabolism, as over 100 mitochondrial proteins can be modified by tyrosine phosphorylation (Cesaro and Salvi, 2010). Abelson (Abl)-family proteins were the first tyrosine kinases found to associate with mitochondria (Kumar et al., 2001; Ito et al., 2001), and their translocation to mitochondria is often associated with apoptosis. Src kinases are a family of non-receptor tyrosine kinases that specifically phosphorylate tyrosine residues and have been found in the intermembrane space and inner mitochondrial membrane (Salvi et al., 2002, 2005; Miyazaki et al., 2003). The regulation of Src kinases is complex, as their own activity is regulated by phosphorylation. The phosphorylation states of two tyrosine residues on Src kinases are key to their activity, with one site associated with inhibition of the enzyme when phosphorylated, and the other associated with activation (Roskoski, 2005). The inhibitory site (Y530) is phosphorylated by C-terminal Src kinase (Csk), which induces a closed conformation of the protein, masking the catalytic site. Several tyrosine phosphatases – including SHP-2, PTP-1B, and PTPMT1 – can dephosphorylate the Y530 site, removing the inhibitory effect (Roskoski, 2004, 2005). Several of the enzymes involved in this regulatory cascade have been found within mitochondria; Csk and SHP-2 has been found in rat brain mitochondria (Salvi et al., 2005; Arachiche et al., 2008), and PTPMT1 is found exclusively in the inner mitochondrial membrane (Pagliarini et al., 2005). The localization of these regulatory kinases and phosphatases suggests that Src kinase activity can be regulated directly in the mitochondria. Src kinases can be regulated by redox conditions; they are activated by H₂O₂ and peroxynitrite (Akhand et al., 1999), as well as cellular hypoxia (Sato et al., 2005).

1.5.2 Regulation of acetylation

Reversible protein acetylation is also a major mechanism for controlling protein function, and occurs as an acetyl group is attached to the ε-amino group in a lysine residue

(reviewed by Drazic et al., 2016). N-terminal acetylation, which is mediated by the action of N-terminal-acetyltransferases, is considered irreversible. In contrast, acetylation of lysine residues, which is reversible, is more important for acute regulation of protein activity in response to cellular conditions. Lysine acetylation can be mediated by lysine acetyltransferases, but also occurs in a non-enzymatic manner when acetyl-CoA concentrations are high (Wagner and Payne, 2013). A key regulator of acetylation state of proteins within mitochondria is the NAD-dependent protein deacetylase Sirt3. The Sirtuin family of is composed of seven proteins in mammals, with Sirt3, Sirt4, and Sirt5 localized to the mitochondrial matrix (He et al., 2012). The binding of NAD⁺ to Sirtuin proteins induces a conformational change which allows deacetylation of lysine residues (Jin et al., 2009). Since NAD⁺ levels increase in response to a decrease in cellular energy status and altered redox status, Sirtuins are believed to be a key mechanism for cells to acutely adjust metabolism. No specific mitochondrial acetyltransferases have been identified in the mitochondria. It has been suggested that most acetylation events are nonenzymatic, since lysine residues are very reactive with acetyl-coA (Baeza et al., 2015). Protein acetylation is most commonly associated with inhibitory effects (Baeza et al., 2016), which could provide negative feedback by inhibiting mitochondrial metabolism when acetyl-CoA is abundant.

1.6 Post-translational modification of proteins during hibernation

For decades, researchers have investigated the role of PTMs in regulating metabolism during hibernation. One of the best-known examples is pyruvate dehydrogenase (PDH). PDH links glycolysis to the TCA cycle through the conversion of pyruvate to acetyl-CoA. Phosphorylation of PDH dramatically decreases its activity, and during hibernation in golden-mantled ground squirrels the amount of active dephosphorylated enzyme decreases from 60-80% to 3-4% of the total enzyme in heart and kidney (Brooks and Storey, 1992). The increased phosphorylation of PDH corresponds with an upregulation of PDH kinase, an enzyme that specifically phosphorylates PDH. Hexokinase, also

involved in glycolysis, is also regulated by reversible phosphorylation during hibernation (Abnous and Storey, 2008). These patterns of phosphorylation likely facilitate an overall inhibition of carbohydrate catabolism during hibernation. Inhibition of membrane ion pumps also occurs during hibernation; as consumption of ATP by ion-motive ATPases can account for up to 50% of total cellular ATP demand (Clausen, 1986), they represent a significant energy sink. Phosphorylation of Na^+/K^+ ATPases occurs during hibernation in golden-mantled ground squirrels, reducing the activity of these membrane pumps by ~50% (MacDonald and Storey, 1999). The activity of sarcoplasmic reticulum Ca^{2+} -ATPase is also reduced by reversible phosphorylation during hibernation (Malysheva et al., 2001).

While there is ample evidence that PTMs (primarily phosphorylation) are involved in regulating metabolism during hibernation, most studies (e.g. Brooks and Storey, 1992) compare animals in torpor with animals during summer when they are euthermic and will not hibernate. Such seasonal patterns may be affected by many factors that change throughout the year including reproductive status, food quantity and quality, and photoperiod. Experiments that compare torpor and IBE eliminate these seasonal effects, and allow a focused examination of acute metabolic changes. The role of PTMs in mediating the torpor-IBE transition, however, remains largely unknown. A recent proteomics study found few changes in PTMs of liver proteins between torpor and IBE in 13-lined ground squirrels (Hindle et al., 2014), and another study found no significant differences in phosphorylation of liver mitochondrial proteins between torpor and IBE (Chung et al., 2013). There is some evidence of differential acetylation during a torpor arousal cycle; in skeletal muscle of 13-lined ground squirrels, the amount of Sirt3 protein increased during late torpor, corresponding with decreased acetylation of the Sirt3 target superoxide dismutase (Rouble and Storey, 2015). It is still unclear if and how differential acetylation contributes to the changes in metabolism that occur between torpor and IBE.

1.7 Inducing metabolic suppression: the search for a “hibernation induction trigger”

The ability of hibernators to suppress metabolic rate and body temperature without disrupting homeostasis is a remarkable feat. When ATP production decreases without a corresponding suppression in ATP demand, homeostasis is disrupted, which can lead to cell death and organ damage, such as that observed in hypoxia (Hochachka, 1986; Boutilier, 2001). In hibernators however, significant cell death and organ damage do not occur (Zancanaro et al., 1999; Fleck and Carey, 2005; van Breukelen et al., 2010). Researchers have long tried to understand the mechanisms by which hibernation and torpor are regulated, as the potential to manipulate such physiological parameters to allow a controlled reduction in metabolism and body temperature could have profound implications for both biological and medical sciences.

Dawe and Spurrier (1969) first proposed the existence of a hibernation “trigger” in the blood. They transfused summer euthermic 13-lined ground squirrels with whole blood, red blood cells, or serum from hibernating ground squirrels, and most animals entered torpor within 60 days of injection (Dawe et al., 1970). This led to the proposition of an unidentified blood-borne “hibernation induction trigger” (HIT). A subsequent study, however, found that when plasma from hibernating Richardson’s ground squirrels (*Urocitellus richardsonii*) was transfused into both Richardson’s ground squirrels and 13-lined ground squirrels, torpor was only induced in 13-lined ground squirrels (Wang et al., 1988). Further, injections of saline were just as effective at inducing torpor as injections with the plasma of hibernators. Though these data contradicted the hypothesis of a universal blood-borne HIT, the search for such a molecule has continued.

Some hormonal changes occur throughout a torpor-IBE cycle (e.g., insulin and leptin; Weitten et al., 2013). Interestingly insulin has been associated with regulating diapause in insects (Sim and Denlinger, 2013), but to my knowledge, there is no evidence that links these hormones to the substantial metabolic changes that occur during hibernation. Several endogenously produced metabolites and signaling molecules that play a role in

metabolic regulation undergo concentration cycles that parallel the annual hibernation cycle in ground squirrels (Epperson et al., 2011). Although most of these changes are seasonal, some plasma metabolites (e.g., riboflavin, ascorbate, and glycerol) differ within the winter among different stages of the torpor-IBE cycle. It has been proposed that 5'-adenosine monophosphate (5'-AMP) is involved in torpor induction; ATP/AMP ratio can be an important regulator of cellular energy status, and plasma levels of 5'-AMP increase during entrance into torpor in fasted mice (Zhang et al., 2006). Furthermore, injection of 5'-AMP into euthermic mice led to a dramatic decrease in body temperature (Zhang et al., 2006). However, in these experiments the patterns of heart rate and cooling do not match the patterns observed during torpor, so doubt has been raised about the role of 5'-AMP in the natural induction of torpor. It has been suggested that the observed temperature effects are either due to the breakdown of 5'-AMP to adenosine which reduces cardiac output, or the activation of AMP-activated kinase which is a key metabolic regulator (Swoap et al., 2007). Other metabolites involved in energy status signaling may play a role in inducing torpor; for example, in 13-lined ground squirrel liver, NAD⁺ concentration increases during entry into a torpor bout (Serkova et al., 2007). This increase in NAD⁺ could activate NAD-dependent Sirtuins and trigger deacetylation of target proteins, which could significantly affect metabolic pathways.

Several pharmacological compounds have been investigated recently for their potential to induce metabolic suppression. One compound that has gained significant attention is hydrogen sulfide (H₂S), an endogenously produced molecule that plays a role in cell signaling. H₂S is a potent inhibitor of ETS complex IV, and results in decreased enzyme activity and cellular respiration (Cooper and Brown, 2008). Inhalation of 80 ppm H₂S was shown to trigger a substantial decrease in body temperature and metabolic rate in mice (Blackstone et al., 2005). After inhalation, metabolic rate decreased by 90% and body temperature dropped to approximately 2 °C above ambient temperature, and these effects were completely reversible following the removal of H₂S. While these results have proven repeatable in mice (Volpato et al., 2008) inconsistent results have been found in larger animals such as pigs (Li et al., 2008) and sheep (Haouzi et al., 2008). Since mice have the capacity to enter torpor whereas pigs and sheep do not, the inability

to induce metabolic suppression in pigs and sheep with H₂S may be because they lack the mechanisms required for metabolic suppression and heterothermy. It is therefore possible that H₂S inhalation triggers metabolic suppression in mice through pathways unique to animals capable of hibernation and torpor.

The role of respiratory acidosis in metabolic suppression has also been investigated. As the body temperature of a hibernator decreases, blood plasma pH remains constant (Malan et al., 1973). Since the pH of neutrality increases as body temperature decreases, the blood of hibernators is considered acidic, relative to the euthermic condition.

Entrance into torpor is also accompanied by a retention in CO₂ as ventilation initially decreases more than metabolic rate, leading to respiratory acidosis (reviewed by Milsom and Jackson, 2011). Hypercapnia alone was shown to significantly reduce metabolic rate in euthermic golden-mantled ground squirrels (Bharma and Milsom, 1993), potentially by direct inhibition of metabolic enzymes. For example, phosphofructokinase, a rate-limiting glycolytic enzyme, is inhibited at low pH (Hand and Carpenter, 1986). This result has been contested by MacDonald and Storey (2001), who found that under conditions with high protein concentrations, such relative acidosis has little effect on phosphofructokinase activity. It is possible that changes in pH contribute to the induction of metabolic suppression in hibernators, but it is difficult to determine independent effects of pH as other biological parameters (e.g. body temperature) change in parallel as animals enter torpor and will affect pH dynamics.

It is important to take a multi-systems and mechanistic approach when trying to elucidate the mechanisms of such a complex physiological phenomenon as metabolic suppression in hibernation. For example, the transcription factor p53 decreased four-fold during torpor in 13-lined ground squirrels (Fleck and Carey, 2005), which led to speculation about its potential role in torpor induction. A subsequent study however found that the changes in p53 levels over a torpor-IBE cycle do not correspond with changes in the expression of any of its target genes (Pan et al., 2014). It is therefore critical that research examines multiple biological levels for a comprehensive, mechanistic understanding of metabolic suppression during hibernation.

1.8 Thesis overview

1.8.1 Rationale

During hibernation, transitions between torpor and interbout euthermia (IBE) involve rapid and substantial changes in metabolic rate. In animals such as the 13-lined ground squirrel, suppression of whole-animal metabolic rate during torpor is paralleled by suppression of mitochondrial metabolism in several tissues including liver. Suppression of liver mitochondrial metabolism occurs prior to decreases in body temperature, indicating active, regulated metabolic suppression. Little is known about the mechanisms that underlie this suppression. Post-translational modifications such as phosphorylation and acetylation can regulate mitochondrial metabolism, but little is known about how such protein modifications may contribute to mitochondrial metabolic suppression during hibernation.

1.8.2 Objectives

The major research goal of my thesis is to understand how changes in liver mitochondrial metabolism are regulated in hibernation. I hypothesize that the substantial changes in mitochondrial metabolism between torpor and IBE are acutely regulated by post-translational modification of mitochondrial ETS complexes. Further, I hypothesize that manipulating these post-translational modifications will induce and reverse suppression in liver mitochondria from hibernators. To address these hypotheses, I have structured my thesis into three main objectives, each of which is addressed in a single chapter. An additional chapter (Chapter 3) supports one of these main objectives by providing unique insights into the potential of PTMs to regulate changes in mitochondrial metabolism between torpor and IBE.

My first objective was to determine which enzymes of the mitochondrial ETS are reversibly suppressed during torpor. In Chapter 2 (Regulation of mitochondrial metabolism during hibernation by reversible suppression of electron transport system enzymes), I measured flux through each of the ETS enzymes in intact liver mitochondria

and related these measurements to the maximal activity of individual ETS complexes. I found that ETS complexes I and II were significantly suppressed in torpor compared to IBE, but that this suppression was not paralleled by changes in protein content. I conclude that changes in liver mitochondrial metabolism during hibernation are regulated by changes in complexes I and II activity, and predict that post-translational modification of these complexes underlies this regulation.

The experiment described in Chapter 3 was initially intended as a methodological study to assess the suitability of using saponin-permeabilization of liver tissue to evaluate mitochondrial respiration in a hibernator. In contrast to isolated mitochondria from the same animals, the permeabilization method yielded no difference in state 3 respiration between torpor and IBE, leading me to hypothesize that the regulatory mechanisms responsible for suppression during torpor were somehow reversed during the permeabilization process. To test this hypothesis, I repeated the experiment with the inclusion of phosphatase and deacetylase inhibitors during permeabilization in an attempt to preserve the phosphorylation and acetylation state of mitochondrial proteins. With phosphatase inhibitors present during permeabilization, the suppression of mitochondrial respiration in torpor was restored. From these results, I conclude that phosphorylation is critical to mitochondrial metabolic suppression during torpor.

My second objective was to determine how post-translational modifications of liver mitochondrial proteins differ between torpor and IBE. In Chapter 4, I conducted a large-scale proteomics analysis of liver mitochondrial proteins that differ in expression or post-translational modification between torpor and IBE. I identified several proteins that differ in phosphorylation and acetylation state, providing potentially novel sites of metabolic regulation. Most significantly, I found differential phosphorylation in ETS complexes I and II between torpor and IBE, providing direct support for my initial hypothesis.

My final objective was to use the mechanistic knowledge gained from my previous studies to manipulate metabolism in liver mitochondria. In Chapter 5, I attempted to induce and reverse metabolic suppression at the enzyme and mitochondrial levels by

manipulating the phosphorylation state of mitochondrial proteins *in vitro*. I treated homogenized liver mitochondria from IBE and torpid ground squirrels with kinases and phosphatases to stimulate phosphorylation and/or dephosphorylation of mitochondrial proteins. I found that the maximal activities of both complexes I and II were differentially altered following treatment with kinases and phosphatases, providing direct evidence for the role of phosphorylation in regulating the activity of these enzymes between torpor and IBE. Following successful manipulation of enzyme activity, I attempted to manipulate the respiration rates of intact mitochondria by stimulating the endogenous protein kinase A (PKA) pathway. Though I was able to induce some changes in mitochondrial respiration, there was no clear effect of PKA pathway activation on mitochondrial respiration. I conclude that it is possible to manipulate enzyme activity directly by manipulating phosphorylation state, but the PKA pathway does not likely regulate the metabolic changes that occur between torpor and IBE.

In Chapter 6 I synthesize the results from these four studies to propose a model by which liver mitochondrial metabolism is reversibly suppressed during hibernation.

1.9 References

- Abnous, K. and Storey, K.B. (2008) Skeletal muscle hexokinase: regulation in mammalian hibernation. *Molecular and Cellular Biochemistry*, 319(1–2) 41–50.
- Acín-Pérez, R., Bayona-Bafaluy, M.P., Fernández-Silva, P., Moreno-Loshuertos, R., Pérez-Martos, A., Bruno, C., Moraes, C.T. and Enríquez, J.A. (2004) Respiratory complex III is required to maintain complex I in mammalian mitochondria. *Molecular Cell*, 13(6) 805–815.
- Acín-Pérez, R. and Enríquez, J.A. (2014) The function of the respiratory supercomplexes: The plasticity model. *Biochimica et Biophysica Acta*, 1837(4) 444–450.
- Acín-Pérez, R., Gatti, D.L., Bai, Y. and Manfredi, G. (2011) Protein phosphorylation and prevention of cytochrome oxidase inhibition by ATP: coupled mechanisms of energy metabolism regulation. *Cell Metabolism*, 13(6) 712–719.
- Acín-Pérez, R., Salazar, E., Kamenetsky, M., Buck, J., Levin, L.R. and Manfredi, G. (2009) Cyclic AMP produced inside mitochondria regulates oxidative phosphorylation. *Cell Metabolism*, 9(3) 265–276.
- Ahn, B.-H., Kim, H.-S., Song, S., Lee, I.H., Liu, J., Vassilopoulos, A., Deng, C.-X. and Finkel, T. (2008) A role for the mitochondrial deacetylase Sirt3 in regulating energy homeostasis. *Proceedings of the National Academy of Sciences*, 105(38) 14447–14452.
- Akhand, A.A., Pu, M., Senga, T., Kato, M., Suzuki, H., Miyata, T., Hamaguchi, M. and Nakashima, I. (1999) Nitric oxide controls Src kinase activity through a sulfhydryl group modification-mediated Tyr-527-independent and Tyr-416-linked mechanism. *The Journal of Biological Chemistry*, 274(36) 25821–25826.
- Arachiche, A., Augereau, O., Decossas, M., Pertuiset, C., Gontier, E., Letellier, T. and Dachary-Prigent, J. (2008) Localization of PTP-1B, SHP-2, and Src exclusively in rat brain mitochondria and functional consequences. *Journal of Biological Chemistry*, 283(36) 24406–24411.
- Arendt, T. and Bullmann, T. (2013) Neuronal plasticity in hibernation and the proposed role of the microtubule-associated protein tau as a ‘master switch’ regulating synaptic gain in neuronal networks. *American Journal of Physiology - Regulatory, Integrative and Comparative Physiology*, 305(5) R478-489.
- Armstrong, C., Thomas, R.H., Price, E.R., Guglielmo, C.G. and Staples, J.F. (2011) Remodeling mitochondrial membranes during arousal from hibernation. *Physiological and Biochemical Zoology*, 84(4) 438–449.

- Arnold, S. and Kadenbach, B. (1997) Cell respiration is controlled by ATP, an allosteric inhibitor of cytochrome-c oxidase. *European Journal of Biochemistry*, 249(1) 350–354.
- Augereau, O., Claverol, S., Boudes, N., Basurko, M.-J., Bonneu, M., Rossignol, R., Mazat, J.-P., Letellier, T. and Dachary-Prigent, J. (2005) Identification of tyrosine-phosphorylated proteins of the mitochondrial oxidative phosphorylation machinery. *Cellular and Molecular Life Sciences*, 62(13) 1478–1488.
- Baeza, J., Smallegan, M.J. and Denu, J.M. (2016) Mechanisms and dynamics of protein acetylation in mitochondria. *Trends in Biochemical Sciences*, 41(3) 231–244.
- Baeza, J., Smallegan, M.J. and Denu, J.M. (2015) Site-specific reactivity of nonenzymatic lysine acetylation. *ACS Chemical Biology*, 10(1) 122–128.
- Bao, J., Scott, I., Lu, Z., Pang, L., Dimond, C.C., Gius, D. and Sack, M.N. (2010) SIRT3 is regulated by nutrient excess and modulates hepatic susceptibility to lipotoxicity. *Free Radical Biology and Medicine*, 49(7) 1230–1237.
- Bender, E. and Kadenbach, B. (2000) The allosteric ATP-inhibition of cytochrome c oxidase activity is reversibly switched on by cAMP-dependent phosphorylation. *FEBS Letters*, 466(1) 130–134.
- Bharma, S. and Milsom, W.K. (1993) Acidosis and metabolic rate in golden mantled ground squirrels (*Spermophilus lateralis*). *Respiration Physiology*, 94(3) 337–351.
- Blackstone, E., Morrison, M. and Roth, M.B. (2005) H₂S induces a suspended animation-like state in mice. *Science*, 308(5721) 518.
- Bouma, H.R., Kroese, F.G.M., Kok, J.W., Talaei, F., Boerema, A.S., Herwig, A., Draghiciu, O., Buiten, A. van, Epema, A.H., Dam, A. van, Strijkstra, A.M. and Henning, R.H. (2011) Low body temperature governs the decline of circulating lymphocytes during hibernation through sphingosine-1-phosphate. *Proceedings of the National Academy of Sciences*, 108(5) 2052–2057.
- Boutilier, R.G. (2001) Mechanisms of cell survival in hypoxia and hypothermia. *The Journal of Experimental Biology*, 204(Pt 18) 3171–3181.
- Brand, M.D. (1998) Top-down elasticity analysis and its application to energy metabolism in isolated mitochondria and intact cells. *Molecular and Cellular Biochemistry*, 184(1–2) 13–20.
- van Breukelen, F., Krumschnabel, G. and Podrabsky, J.E. (2010) Vertebrate cell death in energy-limited conditions and how to avoid it: what we might learn from mammalian hibernators and other stress-tolerant vertebrates. *Apoptosis: An International Journal on Programmed Cell Death*, 15(3) 386–399.

- van Breukelen, F. and Martin, S.L. (2001) Translational initiation is uncoupled from elongation at 18 C during mammalian hibernation. *American Journal of Physiology - Regulatory, Integrative and Comparative Physiology*, 281(5) R1374–R1379.
- Brooks, S.P.J. and Storey, K.B. (1992) Mechanisms of glycolytic control during hibernation in the ground squirrel *Spermophilus lateralis*. *Journal of Comparative Physiology B - Biochemical, Systems, and Environmental Physiology*, 162(1) 23–28.
- Brown, J.C.L., Chung, D.J., Belgrave, K.R. and Staples, J.F. (2012) Mitochondrial metabolic suppression and reactive oxygen species production in liver and skeletal muscle of hibernating thirteen-lined ground squirrels. *American Journal of Physiology - Regulatory, Integrative and Comparative Physiology*, 302(1) R15–28.
- Brown, J.C.L. and Staples, J.F. (2014) Substrate-specific changes in mitochondrial respiration in skeletal and cardiac muscle of hibernating thirteen-lined ground squirrels. *Journal of Comparative Physiology B - Biochemical, Systems, and Environmental Physiology*, 184(3) 401–414.
- Brown, J.C.L. and Staples, J.F. (2010) Mitochondrial metabolism during fasting-induced daily torpor in mice. *Biochimica et Biophysica Acta*, 1797(4) 476–486.
- Brustovetsky, N.N., Egorova, M.V., Iljasova, E.N. and Bakeeva, L.E. (1993) Relationship between structure and function of liver mitochondria from hibernating and active ground squirrels, *Citellus undulatus*. *Comparative Biochemistry and Physiology B - Comparative Biochemistry*, 106(1) 125–130.
- Buck, C.L. and Barnes, B.M. (2000) Effects of ambient temperature on metabolic rate, respiratory quotient, and torpor in an arctic hibernator. *American Journal of Physiology - Regulatory, Integrative and Comparative Physiology*, 279(1) R255–R262.
- Cesaro, L. and Salvi, M. (2010) Mitochondrial tyrosine phosphoproteome: new insights from an up-to-date analysis. *Biofactors* 36(6) 437–450.
- Chance, B. and Williams, G.R. (1955) Respiratory enzymes in oxidative phosphorylation. I. Kinetics of oxygen utilization. *The Journal of Biological Chemistry*, 217(1) 383–393.
- Chance, B. and Williams, G.R. (1956) Respiratory enzymes in oxidative phosphorylation. VI. The effects of adenosine diphosphate on azide-treated mitochondria. *The Journal of Biological Chemistry*, 221(1) 477–489.
- Chang, A.H.K., Sancheti, H., Garcia, J., Kaplowitz, N., Cadenas, E. and Han, D. (2014) Respiratory substrates regulate S-nitrosylation of mitochondrial proteins through a thiol-dependent pathway. *Chemical Research in Toxicology*, 27(5) 794–804.

- Chen, H., Chomyn, A. and Chan, D.C. (2005) Disruption of fusion results in mitochondrial heterogeneity and dysfunction. *Journal of Biological Chemistry*, 280(28) 26185–26192.
- Chung, D., Lloyd, G.P., Thomas, R.H., Guglielmo, C.G. and Staples, J.F. (2011) Mitochondrial respiration and succinate dehydrogenase are suppressed early during entrance into a hibernation bout, but membrane remodeling is only transient. *Journal of Comparative Physiology B*, 181(5) 699–711.
- Chung, D.J., Szyszka, B., Brown, J.C.L., Hüner, N.P.A. and Staples, J.F. (2013) Changes in the mitochondrial phosphoproteome during mammalian hibernation. *Physiological Genomics*, 45(10) 389–399.
- Cimen, H., Han, M.-J., Yang, Y., Tong, Q., Koc, H. and Koc, E.C. (2010) Regulation of succinate dehydrogenase activity by SIRT3 in mammalian mitochondria. *Biochemistry*, 49(2) 304–311.
- Clausen, T. (1986) Regulation of active Na^+ - K^+ transport in skeletal muscle. *Physiological Reviews*, 66(3) 542–580.
- Cooper, C.E. and Brown, G.C. (2008) The inhibition of mitochondrial cytochrome oxidase by the gases carbon monoxide, nitric oxide, hydrogen cyanide and hydrogen sulfide: chemical mechanism and physiological significance. *Journal of Bioenergetics and Biomembranes*, 40(5) 533–539.
- Covian, R., French, S., Kusnetz, H. and Balaban, R.S. (2014) Stimulation of oxidative phosphorylation by calcium in cardiac mitochondria is not influenced by cAMP and PKA activity. *Biochimica et Biophysica Acta*, 1837(12) 1913–1921.
- Daan, S., Barnes, B.M. and Strijkstra, A.M. (1991) Warming up for sleep? Ground squirrels sleep during arousals from hibernation. *Neuroscience Letters*, 128(2) 265–268.
- Dausmann, K.H., Glos, J., Ganzhorn, J.U. and Heldmaier, G. (2004) Physiology: Hibernation in a tropical primate. *Nature*, 429(6994) 825–826.
- Dawe, A.R. and Spurrier, W.A. (1969) Hibernation induced in ground squirrels by blood transfusion. *Science*, 163(3864) 298–299.
- Dawe, A.R., Spurrier, W.A. and Armour, J.A. (1970) Summer hibernation induced by cryogenically preserved blood ‘trigger’. *Science*, 168(3930) 497–498.
- DeLuca, M. and McElroy, W.D. (1974) Kinetics of the firefly luciferase catalyzed reactions. *Biochemistry*, 13(5) 921–925.

- DiPilato, L.M., Cheng, X. and Zhang, J. (2004) Fluorescent indicators of cAMP and Epac activation reveal differential dynamics of cAMP signaling within discrete subcellular compartments. *Proceedings of the National Academy of Sciences of the United States of America*, 101(47) 16513–16518.
- Drazic, A., Myklebust, L.M., Ree, R. and Arnesen, T. (2016) The world of protein acetylation. *Biochimica et Biophysica Acta*, 1864(10) 1372–1401.
- Dudkina, N.V., Sunderhaus, S., Boekema, E.J. and Braun, H.-P. (2008) The higher level of organization of the oxidative phosphorylation system: mitochondrial supercomplexes. *Journal of Bioenergetics and Biomembranes*, 40(5) 419–424.
- Else, P.L. and Hulbert, A.J. (1981) Comparison of the ‘mammal machine’ and the ‘reptile machine’: energy production. *The American Journal of Physiology*, 240(1) R3-9.
- Epperson, L.E., Karimpour-Fard, A., Hunter, L.E. and Martin, S.L. (2011) Metabolic cycles in a circannual hibernator. *Physiological Genomics*, 43(13) 799–807.
- Finley, L.W.S., Carracedo, A., Lee, J., Souza, A., Egia, A., Zhang, J., Teruya-Feldstein, J., Moreira, P.I., Cardoso, S.M., Clish, C.B., Pandolfi, P.P. and Haigis, M.C. (2011) SIRT3 opposes reprogramming of cancer cell metabolism through HIF1 α destabilization. *Cancer Cell*, 19(3) 416–428.
- Fleck, C.C. and Carey, H.V. (2005) Modulation of apoptotic pathways in intestinal mucosa during hibernation. *American Journal of Physiology - Regulatory, Integrative and Comparative Physiology*, 289(2) R586–R595.
- Frick, N.T., Bystriansky, J.S., Ip, Y.K., Chew, S.F. and Ballantyne, J.S. (2010) Cytochrome *c* oxidase is regulated by modulations in protein expression and mitochondrial membrane phospholipid composition in estivating African lungfish. *American Journal of Physiology - Regulatory, Integrative and Comparative Physiology*, 298(3) R608–R616.
- Fry, M. and Green, D.E. (1980) Cardiolipin requirement by cytochrome oxidase and the catalytic role of phospholipid. *Biochemical and Biophysical Research Communications*, 93(4) 1238–1246.
- Fukuda, R., Zhang, H., Kim, J., Shimoda, L., Dang, C.V. and Semenza, G.L. (2007) HIF-1 regulates cytochrome oxidase subunits to optimize efficiency of respiration in hypoxic cells. *Cell*, 129(1) 111–122.
- Gallagher, K. and Staples, J.F. (2013) Metabolism of brain cortex and cardiac muscle mitochondria in hibernating 13-lined ground squirrels *Ictidomys tridecemlineatus*. *Physiological and Biochemical Zoology*, 86(1) 1–8.
- Geiser, F. (2004) Metabolic rate and body temperature reduction during hibernation and daily torpor. *Annual Review of Physiology*, 66 239–274.

- Glancy, B., Hartnell, L.M., Malide, D., Yu, Z.-X., Combs, C.A., Connelly, P.S., Subramaniam, S. and Balaban, R.S. (2015) Mitochondrial reticulum for cellular energy distribution in muscle. *Nature*, 523(7562) 617–620.
- Gray, M.W., Burger, G. and Lang, B.F. (1999) Mitochondrial evolution. *Science*, 283(5407) 1476–1481.
- Grodums, E.I. (1977) Ultrastructural changes in the mitochondria of brown adipose cells during the hibernation cycle of *Citellus lateralis*. *Cell and Tissue Research*, 185(2) 231–237.
- Hand, S.C. and Carpenter, J.F. (1986) pH-induced hysteretic properties of phosphofructokinase purified from rat myocardium. *The American Journal of Physiology*, 250(3 Pt 2) R505-511.
- Haouzi, P., Notet, V., Chenuel, B., Chalon, B., Sponne, I., Ogier, V. and Bihain, B. (2008) H₂S induced hypometabolism in mice is missing in sedated sheep. *Respiratory Physiology & Neurobiology*, 160(1) 109–115.
- Hazel, J.R. (1972) The effect of temperature acclimation upon succinic dehydrogenase activity from the epaxial muscle of the common goldfish (*Carassius auratus*) – II. Lipid reactivation of the soluble enzyme. *Comparative Biochemistry and Physiology B - Comparative Biochemistry*, 43(4) 863–882.
- He, W., Newman, J.C., Wang, M.Z., Ho, L. and Verdin, E. (2012) Mitochondrial sirtuins: regulators of protein acylation and metabolism. *Trends in Endocrinology & Metabolism*, 23(9) 467–476.
- Heller, H.C., Colliver, G.W. and Beard, J. (1977) Thermoregulation during entrance into hibernation. *Pflügers Archiv*, 369(1) 55–59.
- Helling, S., Hüttemann, M., Ramzan, R., Kim, S.H., Lee, I., Müller, T., Langenfeld, E., Meyer, H.E., Kadenbach, B., Vogt, S. and Marcus, K. (2012) Multiple phosphorylations of cytochrome c oxidase and their functions. *Proteomics*, 12(7) 950–959.
- Hindle, A.G., Grabek, K.R., Epperson, L.E., Karimpour-Fard, A. and Martin, S.L. (2014) Metabolic changes associated with the long winter fast dominate the liver proteome in 13-lined ground squirrels. *Physiological Genomics*, 46(10) 348–361.
- Hochachka, P.W. (1986) Defense strategies against hypoxia and hypothermia. *Science*, 231(4735) 234–241.
- Hwang, Y.T., Larivière, S. and Messier, F. (2007) Energetic consequences and ecological significance of heterothermy and social thermoregulation in striped skunks (*Mephitis mephitis*). *Physiological and Biochemical Zoology*, 80(1) 138–145.

- Ito, Y., Pandey, P., Mishra, N., Kumar, S., Narula, N., Kharbanda, S., Saxena, S. and Kufe, D. (2001) Targeting of the c-Abl tyrosine kinase to mitochondria in endoplasmic reticulum stress-induced apoptosis. *Molecular and Cellular Biology*, 21(18) 6233–6242.
- Jin, L., Wei, W., Jiang, Y., Peng, H., Cai, J., Mao, C., Dai, H., Choy, W., Bemis, J.E., Jirousek, M.R., Milne, J.C., Westphal, C.H. and Perni, R.B. (2009) Crystal structures of human SIRT3 displaying substrate-induced conformational changes. *The Journal of Biological Chemistry*, 284(36) 24394–24405.
- Karpovich, S.A., Tøien, Ø., Buck, C.L. and Barnes, B.M. (2009) Energetics of arousal episodes in hibernating arctic ground squirrels. *Journal of Comparative Physiology B - Biochemical, Systems, and Environmental Physiology*, 179(6) 691–700.
- Kim, S.C., Sprung, R., Chen, Y., Xu, Y., Ball, H., Pei, J., Cheng, T., Kho, Y., Xiao, H., Xiao, L., Grishin, N.V., White, M., Yang, X.-J. and Zhao, Y. (2006) Substrate and functional diversity of lysine acetylation revealed by a proteomics survey. *Molecular Cell*, 23(4) 607–618.
- Ko, Y.H., Delannoy, M., Hullihen, J., Chiu, W. and Pedersen, P.L. (2003) Mitochondrial ATP synthasome. Cristae-enriched membranes and a multiwell detergent screening assay yield dispersed single complexes containing the ATP synthase and carriers for Pi and ADP/ATP. *The Journal of Biological Chemistry*, 278(14) 12305–12309.
- Krieger, D.A., Tate, C.A., McMillin-Wood, J. and Booth, F.W. (1980) Populations of rat skeletal muscle mitochondria after exercise and immobilization. *Journal of Applied Physiology: Respiratory, Environmental and Exercise Physiology*, 48(1) 23–28.
- Kumar, S., Bharti, A., Mishra, N.C., Raina, D., Kharbanda, S., Saxena, S. and Kufe, D. (2001) Targeting of the c-Abl tyrosine kinase to mitochondria in the necrotic cell death response to oxidative stress. *The Journal of Biological Chemistry*, 276(20) 17281–17285.
- Kuznetsov, A.V., Veksler, V., Gellerich, F.N., Saks, V., Margreiter, R. and Kunz, W.S. (2008) Analysis of mitochondrial function in situ in permeabilized muscle fibers, tissues and cells. *Nature Protocols*, 3(6) 965–976.
- Lanza, I.R. and Nair, K.S. (2009) Functional assessment of isolated mitochondria in vitro. *Methods in Enzymology*, 457 349–372.
- Larivée, M.L., Boutin, S., Speakman, J.R., McAdam, A.G. and Humphries, M.M. (2010) Associations between over-winter survival and resting metabolic rate in juvenile North American red squirrels. *Functional Ecology*, 24(3) 597–607.

- Lee, I., Salomon, A.R., Ficarro, S., Mathes, I., Lottspeich, F., Grossman, L.I. and Hüttemann, M. (2005) cAMP-dependent tyrosine phosphorylation of subunit I inhibits cytochrome c oxidase Activity. *Journal of Biological Chemistry*, 280(7) 6094–6100.
- Lehmer, E.M., Savage, L.T., Antolin, M.F. and Biggins, D.E. (2006) Extreme plasticity in thermoregulatory behaviors of free-ranging black-tailed prairie dogs. *Physiological and Biochemical Zoology*, 79(3) 454–467.
- Li, J., Zhang, G., Cai, S. and Redington, A.N. (2008) Effect of inhaled hydrogen sulfide on metabolic responses in anesthetized, paralyzed, and mechanically ventilated piglets. *Pediatric Critical Care Medicine: A Journal of the Society of Critical Care Medicine and the World Federation of Pediatric Intensive and Critical Care Societies*, 9(1) 110–112.
- Li, Y., D'Aurelio, M., Deng, J.-H., Park, J.-S., Manfredi, G., Hu, P., Lu, J. and Bai, Y. (2007) An assembled complex IV maintains the stability and activity of complex I in mammalian mitochondria. *The Journal of Biological Chemistry*, 282(24) 17557–17562.
- Liko, I., Degiacomi, M.T., Mohammed, S., Yoshikawa, S., Schmidt, C. and Robinson, C.V. (2016) Dimer interface of bovine cytochrome c oxidase is influenced by local posttranslational modifications and lipid binding. *Proceedings of the National Academy of Sciences*, 201600354.
- Liu, X. and Hajnóczky, G. (2011) Altered fusion dynamics underlie unique morphological changes in mitochondria during hypoxia-reoxygenation stress. *Cell Death and Differentiation*, 18(10) 1561–1572.
- Lovegrove, B.G. (2012) The evolution of endothermy in Cenozoic mammals: a plesiomorphic-apomorphic continuum. *Biological Reviews of the Cambridge Philosophical Society*, 87(1) 128–162.
- Lovegrove, B.G., Lobban, K.D. and Levesque, D.L. (2014) Mammal survival at the Cretaceous–Palaeogene boundary: metabolic homeostasis in prolonged tropical hibernation in tenrecs. *Proceedings of the Royal Society B*, 281(1796) 20141304.
- MacCannell, A.D.V., Jackson, E.C., Mathers, K.E. and Staples, J.F. An improved method for detecting torpor entrance and arousal in a mammalian hibernator using heart rate data. Submitted to *Journal of Experimental Biology*.
- MacCannell, A.D.V., Sinclair, K., Friesen-Waldner, L., McKenzie, C. and Staples, J.F. (2017) Water-fat MRI reveals growth of brown adipose tissue without cold exposure in a hibernator. *Journal of Comparative Physiology B - Biochemical, Systems, and Environmental Physiology*, 187 759–767.

- MacDonald, J.A. and Storey, K.B. (2001) Reassessment of the cold-labile nature of phosphofructokinase from a hibernating ground squirrel. *Molecular and Cellular Biochemistry*, 225(1–2) 51–57.
- MacDonald, J.A. and Storey, K.B. (1999) Regulation of ground squirrel Na⁺K⁺-ATPase activity by reversible phosphorylation during hibernation. *Biochemical and Biophysical Research Communications*, 254(2) 424–429.
- Malan, A. (2014) The Evolution of Mammalian Hibernation: Lessons from Comparative Acid-Base Physiology. *Integrative and Comparative Biology*, 54(3) 484–496.
- Malan, A., Arens, H. and Waechter, A. (1973) Pulmonary respiration and acid-base state in hibernating marmots and hamsters. *Respiration Physiology*, 17(1) 45–61.
- Malysheva, A.N., Storey, K.B., Ziganshin, R.K., Lopina, O.D. and Rubtsov, A.M. (2001) Characteristics of sarcoplasmic reticulum membrane preparations isolated from skeletal muscles of active and hibernating ground squirrel *Spermophilus undulatus*. *Biochemistry*, 66(8) 918–925.
- McClure, M., Cannell, E. and Despland, E. (2011) Thermal ecology and behaviour of the nomadic social forager *Malacosoma disstria*. *Physiological Entomology*, 36(2) 120–127.
- McFarlane, S.V., Mathers, K.E. and Staples, J.F. (2017) Reversible temperature-dependent differences in brown adipose tissue respiration during torpor in a mammalian hibernator. *American Journal of Physiology - Regulatory, Integrative and Comparative Physiology*, 312(3) R434–R442.
- McKechnie, A.E. and Lovegrove, B.G. (2002) Avian facultative hypothermic responses: a review. *The Condor*, 104(4) 705–724.
- Mileykovskaya, E. and Dowhan, W. (2014) Cardiolipin-dependent formation of mitochondrial respiratory supercomplexes. *Chemistry and Physics of Lipids*, 179 42–48.
- Milsom, W.K. and Jackson, D.C. (2011) Hibernation and gas exchange. *Comprehensive Physiology*, 1(1) 397–420.
- Mitra, K., Wunder, C., Roysam, B., Lin, G. and Lippincott-Schwartz, J. (2009) A hyperfused mitochondrial state achieved at G1–S regulates cyclin E buildup and entry into S phase. *Proceedings of the National Academy of Sciences*, 106(29) 11960–11965.
- Miyazaki, T., Neff, L., Tanaka, S., Horne, W.C. and Baron, R. (2003) Regulation of cytochrome c oxidase activity by c-Src in osteoclasts. *The Journal of Cell Biology*, 160(5) 709–718.

- Muleme, H.M., Walpole, A.C. and Staples, J.F. (2006) Mitochondrial metabolism in hibernation: Metabolic suppression, temperature effects, and substrate preferences. *Physiological and Biochemical Zoology*, 79(3) 474–483.
- Nath, A.K., Ryu, J.H., Jin, Y.N., Roberts, L.D., Dejam, A., Gerszten, R.E. and Peterson, R.T. (2015) PTPMT1 inhibition lowers glucose through phosphorylation of SDH. *Cell Reports*, 10(5) 694–701.
- Ogura, M., Yamaki, J., Homma, M.K. and Homma, Y. (2012) Mitochondrial c-Src regulates cell survival through phosphorylation of respiratory chain components. *The Biochemical Journal*, 447(2) 281–289.
- Pagliarini, D.J., Wiley, S.E., Kimple, M.E., Dixon, J.R., Kelly, P., Worby, C.A., Casey, P.J. and Dixon, J.E. (2005) Involvement of a mitochondrial phosphatase in the regulation of ATP production and insulin secretion in pancreatic β cells. *Molecular Cell*, 19(2) 197–207.
- Papa, S., Sardanelli, A.M., Cocco, T., Speranza, F., Scacco, S.C. and Technikova-Dobrova, Z. (1996) The nuclear-encoded 18 kDa (IP) AQP subunit of bovine heart complex I is phosphorylated by the mitochondrial cAMP-dependent protein kinase. *FEBS Letters*, 379(3) 299–301.
- Pan, P., Treat, M.D. and Breukelen, F. van (2014) A systems-level approach to understanding transcriptional regulation by p53 during mammalian hibernation. *Journal of Experimental Biology*, 217(14) 2489–2498.
- Paradies, G., Paradies, V., De Benedictis, V., Ruggiero, F.M. and Petrosillo, G. (2014) Functional role of cardiolipin in mitochondrial bioenergetics. *Biochimica et Biophysica Acta*, 1837(4) 408–417.
- Park, J., Chen, Y., Tishkoff, D.X., Peng, C., Tan, M., Dai, L., Xie, Z., Zhang, Y., Zwaans, B.M.M., Skinner, M.E., Lombard, D.B. and Zhao, Y. (2013) SIRT5-mediated lysine desuccinylation impacts diverse metabolic pathways. *Molecular Cell*, 50(6) 919–930.
- Pengelley, E.T., Asmundson, S.J., Barnes, B. and Aloia, R.C. (1976) Relationship of light intensity and photoperiod to circannual rhythmicity in the hibernating ground squirrel, *Citellus lateralis*. *Comparative Biochemistry and Physiology A - Physiology*, 53(3) 273–277.
- Pesta, D. and Gnaiger, E. (2012) High-resolution respirometry: OXPHOS protocols for human cells and permeabilized fibers from small biopsies of human muscle. *Methods in Molecular Biology*, 810 25–58.
- Picard, M., Taivassalo, T., Ritchie, D., Wright, K.J., Thomas, M.M., Romestaing, C. and Hepple, R.T. (2011) Mitochondrial structure and function are disrupted by standard isolation methods. *PLoS ONE*, 6(3) e18317.

- Popov, V.I., Bocharova, L.S. and Bragin, A.G. (1992) Repeated changes of dendritic morphology in the hippocampus of ground squirrels in the course of hibernation. *Neuroscience*, 48(1) 45–51.
- Porras, C.A. and Bai, Y. (2015) Respiratory supercomplexes: plasticity and implications. *Frontiers in Bioscience (Landmark edition)*, 20 621–634.
- Prendergast, B.J., Freeman, D.A., Zucker, I. and Nelson, R.J. (2002) Periodic arousal from hibernation is necessary for initiation of immune responses in ground squirrels. *American Journal of Physiology - Regulatory, Integrative and Comparative Physiology*, 282(4) R1054-1062.
- Roskoski, R. (2005) Src kinase regulation by phosphorylation and dephosphorylation. *Biochemical and Biophysical Research Communications*, 331(1) 1–14.
- Roskoski, R. (2004) Src protein–tyrosine kinase structure and regulation. *Biochemical and Biophysical Research Communications*, 324(4) 1155–1164.
- Rouble, A.N. and Storey, K.B. (2015) Characterization of the SIRT family of NAD-dependent protein deacetylases in the context of a mammalian model of hibernation, the thirteen-lined ground squirrel. *Cryobiology*, 71(2) 334–343.
- Ruf, T. and Geiser, F. (2015) Daily torpor and hibernation in birds and mammals. *Biological Reviews of the Cambridge Philosophical Society*, 90(3) 891–926.
- Saks, V., Guzun, R., Timohhina, N., Tepp, K., Varikmaa, M., Monge, C., Beraud, N., Kaambre, T., Kuznetsov, A., Kadaja, L., Eimre, M. and Seppet, E. (2010) Structure–function relationships in feedback regulation of energy fluxes in vivo in health and disease: Mitochondrial Interactosome. *Biochimica et Biophysica Acta*, 1797(6) 678–697.
- Salvi, M., Brunati, A.M., Bordin, L., La Rocca, N., Clari, G. and Toninello, A. (2002) Characterization and location of Src-dependent tyrosine phosphorylation in rat brain mitochondria. *Biochimica et Biophysica Acta*, 1589(2) 181–195.
- Salvi, M., Brunati, A.M. and Toninello, A. (2005) Tyrosine phosphorylation in mitochondria: A new frontier in mitochondrial signaling. *Free Radical Biology and Medicine*, 38(10) 1267–1277.
- Sato, H., Sato, M., Kanai, H., Uchiyama, T., Iso, T., Ohyama, Y., Sakamoto, H., Tamura, J., Nagai, R. and Kurabayashi, M. (2005) Mitochondrial reactive oxygen species and c-Src play a critical role in hypoxic response in vascular smooth muscle cells. *Cardiovascular Research*, 67(4) 714–722.

- Scacco, S., Vergari, R., Scarpulla, R.C., Technikova-Dobrova, Z., Sardanelli, A., Lambo, R., Lorusso, V. and Papa, S. (2000) cAMP-dependent phosphorylation of the nuclear encoded 18-kDa (IP) subunit of respiratory complex I and activation of the complex in serum-starved mouse fibroblast cultures. *Journal of Biological Chemistry*, 275(23) 17578–17582.
- Serkova, N.J., Rose, J.C., Epperson, L.E., Carey, H.V. and Martin, S.L. (2007) Quantitative analysis of liver metabolites in three stages of the circannual hibernation cycle in 13-lined ground squirrels by NMR. *Physiological Genomics*, 31(1) 15–24.
- Sheriff, M.J., Fridinger, R.W., Tøien, Ø., Barnes, B.M. and Buck, C.L. (2013) Metabolic rate and prehibernation fattening in free-living arctic ground squirrels. *Physiological and Biochemical Zoology*, 86(5) 515–527.
- Sim, C. and Denlinger, D.L. (2013) Insulin signaling and the regulation of insect diapause. *Frontiers in Physiology*, 4 1–185.
- Staples, J.F. (2016) Metabolic flexibility: Hibernation, torpor, and estivation. *Comprehensive Physiology*, 6(2) 737–771.
- Staples, J.F. and Brown, J.C. (2008) Mitochondrial metabolism in hibernation and daily torpor: a review. *Journal of Comparative Physiology B - Biochemical, Systems, and Environmental Physiology*, 178(7) 811–827.
- Swoap, S.J., Rathvon, M. and Gutilla, M. (2007) AMP does not induce torpor. *American Journal of Physiology - Regulatory, Integrative and Comparative Physiology*, 293(1) R468–R473.
- Taylor, S.S., Yang, J., Wu, J., Haste, N.M., Radzio-Andzelm, E. and Anand, G. (2004) PKA: a portrait of protein kinase dynamics. *Biochimica et Biophysica Acta*, 1697(1–2) 259–269.
- Tomitsuka, E., Kita, K. and Esumi, H. (2009) Regulation of succinate-ubiquinone reductase and fumarate reductase activities in human complex II by phosphorylation of its flavoprotein subunit. *Proceedings of the Japan Academy, Series B*, 85(7) 258–265.
- Tondera, D., Grandemange, S., Jourdain, A., Karbowski, M., Mattenberger, Y., Herzig, S., Cruz, S.D., Clerc, P., Raschke, I., Merkwirth, C., Ehses, S., Krause, F., Chan, D.C., Alexander, C., Bauer, C., Youle, R., Langer, T. and Martinou, J.-C. (2009) SLP-2 is required for stress-induced mitochondrial hyperfusion. *The EMBO Journal*, 28(11) 1589–1600.
- Volpato, G.P., Searles, R., Yu, B., Scherrer-Crosbie, M., Bloch, K.D., Ichinose, F. and Zapol, W.M. (2008) Inhaled hydrogen sulfide: A rapidly reversible inhibitor of cardiac and metabolic function in the mouse. *Journal of the American Society of Anesthesiologists*, 108(4) 659–668.

- Wagner, G.R. and Payne, R.M. (2013) Widespread and enzyme-independent N ϵ -acetylation and N ϵ -succinylation of proteins in the chemical conditions of the mitochondrial matrix. *Journal of Biological Chemistry*, 288(40) 29036–29045.
- Wang, L.C. (1979) Time patterns and metabolic rates of natural torpor in the Richardson's ground squirrel. *Canadian Journal of Zoology*, 57(1) 149–155.
- Wang, L.C., McArthur, M., Jourdan, M.L. and Lee, T.F. (1990) Depressed metabolic rate in hibernation and hypothermia: can these be compared meaningfully? In: J.R. Sutton, G. Coates, J.E. Remmers (eds.) *Hypoxia: the adaptations*. Toronto: B.C. Decker Inc., 78–83.
- Wang, L.C., Belke, D., Jourdan, M.L., Lee, T.F., Westly, J. and Nurnberger, F. (1988) The 'hibernation induction trigger': specificity and validity of bioassay using the 13-lined ground squirrel. *Cryobiology*, 25(4) 355–362.
- Wang, P., Walter, R.D., Bhat, B.G., Florant, G.L. and Coleman, R.A. (1997) Seasonal changes in enzymes of lipogenesis and triacylglycerol synthesis in the golden-mantled ground squirrel (*Spermophilus lateralis*). *Comparative Biochemistry and Physiology B - Biochemistry and Molecular Biology*, 118(2) 261–267.
- Weitten, M., Robin, J.-P., Oudart, H., Pévet, P. and Habol, C. (2013) Hormonal changes and energy substrate availability during the hibernation cycle of Syrian hamsters. *Hormones and Behavior*, 64(4) 611–617.
- Wodtke, E. (1978) Lipid adaptation in liver mitochondrial membranes of carp acclimated to different environmental temperatures: phospholipid composition, fatty acid pattern, and cholesterol content. *Biochimica et Biophysica Acta*, 529(2) 280–291.
- Wodtke, E. (1981) Temperature adaptation of biological membranes. Compensation of the molar activity of cytochrome c oxidase in the mitochondrial energy-transducing membrane during thermal acclimation of the carp (*Cyprinus carpio* L.). *Biochimica et Biophysica Acta*, 640(3) 710–720.
- Wu, Y.-T., Lee, H.-C., Liao, C.-C. and Wei, Y.-H. (2013) Regulation of mitochondrial FoF1ATPase activity by Sirt3-catalyzed deacetylation and its deficiency in human cells harboring 4977bp deletion of mitochondrial DNA. *Biochimica et Biophysica Acta*, 1832(1) 216–227.
- Zancanaro, C., Malatesta, M., Mannello, F., Vogel, P. and Fakan, S. (1999) The kidney during hibernation and arousal from hibernation. A natural model of organ preservation during cold ischaemia and reperfusion. *Nephrology Dialysis Transplantation*, 14(8) 1982–1990.
- Zhang, J., Kaasik, K., Blackburn, M.R. and Lee, C.C. (2006) Constant darkness is a circadian metabolic signal in mammals. *Nature*, 439(7074) 340–343.

CHAPTER 2

2 Regulation of mitochondrial metabolism during hibernation by reversible suppression of electron transport system enzymes

A version of this chapter has been previously published in *Journal of Comparative Physiology B*¹.

2.1 Introduction

Many small mammals, such as the 13-lined ground squirrel (*Ictidomys tridecemlineatus*), hibernate seasonally to conserve energy when environmental conditions are unfavourable. For these animals, hibernation is characterized by a distinct cycle of body temperature and metabolic suppression as animals cycle between periods of torpor and interbout euthermia (IBE) during the hibernation season (reviewed in Chapter 1.2.2). It is estimated that 40-70% of the decrease in metabolic rate as an animal enters torpor is due to active suppression, with the rest of the decline in metabolic rate being due to passive thermal effects as body temperature decreases (Guppy and Withers, 1999; Heldmaier and Elvert, 2004; Staples and Brown, 2008). Suppression of liver metabolism likely contributes to the substantial reduction of whole animal metabolic rate, as the liver is a metabolically important organ for rodents, contributing 12-17% to total metabolism but only 6-7% to whole-animal mass (Martin and Fuhrman, 1955). In isolated liver mitochondria, state 3 (phosphorylating) respiration is suppressed by up to 70% during torpor relative to IBE (Muleme et al., 2006). Recently, work from the Staples lab has shown that this suppression of mitochondrial metabolism is rapid and independent of body temperature, since maximal suppression of succinate-fueled state 3 respiration

¹ Mathers, K.E., McFarlane, S.V., Zhao, L. and Staples, J.F. (2017). *Journal of Comparative Physiology B* 187:227-234.

occurs before body temperature falls below 30 °C (Chung et al., 2011). In contrast, the increase in the respiration rate of liver mitochondria during arousal from torpor into IBE is slow, with increases in succinate-fueled state 3 respiration rates roughly paralleling increases in body temperature.

Suppression of liver mitochondrial metabolism in hibernators is greatest with succinate as an oxidative substrate, which suggests that most of the suppression occurs at or downstream of ETS complex II (Staples, 2014). The regulatory mechanism(s) underlying this suppression remain largely unknown. Significant changes in the concentration for metabolites related to mitochondrial metabolism (e.g. isovaleryl carnitine, uridine, and flavin adenine dinucleotide) occur between torpor and IBE in liver (Nelson et al., 2009), but metabolite inhibition can explain a maximum of 25% of the suppression of complex II seen during torpor (Armstrong and Staples, 2010). Changes in mitochondrial membrane composition, such as degree of phospholipid fatty acid saturation, can affect the activity of complex II and other proteins in the inner mitochondrial membrane (Hazel, 1972), but in 13-lined ground squirrels, there appear to be no differences in membrane composition between torpor and IBE (Chung et al., 2011).

Given the rapid nature of the suppression that occurs in liver mitochondria, especially during entrance into torpor (within approximately two hours), it is unlikely that differential transcription and translation are responsible. In addition, initiation of transcription does not occur at body temperatures below 18 °C in ground squirrels (van Breukelen and Martin, 2001). It is more likely that ETS enzyme activity is directly and reversibly suppressed during torpor, perhaps through post-translational modifications. Such modifications can be powerful regulators of mitochondrial metabolism (Hofer and Wenz, 2014), though their role in regulating mitochondrial metabolism between torpor and IBE remains largely unexplored.

In this Chapter I aimed to better characterize the regulation of the rapid, reversible metabolic suppression displayed by liver mitochondria during hibernation. Our research group has demonstrated previously that liver mitochondrial metabolism of succinate and

pyruvate is reversibly suppressed during torpor (Muleme et al., 2006; Chung et al., 2011), but the role of individual complexes and their effect on overall mitochondrial metabolism is not yet clear. Specifically, the roles of individual complexes downstream of complex II (complexes III, IV, and V) are completely unknown.

I hypothesized that complex II is the main site of suppression in liver mitochondria, and that this suppression is mediated by differential post-translational modification between torpor and IBE. To test this hypothesis, I first measured flux through each of the ETS complexes in intact liver mitochondria. I then measured the maximal activity of each complex in liver mitochondria and liver tissue to estimate their contributions to suppression of mitochondrial respiration. I also measured the protein content of each ETS complex. Since I hypothesized that changes in activity are mediated by PTM to existing proteins rather than changes in transcription or translation, I predicted that the protein content of all ETS complexes would not change between torpor and IBE.

2.2 Materials and methods

2.2.1 Animals

All procedures were approved by the University of Western Ontario Animal Use Subcommittee (Protocol number: 2012-016; Appendix A). Thirteen-lined ground squirrels (*Ictidomys tridecemlineatus*) were live-trapped in Carman, MB, Canada (49°30'N, 98°01'W, with approval from the Manitoba Ministry of Conservation; Appendix B) or bred in captivity, following previously established protocols (Vaughan et al., 2006). All squirrels were housed at the University of Western Ontario. Squirrels were individually housed in plastic shoe-box style cages (26.7 x 48.3 x 20.3 cm) and provided with dried, shredded corn cob bedding (Bed-o'Cobs ¼", The Andersons, Maumee, OH), shredded paper nesting material (Crink-I'Nest, The Andersons, Inc.), and a cardboard tube (8 x 15 cm, Bio-Serv, Flemington, NJ) for enrichment. Rat chow (5P00, LabDiet, St. Louis, MO) and water were provided *ad libitum*. During the spring and summer, squirrels were housed at 22 °C ± 3 °C with a photoperiod matching that of Carman, MB (adjusted

weekly) under full-spectrum, fluorescent lighting. In early October, squirrels were transferred to environmental chambers where the temperature was reduced by 1 °C per day until it reached 4 °C ± 2°C and photoperiod was reduced to 2 h of light and 22 h of dark (with lights on at 10:00 h). This photoperiod mimics that of the inside of a burrow during the hibernation season while allowing sufficient light for animal care.

2.2.2 Radiotelemetry implants

Radiotelemeters were surgically implanted in adult ground squirrels to continuously monitor core body temperature during hibernation (Muleme et al., 2006). Radio telemeters (Model TA-ETA10, Data Sciences International, New Brighton, MN) were implanted intraperitoneally under isoflurane gas anesthesia. Squirrels were provided with postoperative analgesia (subcutaneous meloxicam, 0.05 mg/kg) prior to surgery, and once daily for three days following surgery. Core body temperature measurements were collected every four minutes using telemetry receivers (model RA1010, Data Sciences International) using DataQuest ART software (Data Science International).

2.2.3 Experimental groups

This study compared animals that were either in torpor (a stable body temperature near 5 °C for 3-5 days) or IBE (a stable body temperature near 37 °C for 3-4 h following a spontaneous arousal). Torpid animals were sampled at 8:30am EST, but IBE animals could not be sampled at a standardized time due to the spontaneous nature of interbout arousals. Animals sampled during IBE were euthanized by anesthetic overdose (intraperitoneal injection of Euthanyl; 54 mg/100g). Euthanyl has no known effects on mitochondrial metabolism (Takaki et al., 1997). Torpid animals were euthanized by cervical dislocation, since anaesthetic injection would cause arousal. Liver was dissected immediately following euthanasia, and a small section was frozen in liquid nitrogen for enzyme assays.

2.2.4 Isolation of mitochondria

Following excision, liver tissue was immediately submerged in ice-cold homogenization buffer 1 (HB1; 250 mM sucrose, 1 mM EGTA, 10 mM HEPES, 1% (w/v) BSA, pH 7.4) and minced into 1 mm³ pieces using surgical scissors. Minced tissue was then homogenized in approximately 30 ml HB1 in a 50 ml glass mortar, using three passes (100 rpm for approximately 30 sec) of a loose-fitting Teflon pestle. The homogenate was subsequently filtered through one layer of cheesecloth and centrifuged at 1000 g for 10 min at 4 °C (Centrifuge 5804R, Eppendorf, Mississauga ON), and this step was repeated once with the resulting supernatant. Following the second centrifugation, the supernatant was filtered through four layers of cheesecloth and centrifuged at 8700 g for 10 min at 4 °C. The supernatant was then aspirated, and the resulting crude mitochondrial pellet was resuspended in 1 ml ice-cold homogenization buffer 2 (HB2; 250 mM sucrose, 1 mM EGTA, 10 mM HEPES, pH 7.4). This sample of crude mitochondria was purified using a Percoll gradient centrifugation technique outlined by Petit et al. (1990). Crude mitochondria (1 ml) were layered on top of a Percoll (Sigma-Aldrich) gradient solution composed of 10 ml layers of 10, 18, 30, and 70% (v/v) solutions, diluted in HB2, layered with the densest at the bottom of a 50 ml centrifuge tube. The mitochondria and Percoll solution was then centrifuged at 13,000 g for 35 min at 4 °C. Following centrifugation, approximately 1 ml of purified mitochondria was isolated from the boundary between the 30 and 70% Percoll layers and resuspended in 40 ml HB2. The mitochondrial suspension was centrifuged at 8700 g for 10 min at 4 °C, with this wash step repeated once more to remove all Percoll. The final, purified mitochondrial pellet was resuspended in 1 ml HB2 and kept on ice until respiration measurements were made, with aliquots flash frozen in liquid nitrogen and stored at -80 °C for subsequent enzyme assays. This mitochondrial isolation and purification technique results in mitochondrial samples with 85 to 96% of contaminants (endoplasmic reticulum, peroxisomes, lysosomes, and plasma membranes) removed, demonstrated by assays of marker enzyme activity (Armstrong and Staples, 2010).

2.2.5 Mitochondrial respiration and ETS complex flux

Mitochondrial oxygen consumption was measured using an Oxygraph-O2K high-resolution respirometer (Oroboros Instruments, Austria). Mitochondria (10 μ l, ~150 μ g protein) were transferred to respiration chambers containing 2 ml of mitochondrial respiration medium (0.5 mM EGTA, 3 mM MgCl₂, 60 mM L-lactobionate, 20 mM taurine, 10 mM KH₂PO₄, 20 mM HEPES, 110 mM sucrose, 1 g/l fatty acid free BSA, pH 7.1; (Kuznetsov et al., 2008) under constant stirring (750 rpm) at 37 °C. Oxygen partial pressure was sensed by polarographic electrodes and converted to dissolved oxygen concentration using DatLab software (version 4.3.2.7, Oroboros Instruments, Austria) following calibration with air-saturated respiration medium and oxygen-depleted medium (obtained with the use of a yeast suspension). Unless indicated otherwise, all substrates and inhibitors were dissolved in respiration medium. Flux through each ETS complex was assessed in one mitochondrial sample from each animal by measuring oxygen consumption rates following sequential stimulation and inhibition of each complex. Flux values were calculated from the mean of duplicates for each animal. Flux through complexes I-IV was measured following the addition of ADP (1 mM), pyruvate (1 mM), and malate (1 mM). Once a stable rate was reached, rotenone (0.5 μ M, dissolved in 95% (v/v) ethanol) was added to inhibit complex I, and flux through complexes II-IV was measured by adding succinate (6 mM). Complex II was then inhibited by the addition of malonate (5 mM), and flux through complexes III-IV was determined after the addition of reduced ubiquinone₂ (10 μ l of 10 mg/ml, reduced as described by (Rieske, 1967)). Antimycin A (2.5 μ M, dissolved in 95% (v/v) ethanol) was added to inhibit complex III, and flux through complex IV was measured following the addition of N, N', N'-tetramethyl-p-phenylenediamine (TMPD; 0.5 mM) and ascorbate (2 mM). Parallel measurements were made with and without potassium cyanide (1 mM) to correct for uncatalyzed oxidation of TMPD. Flux through each ETS complex was expressed relative to total protein content of each isolated mitochondria sample. The protein content of each mitochondrial sample was determined with protein assay dye (Bio-Rad) using BSA dissolved in homogenization buffer as protein standards.

2.2.6 ETS complex activity assays

Aliquots of liver mitochondria from animals sampled during torpor and IBE were thawed in an ice/water slurry and centrifuged for 10 min at 20,000 *g* and 4 °C. The resulting pellets were resuspended in an isotonic assay medium (100 mM KCl, 25 mM K₂HPO₄, 5 mM MgCl₂, pH 7.4) to a concentration of 1 mg protein/ml and freeze-thawed three times in liquid nitrogen and an ice/water slurry and used for assays. Frozen liver tissue from the same animals was homogenized in 10 volumes of buffer (20 mM Tris, 1 mM EDTA, 0.1% Triton X-100, pH 7.2). These homogenates were diluted to 2 mg tissue/ml and used for assays.

All assays were performed as described by Kirby et al. (2007), using a Spectromax plate spectrometer (Molecular Devices, Sunnyvale, CA) at 37 °C. For all assays, samples were run in triplicates and V_{\max} values for individuals were calculated from the mean of the triplicates. Complex I activity was measured following the addition of 10 μ l mitochondrial or tissue homogenate (corresponding to 10 μ g mitochondrial protein and 20 μ g liver tissue) to 290 μ l of assay mixture containing 25 mM K₂HPO₄ (pH 7.4), 2 μ g/ml antimycin A, 2 mM KCN, 2.5 mg/ml BSA, and 0.2 mM NADH. The oxidation of NADH was tracked by measuring absorbance (340 nm) for 3-5 mins. Complex II activity was measured following the addition of 5 μ l mitochondrial or tissue homogenates (corresponding to 5 μ g mitochondrial protein and 10 μ g liver tissue) to 294 μ l of assay mixture containing 25 mM K₂HPO₄ (pH 7.4), 2 μ g/ml rotenone, 2 μ g/ml antimycin A, 2 mM KCN, 20 mM succinate, and 50 μ M dichlorophenolindophenol (DCPIP). The reaction was started with 1 μ l of 10 μ M ubiquinone₁, and the oxidation state of DCPIP was tracked by measuring absorbance (600 nm) for 3-5 min. Complex III activity was measured following the addition of 3 μ l mitochondrial or tissue homogenates (corresponding to 3 μ g mitochondrial protein and 6 μ g liver tissue) to 296 μ l of assay mixture containing 25 mM K₂HPO₄ (pH 7.2), 2 μ g/ml rotenone, 2 mM KCN, 2.5 mg/ml BSA, 0.6 mM n-dodecyl- β -D-maltoside, and 15 mM oxidized cytochrome c. The reaction was started with 1 μ l of reduced ubiquinone₂ (10 mg/ml), and the oxidation state of cytochrome c was tracked by measuring absorbance values (550 nm) for 2-5 min.

Complex IV activity was measured following the addition of 1 μ l mitochondrial or tissue homogenates (corresponding to 1 μ g mitochondrial protein and 2 μ g liver tissue) to 299 μ l of assay mixture containing 25 mM K_2HPO_4 (pH 7.2), 5 mM $MgCl_2$, 2.5 mg/ml BSA, 0.6 mM lauryl maltoside, and 50 μ M reduced cytochrome c. Cytochrome c was reduced by adding a few grains of sodium hydrosulfite to 250 μ l of oxidized cytochrome c immediately before the complex IV assays. The reduction state of the cytochrome c was determined by measuring its absorbance at 550 nm and at 565 nm, and was considered sufficient only if the ratio of A_{550}/A_{565} was greater than 6 (Kirby et al., 2007). Parallel assays were run with and without 150 mM sodium azide to account for non-enzymatic oxidation of TMPD. Absorbance values (550 nm) were collected for 3-5 min. Complex V activity was measured following the addition of 1 μ l mitochondrial or tissue homogenates (corresponding to 1 μ g mitochondrial protein and 2 μ g liver tissue) to 299 μ l of assay mixture containing 5 mM ATP, 1 mM phosphoenolpyruvate, 0.2 mM NADH, 1 U/ml pyruvate kinase, and 1 U/ml lactate dehydrogenase. Absorbance values (340 nm), corresponding with concentration of NADH, were collected for 3-5 min, with complex V rates calculated from the difference between rates collected with and without oligomycin inhibition.

2.2.7 Immunoblots

Samples of isolated liver mitochondria from animals sampled during torpor and IBE were denatured in loading buffer (100 mM Tris, 10% (v/v) glycerol, 2% (w/v) lithium dodecyl sulfate (LDS), 0.175 mM Phenol Red, 100 mM dithiothreitol (DTT), pH 8.5) at 37 °C for 10 minutes and electrophoresed on sodium dodecyl sulfate (SDS) polyacrylamide gels (10% (w/v) acrylamide). Gels were loaded with 10 ng of protein from each liver mitochondria sample. Gels were run at 180V for 1 hr in a running buffer (25 mM Tris, 190 mM glycine, 0.1% (w/v) SDS), then transferred to polyvinylidene fluoride membranes. Transfers were conducted at 4 °C at 100V for 2 hours. After transfer, membranes were blocked with 5% BSA in Tris-buffered saline and Tween-20 (TBST; 30 mM Tris, 137 mM NaCl, 0.1% (v/v) Tween-20, pH 7.6) under steady agitation (300 rpm)

Table 2-1. Subunits of ETS complexes targeted by MitoProfile antibody cocktail (AbCam, ab6820).

ETS Complex	Subunit targeted
Complex I	NDUFB8
Complex II	Iron-sulfur protein (IP) subunit
Complex III	Core protein II
Complex IV	Subunit I
Complex V	Alpha subunit

for 2 hours and probed with the mouse MitoProfile primary antibody (Abcam, ab110413 1:1000 dilution in TBST), which binds to one subunit of each ETS complex (Table 2-1), overnight at 4 °C. Membranes were then incubated with donkey polyclonal Secondary Antibody to Mouse IgG (Abcam, ab6820, 1:10,000 dilution in TBST) for 1 hr at room temperature under steady agitation. The membrane was washed four times for 15 min in TBST. Bands were visualized following the addition of Luminata Forte chemiluminescent substrate (Millipore) to membranes, using a VersaDoc MP5000 imaging system (BioRad). Bands were quantified using the densitometry analysis tool in ImageLab 3.0 (BioRad) and standardized to total protein in each lane, determined by Amido Black staining of the same membranes. The total protein loaded (10 ng per well) corresponds with bands within the linear range of detection for all five ETS subunits, determined by a preliminary immunoblot with a dilution series of protein (data not shown).

2.2.8 Statistical analysis

All statistical analyses were conducted using R. One-tailed, unpaired t-tests were used to compare fluxes between torpor and IBE for each ETS complex in intact liver mitochondria. One-tailed, unpaired t-tests were used to compare maximal activity of each ETS complex between torpor and IBE for both isolated mitochondria and homogenized liver tissue. For immunoblots, two-tailed, unpaired t-tests were used to compare the content of each ETS protein between torpor and IBE. Differences were considered significant for p-values <0.05.

2.3 Results

I measured flux through the ETS in intact mitochondria by sequentially stimulating and inhibiting each complex, and compared rates between IBE and torpor (Figure 2-1). During torpor, flux through complexes I-IV was significantly suppressed by 40% (p=0.012) and flux through complexes II-IV was suppressed by 60% (p=0.002),

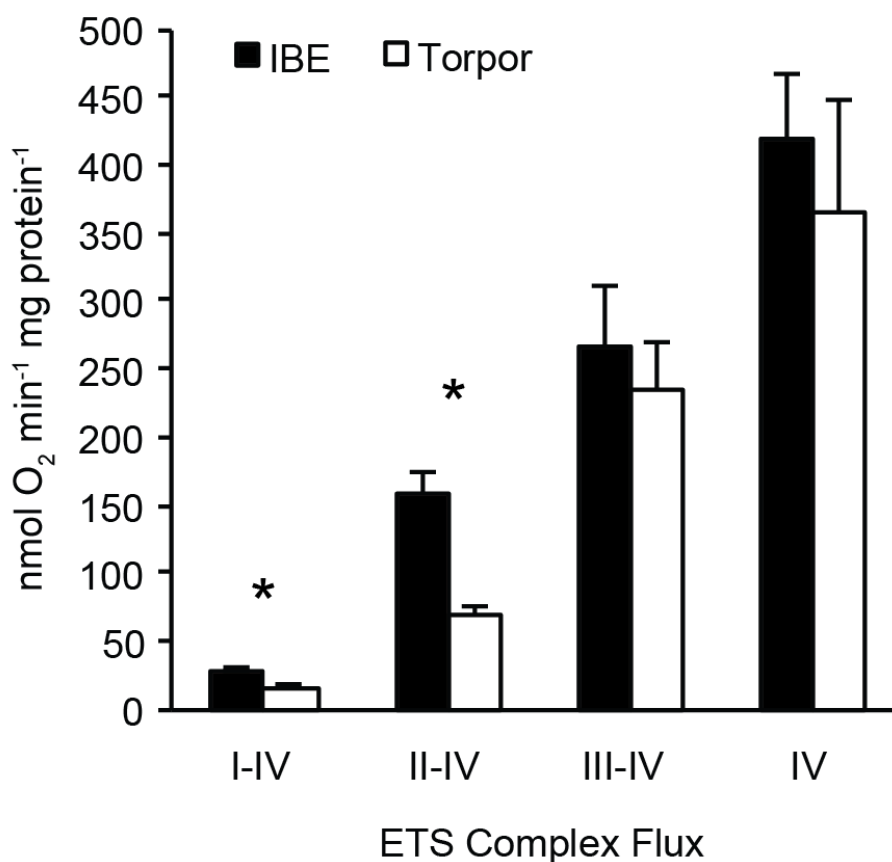


Figure 2-1. Flux through electron transport system (ETS) complexes in liver mitochondria isolated from torpid and IBE ground squirrels. State 3 (ADP-phosphorylating) oxygen consumption rates were measured in liver mitochondrial isolated from animals sampled during torpor (n=9) and IBE (n=8), following sequential stimulation and inhibition of each ETS complex. Values represent means \pm SE. Asterisks denote a significant difference ($p \leq 0.05$, one-tailed t-test) between torpor and IBE.

compared with IBE. Flux through complexes III-IV and IV did not differ significantly between torpor and IBE.

I measured the maximal activity of each ETS complex using spectrophotometric assays for each complex in isolated mitochondria (Table 2-2) from the same samples used to measure ETS fluxes. In homogenized liver mitochondria, complexes I and II were each suppressed by 20% during torpor compared with IBE ($p=0.005$ and $p=0.006$, respectively). Complexes III, IV and V showed no significant difference between torpor and IBE.

I also measured maximal activities of the five ETS complexes in homogenized liver tissue from the same animals, and found significant suppression of complexes I, II, III and V during torpor relative to IBE (Table 2-3). Complex I was suppressed by 14% ($p=0.03$), complex II by 30% ($p<0.001$), complex III by 10% ($p=0.04$), and complex V by 14% ($p=0.03$). There was no significant difference in complex IV activity between torpor and IBE.

I conducted immunoblots to compare the protein content of each ETS complex between torpor and IBE (Figure 2-2). There was 30% more complex III protein present during torpor relative to IBE ($p=0.049$). There were no significant differences between torpor and IBE in the protein content of complexes I, II, IV, or V.

2.4 Discussion

To date, this is the most comprehensive study of the regulation of mitochondrial electron transport system proteins in a hibernator. My results show that the suppression of liver mitochondrial metabolism in 13-lined ground squirrels during torpor corresponds closely with suppression of ETS complexes I and II. Furthermore, my immunoblot data most likely rule out differences in transcription, translation or degradation as underlying causes of this suppression, as the content of these proteins did not differ between torpor and IBE.

Table 2-2. Maximal activity of ETS complexes in isolated liver mitochondria. Enzyme activities ($\mu\text{mol min}^{-1} \text{mg protein}^{-1}$) were measured in homogenized mitochondria from animals sampled during torpor (n=8) and IBE (n=6). Asterisks indicate a significantly lower value in torpor compared with IBE.

		Complex I	Complex II	Complex III	Complex IV	Complex V
IBE	Mean	83.5	181.9	392.7	1240.5	482.1
	SE	3.96	9.21	21.28	88.08	48.43
Torpor	Mean	67.98*	146.6*	379.1	1123.5	468.2
	SE	1.29	7.03	24.1	88.6	13.39

Table 2-3. Maximal activity of ETS complexes in liver tissue. Enzyme activities ($\mu\text{mol min}^{-1} \text{mg tissue}^{-1}$) were measured in homogenized liver tissue from animals sampled during torpor (n=8) and IBE (n=6). Asterisks indicate a significantly lower value in torpor compared with IBE.

		Complex I	Complex II	Complex III	Complex IV	Complex V
IBE	Mean	142.8	412.5	1661.0	5403.2	2460.3
	SE	7.52	16.90	88.20	292.20	120.34
Torpor	Mean	122.7*	285.0*	1476.0*	4946.7	2104.0*
	SE	6.63	19.77	63.05	339.08	139.64

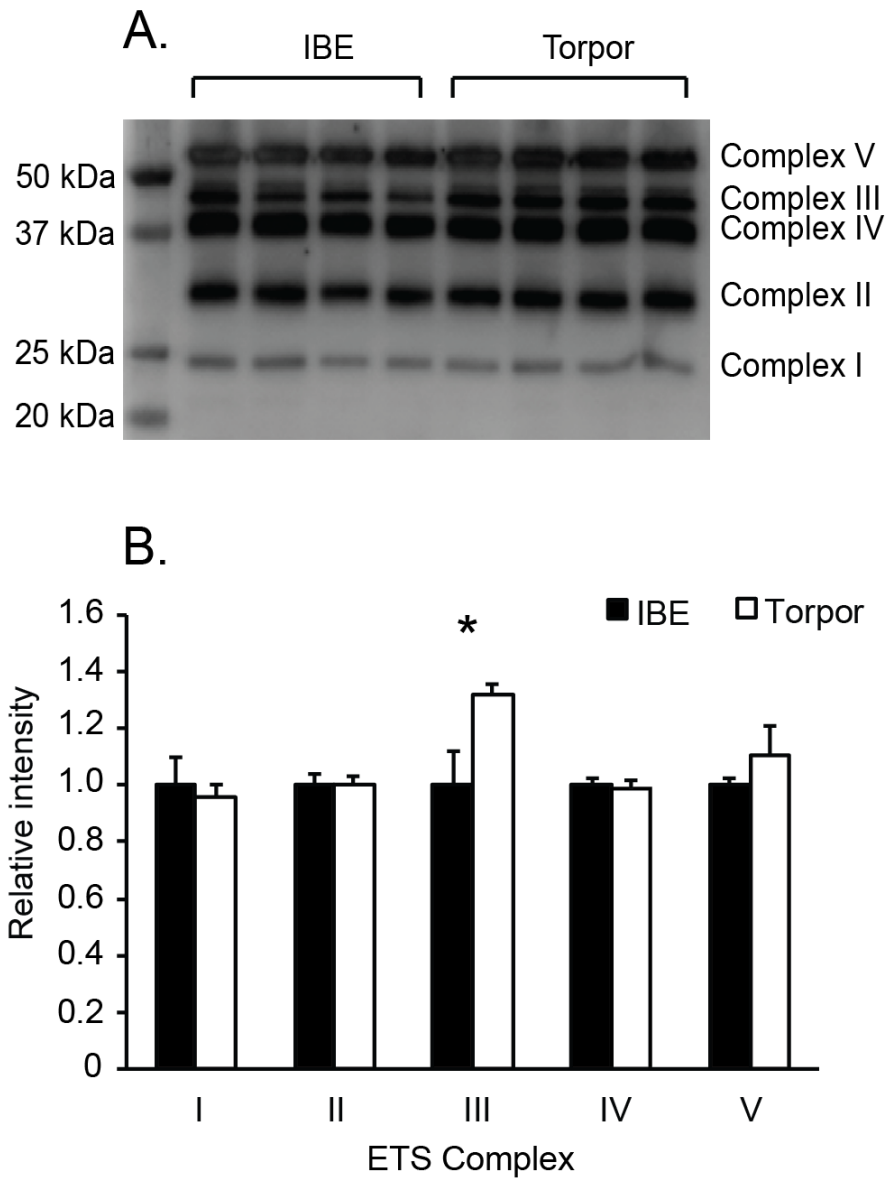


Figure 2-2. Protein content of ETS complexes in liver mitochondria of torpid and IBE ground squirrels. Immunoblots (A) were performed on isolated mitochondria from animals sampled during torpor (n=4) and IBE (n=4). The subunits targeted by each antibody are shown in Table 2-1. Bands were quantified and standardized to total protein, then expressed relative to IBE (B).

In liver mitochondria, there was significant suppression of flux through complexes I and II during torpor (Figure 2-1). Flux through complexes I-IV was suppressed by 40% and flux through complexes II-IV was suppressed by 60%, comparable to previous studies (Muleme et al., 2006; Chung et al., 2011). There was no suppression in flux through complexes III-IV or complex IV. A recent study of liver mitochondrial metabolism during hibernation in the long-tailed ground squirrel also found significant suppression of complexes I and II during torpor (Komelina et al., 2015). In contrast to my results, this study found that complex I was suppressed to a greater degree than complex II, perhaps suggesting differences among species. My study agrees with Komelina et al., (2015) in concluding that a significant portion of the liver mitochondrial suppression occurs between complexes II and III. However, because I found no differences in flux through complex III-IV and complexes IV between torpor and IBE, I can further conclude that the most significant suppression occurs at complex II.

I measured maximal activity (V_{\max}) of each ETS complex in the same liver mitochondria using spectrophotometric assays to determine the activity of each complex (Table 2-2). This approach allowed me to examine each complex individually rather than flux through multiple complexes, the rate of which depends not only on the maximal capacity of the initial enzyme, but also on the capacity of downstream enzymes to metabolize the products of upstream complexes. Complexes I and II both showed significantly lower V_{\max} during torpor relative to IBE. The maximal activities of complexes III, IV and V did not differ between torpor and IBE. These data parallel the pattern of flux measurements from intact mitochondria, further suggesting that suppression of complexes I and II is important for the observed reversible suppression seen in intact mitochondria.

I also measured V_{\max} of each ETS complex in homogenized liver tissue from the same animals used for liver mitochondria isolation (Table 2-3). In homogenized liver tissue, the maximal activities of complexes I, II, III, and V were each significantly lower in torpor relative to IBE. Complex IV showed no difference in V_{\max} between torpor and IBE. It is unclear why complexes III and V would be suppressed during torpor in homogenized tissue but not in isolated mitochondria. It is likely not due to differences in

mitochondrial content, as previous work has shown that, in liver, mitochondrial content does not change between torpor and IBE (Mathers and Staples, 2015). It is worthwhile to note, however, that complexes I and II showed significant suppression during torpor whether measured in isolated mitochondria or whole liver tissue.

Changes in V_{\max} and total flux through each mitochondrial complex could be due to changes in either enzyme active site turnover number (K_{cat}) or the amount of each protein, since V_{\max} is the product of K_{cat} and enzyme concentration. Immunoblots for the five ETS complexes allow a comparison of content of these proteins between torpor and IBE in isolated liver mitochondria (Figure 2-2). The complex III Core protein II was more abundant in torpor relative to IBE; but this does not correspond with changes in flux or V_{\max} . In fact, in liver tissue, V_{\max} of complex III is lower in torpor, so the significance of this increase in Core protein II remains unknown. There were no differences in the protein content of complexes I, II, IV, and V between torpor and IBE.

Despite significant suppression of flux and V_{\max} during torpor for both complexes I and II, there is no difference in the content of either of these proteins. These results indicate that the reversible suppression that occurs during torpor is due to changes in the K_{cat} of these two proteins rather than changes in their overall expression. Given that the rapid reversible, temperature-sensitive pattern of suppression, and that the changes in activity of complexes I and II are not paralleled by changes in protein content, post-translational modification is a probable mechanism underlying these changes. Post-translational modification (PTM) is a powerful regulator of mitochondrial metabolism (Hofer and Wenz, 2014). Complex II in particular is a target for several post-translational modifications that alter its activity; Subunit A (SDHA) is a target for both deacetylation by SIRT3 (Cimen et al., 2010; Finley et al., 2011) and phosphorylation by Src kinases (Augereau et al., 2005; Salvi et al., 2005; Ogura et al., 2010). Complex I is also a target for both deacetylation (Ahn et al., 2008) and phosphorylation (Augereau et al., 2005; Ogura et al., 2010; Hébert-Chatelain et al., 2010). The effects of PTMs on mitochondrial metabolism is complex, with modifications having antagonistic effects on enzyme activity depending on the site that is modified (reviewed in Chapter 1.4.5).

The role of PTMs in regulating mitochondrial metabolism throughout torpor-arousal cycles remains largely unexplored. One study on liver tissue in 13-lined ground squirrels found few differences in total phosphorylation and acetylation between torpor and arousal (Hindle et al., 2014). This study used whole liver tissue, however, so subtle differences in PTMs of mitochondrial proteins might have been difficult to detect as mitochondrial proteins represent only a small fraction of total liver protein. Recent work from the Staples lab found no difference in total phosphorylation of liver mitochondrial proteins between torpor and IBE, although Chung et al. (2013) reported seasonal differences in phosphorylation of some ETS proteins. However, it is possible that the techniques used by Chung et al. (2013) lacked the resolution to detect subtle changes in phosphorylation of specific proteins. It is also possible that types of PTMs other than phosphorylation (e.g. acetylation) are involved in regulating mitochondrial during hibernation.

2.5 Conclusions

This study has helped narrow the search for the mechanisms that are responsible for reversible suppression of mitochondrial metabolism during hibernation. ETS complexes I and II are clearly altered between torpor and IBE. Since the activity of these proteins changes rapidly with no corresponding change in protein content, I propose that differential post-translational modification is responsible for their regulation. In the following chapters, I investigate the role of post-translational modifications in regulating liver mitochondrial metabolism between torpor and IBE.

2.6 References

- Ahn, B.-H., Kim, H.-S., Song, S., Lee, I.H., Liu, J., Vassilopoulos, A., Deng, C.-X. and Finkel, T. (2008) A role for the mitochondrial deacetylase Sirt3 in regulating energy homeostasis. *Proceedings of the National Academy of Sciences*, 105(38) 14447–14452.
- Armstrong, C. and Staples, J.F. (2010) The role of succinate dehydrogenase and oxaloacetate in metabolic suppression during hibernation and arousal. *Journal of Comparative Physiology B - Biochemical, Systems, and Environmental Physiology*, 180(5) 775–783.
- Augereau, O., Claverol, S., Boudes, N., Basurko, M.-J., Bonneu, M., Rossignol, R., Mazat, J.-P., Letellier, T. and Dachary-Prigent, J. (2005) Identification of tyrosine-phosphorylated proteins of the mitochondrial oxidative phosphorylation machinery. *Cellular and Molecular Life Sciences*, 62(13) 1478–1488.
- van Breukelen, F. and Martin, S.L. (2001) Translational initiation is uncoupled from elongation at 18 C during mammalian hibernation. *American Journal of Physiology - Regulatory, Integrative and Comparative Physiology*, 281(5) R1374–R1379.
- Chung, D., Lloyd, G.P., Thomas, R.H., Guglielmo, C.G. and Staples, J.F. (2011) Mitochondrial respiration and succinate dehydrogenase are suppressed early during entrance into a hibernation bout, but membrane remodeling is only transient. *Journal of Comparative Physiology B - Biochemical, Systems, and Environmental Physiology*, 181(5) 699–711.
- Chung, D.J., Szyszka, B., Brown, J.C.L., Hüner, N.P.A. and Staples, J.F. (2013) Changes in the mitochondrial phosphoproteome during mammalian hibernation. *Physiological Genomics*, 45(10) 389–399.
- Cimen, H., Han, M.-J., Yang, Y., Tong, Q., Koc, H. and Koc, E.C. (2010) Regulation of succinate dehydrogenase activity by SIRT3 in mammalian mitochondria. *Biochemistry*, 49(2) 304–311.
- Finley, L.W.S., Carracedo, A., Lee, J., Souza, A., Egia, A., Zhang, J., Teruya-Feldstein, J., Moreira, P.I., Cardoso, S.M., Clish, C.B., Pandolfi, P.P. and Haigis, M.C. (2011) SIRT3 opposes reprogramming of cancer cell metabolism through HIF1 α destabilization. *Cancer Cell*, 19(3) 416–428.
- Guppy, M. and Withers, P. (1999) Metabolic depression in animals: physiological perspectives and biochemical generalizations. *Biological Reviews of the Cambridge Philosophical Society*, 74(01) 1–40.

- Hazel, J.R. (1972) The effect of temperature acclimation upon succinic dehydrogenase activity from the epaxial muscle of the common goldfish (*Carassius auratus*) – II. Lipid reactivation of the soluble enzyme. *Comparative Biochemistry and Physiology B - Comparative Biochemistry*, 43(4) 863–882.
- Hébert-Chatelain, E.H., Dupuy, J.-W., Letellier, T. and Dachary-Prigent, J. (2010) Functional impact of PTP1B-mediated Src regulation on oxidative phosphorylation in rat brain mitochondria. *Cellular and Molecular Life Sciences*, 68(15) 2603–2613.
- Heldmaier, G. and Elvert, R. (2004) How to enter torpor: thermodynamic and physiological mechanisms of metabolic depression. In: B.M. Barnes, H.V. Carey (eds.) *Life in the Cold*. Fairbanks: University of Alaska Fairbanks, 185–198.
- Hindle, A.G., Grabek, K.R., Epperson, L.E., Karimpour-Fard, A. and Martin, S.L. (2014) Metabolic changes associated with the long winter fast dominate the liver proteome in 13-lined ground squirrels. *Physiological Genomics*, 46(10) 348–361.
- Hofer, A. and Wenz, T. (2014) Post-translational modification of mitochondria as a novel mode of regulation. *Experimental Gerontology*, 56 202–220.
- Kirby, D.M., Thorburn, D.R., Turnbull, D.M. and Taylor, R.W. (2007) Biochemical assays of respiratory chain complex activity. *Methods in Cell Biology*, 80 93–119.
- Komelina, N.P., Polskaya, A.I. and Amerkhanov, Z.G. (2015) Artificial hypothermia in rats, unlike natural hibernation in ground squirrels *Spermophilus undulatus*, is not accompanied by the inhibition of respiration in liver mitochondria. *Biochemistry (Moscow) Supplement Series A: Membrane and Cell Biology*, 9(4) 293–302.
- Kuznetsov, A.V., Veksler, V., Gellerich, F.N., Saks, V., Margreiter, R. and Kunz, W.S. (2008) Analysis of mitochondrial function in situ in permeabilized muscle fibers, tissues and cells. *Nature Protocols*, 3(6) 965–976.
- Martin, A.W. and Fuhrman, F.A. (1955) The relationship between summated tissue respiration and metabolic rate in the mouse and dog. *Physiological Zoology*, 18–34.
- Mathers, K.E. and Staples, J.F. (2015) Saponin-permeabilization is not a viable alternative to isolated mitochondria for assessing oxidative metabolism in hibernation. *Biology Open*, 4(7) 858–864.
- Muleme, H.M., Walpole, A.C. and Staples, J.F. (2006) Mitochondrial metabolism in hibernation: Metabolic suppression, temperature effects, and substrate preferences. *Physiological and Biochemical Zoology*, 79(3) 474–483.
- Nelson, C.J., Otis, J.P., Martin, S.L. and Carey, H.V. (2009) Analysis of the hibernation cycle using LC-MS-based metabolomics in ground squirrel liver. *Physiological Genomics*, 37(1) 43–51.

- Ogura, M., Nakamura, Y., Tanaka, D., Zhuang, X., Fujita, Y., Obara, A., Hamasaki, A., Hosokawa, M. and Inagaki, N. (2010) Overexpression of SIRT5 confirms its involvement in deacetylation and activation of carbamoyl phosphate synthetase 1. *Biochemical and Biophysical Research Communications*, 393(1) 73–78.
- Park, J., Chen, Y., Tishkoff, D.X., Peng, C., Tan, M., Dai, L., Xie, Z., Zhang, Y., Zwaans, B.M.M., Skinner, M.E., Lombard, D.B. and Zhao, Y. (2013) SIRT5-mediated lysine desuccinylation impacts diverse metabolic pathways. *Molecular Cell*, 50(6) 919–930.
- Petit, P.X., O'Connor, J.E., Grunwald, D. and Brown, S.C. (1990) Analysis of the membrane potential of rat- and mouse-liver mitochondria by flow cytometry and possible applications. *European Journal of Biochemistry*, 194(2) 389–397.
- Rieske, J.S. (1967) Preparation and properties of reduced coenzyme Q-cytochrome c reductase (complex III of the respiratory chain). *Methods in Enzymology*, 10 239–245.
- Salvi, M., Brunati, A.M. and Toninello, A. (2005) Tyrosine phosphorylation in mitochondria: A new frontier in mitochondrial signaling. *Free Radical Biology and Medicine*, 38(10) 1267–1277.
- Staples, J.F. (2014) Metabolic suppression in mammalian hibernation: the role of mitochondria. *Journal of Experimental Biology*, 217(12) 2032–2036.
- Staples, J.F. and Brown, J.C. (2008) Mitochondrial metabolism in hibernation and daily torpor: a review. *Journal of Comparative Physiology B - Biochemical, Systems, and Environmental Physiology*, 178(7) 811–827.
- Takaki, M., Nakahara, H., Kawatani, Y., Utsumi, K. and Suga, H. (1997) No suppression of respiratory function of mitochondria isolated from the hearts of anesthetized rats with high-dose pentobarbital sodium. *The Japanese Journal of Physiology*, 47(1) 87–92.
- Vaughan, D.K., Gruber, A.R., Michalski, M.L., Seidling, J. and Schlink, S. (2006) Capture, care, and captive breeding of 13-lined ground squirrels, *Spermophilus tridecemlineatus*. *Lab Animal*, 35 33–40.

CHAPTER 3

3 Suppression of liver mitochondria during hibernation is reversed during saponin permeabilization

A version of this chapter has been previously published in *Biology Open*².

3.1 Introduction

Mitochondria transform chemical energy obtained from the environment into ATP that can be utilized by animal cells for development, growth, survival and reproduction. Many animals are periodically faced with environmental conditions that constrain the ability of mitochondria to fulfill this role. For example, seasonal changes in temperature, sunlight and water may limit the amount of energy available for animals. Reversible suppression of oxidative phosphorylation is a strategy used by many organisms to conserve energy under such natural environmental stresses. Understanding the mechanisms that underlie this mitochondrial metabolic suppression will offer insights into how these animals survive in extreme conditions, and this line of inquiry has been the focus of many recent studies (e.g., Galli and Richards, 2012). In addition, changes in mitochondrial metabolism contribute to many pathological conditions including myopathies (Kunz et al., 1993), neuropathies (Yao et al., 2009), and liver cirrhosis (Krähenbühl et al., 2000). For these reasons, accurate analysis of mitochondrial function is crucial for both basic and applied research.

Since at least 1955, oxidative metabolism has been assessed using mitochondria isolated from tissues by homogenization and differential centrifugation (Chance and Williams, 1955). For fibrous animal tissue (e.g. skeletal muscle), homogenization is often combined

² Mathers, K.E. and Staples, J.F. (2015). *Biology Open* 4:858-864.

with mild proteolytic digestion (e.g., Chance and Williams, 1955). Density gradient centrifugation can further purify these “crude” mitochondrial fractions, removing extra-mitochondrial components (Petit et al., 1990), improving resolution for techniques such as protein electrophoresis. These techniques have been helpful in characterizing many aspects of mitochondrial metabolism but, as pointed out by Kuznetsov et al. (2008) they have several limitations. Mitochondrial isolation involves mechanical homogenization, which may alter mitochondrial morphology and interactions with other cellular components (e.g., cytoskeleton, endoplasmic reticulum), and perhaps impact function. Some methods of mitochondrial isolation preferentially retain certain mitochondrial subpopulations (Krieger et al., 1980), potentially biasing results, especially when extrapolating conclusions to higher levels of organization. In addition, mitochondrial isolation requires substantial amounts of tissue, a costly refrigerated centrifuge and considerable amounts of time and skill. As a result of these limitations, many researchers (e.g. Kuznetsov et al., 2008) have opted recently to analyze mitochondrial function in permeabilized tissue slices.

Prior to permeabilization, tissues are gently disrupted mechanically, either by slicing or separation using fine forceps. Subsequently, tissues are incubated with steroid-containing compounds such as saponin. Because of its high affinity for cholesterol, saponin binds to cholesterol within plasma membranes, causing it to aggregate, thereby creating pores in the membrane (Kuznetsov et al. 2008). These pores allow diffusion of relatively small molecules (e.g., pyruvate, succinate, ADP) from the incubation medium to the mitochondria within otherwise intact cells. Because mitochondrial membranes contain much less cholesterol than the plasma membrane (reviewed by Yeagle, 1985), brief treatment with saponin should not uncouple mitochondrial substrate oxidation from ADP phosphorylation. In fact, an early study found that oxidative phosphorylation in saponin-permeabilized muscle fibers was almost identical to mitochondria isolated from the same tissue (Kunz et al., 1993). In addition, maximal respiration rates showed very good correspondence between the two techniques.

In recent years the use of saponin permeabilization has expanded greatly, and, in conjunction with high-resolution respirometry, has been used to analyze mitochondrial metabolism in skeletal (Casas et al., 2008) and cardiac muscle (Galli and Richards, 2012), gastric mucosa (Gruno et al., 2008), and brain tissue (Benani et al., 2009; Clerc and Polster, 2012). It is particularly useful for small organisms such as *Drosophila* (Pichaud et al., 2010), and small biopsies from larger animals, including humans (Brands et al., 2011). However, while “mechanical permeabilization” has been used to assess mitochondrial function in liver biopsies (Kuznetsov et al., 2002), to my knowledge, no study has used saponin or similar compounds to permeabilize liver tissue for mitochondrial studies. Therefore, the first goal of this study was to assess the utility of saponin permeabilization for analysis of liver mitochondrial metabolism. Similar to other tissues, mammalian liver mitochondria contain little cholesterol relative to phospholipid, so I predicted that brief incubation with saponin would cause minimal uncoupling of mitochondrial oxidative phosphorylation. I employed a similar strategy to Kunz et al. (1993) and compared small liver slices, permeabilized using saponin, with mitochondria isolated from the remaining liver tissue of the same animals.

A further goal of this study was to evaluate whether saponin permeabilization of liver is an appropriate technique for assessing mitochondrial metabolism during whole-animal metabolic states that are known to change the function of isolated mitochondria. Saponin permeabilization of rat brain has been used to assess mitochondrial function among some physiological conditions, such as fasting, that are known to alter whole-animal metabolism over fairly long time periods (Kuznetsov et al., 2008). However, this technique may not be appropriate for other tissues or conditions where metabolism changes acutely. For example, in cardiac muscle, the activities of some mitochondrial enzymes differ depending on whether they are assayed in isolated mitochondria or tissue biopsies (Phillips et al., 2012). Since hibernation involves acute metabolic changes, the mammalian hibernation model is well-suited to evaluate the utility of the saponin permeabilization technique for evaluating changes in liver mitochondrial metabolism.

Throughout the late autumn and winter, ground squirrels undergo bouts of torpor, characterized by low and constant body temperature (approximately 5 °C) and metabolic rate (<10% of euthermic rates) for several days. These bouts are spontaneously interrupted every 7-12 days by arousals, during which body temperature and metabolic rate rapidly increase over several hours. Once core body temperature reaches approximately 37 °C during an arousal, metabolic rate and body temperature stabilize for approximately 8 hours; a period referred to as interbout euthermia (IBE). IBE is followed by entrance into another bout of torpor when metabolic rate and body temperature decline again over a few hours. In 13-lined ground squirrels (*Ictidomys tridecemlineatus*), whole-animal metabolic rate decreases by over 90% in the short time it takes to enter a bout of torpor. This drop in whole-animal metabolism corresponds with a ~70% suppression of succinate-fueled state 3 respiration of isolated liver mitochondria, even when assayed at a constant *in vitro* temperature (37 °C) (Brown et al., 2012). In Chapter 2 I demonstrated that this suppression corresponds with suppression of ETS complexes I and II during torpor, and suggest that the underlying regulatory mechanism is differential phosphorylation. This natural model of metabolic plasticity allowed us to investigate the effectiveness of the saponin permeabilization technique for evaluating acute changes in liver mitochondrial function. I predicted that the large decreases in respiration rates seen in isolated mitochondria during torpor would be paralleled by respiration rates measured in saponin-permeabilized liver tissue.

3.2 Materials and Methods

3.2.1 Animals

Thirteen-lined ground squirrels (*Ictidomys tridecemlineatus*) were live-trapped and housed as described in section 2.2.1. Body temperature was continuously monitored over the hibernation season using surgically implanted radiotelemeters (section 2.2.2), and animals were sampled during torpor and IBE (section 2.2.3).

3.2.2 Permeabilization of Liver Tissue

My permeabilization technique incorporated saponin with a previously described mechanical disruption technique (Kuznetsov et al., 2002). Following euthanasia, a small (~100 mg) portion of the left liver lobe was transferred into ice cold isolation buffer (20 mM taurine, 20 mM imidazole, 0.5 mM DTT, 10 mM Ca²⁺EGTA, 5.77 mM ATP, 6.56 mM MgCl₂, 57.5 mM K⁺-MES, pH 7.0), while the rest of the liver was reserved for mitochondrial isolation. This buffer was modified from that used for permeabilization of mammalian brain (Benani et al., 2009) and muscle (Kuznetsov et al., 2008) by omitting phosphocreatine, as liver does not express creatine kinase (Meffert et al., 2005). The outer serosal capsule of the liver was removed, and the inner portion of the liver tissue was sliced into smaller portions of approximately 10 mg (~1 mm across) using a single-sided razor blade.

Liver tissue slices were placed individually into wells of 12-well plates containing 3 ml of ice-cold isolation buffer, covered and gently agitated (30 RPM) on ice using a metabolic shaker. Following 5 min of agitation, 2.5 µl of freshly prepared saponin (Sigma) solution (5 mg/ml isolation buffer) was added to each well. Following the addition of saponin, agitation continued for an additional 20 min. The concentration of saponin and exposure time were empirically optimized in preliminary experiments to yield the highest respiratory control ratio (state 3/state 4), and were similar to those used in the preparation of mammalian brain (Benani et al., 2009), cardiac muscle (Galli and Richards, 2012), and skeletal muscle (Casas et al., 2008). Following incubation with saponin, tissue slices were gently transferred to 3 ml of ice-cold mitochondrial respiration buffer (0.5 mM EGTA, 3 mM MgCl₂, 60 mM K-lactobionate, 20 mM taurine, 10 mM KH₂PO₄, 20 mM HEPES, 110 mM sucrose, 1 g/l fatty acid free BSA, pH 7.1; (Kuznetsov et al., 2008) and agitated for 5 min. This step was repeated twice more to remove any residual saponin. Tissue slices were then immediately used for assessment of mitochondrial respiration (see section 3.2.5).

3.2.3 Phosphatase/Deacetylase inhibitor incubations

To assess the possibility that regulatory PTMs undergo changes during permeabilization, separate liver tissue slices from each animal were simultaneously incubated under standard conditions and in the presence of phosphatase and deacetylase inhibitors. Phosphatase inhibitors (PI) and deacetylase inhibitors (DI) were added to isolation buffer prior to incubation with the following treatments: 1) Control, without any added phosphatase or deacetylase inhibitors, 2) +PI, with the addition of 1% (v/v) Phosphatase Inhibitor Cocktail 3 (Sigma), 3) +DI, with the addition of 1% (v/v) Deacetylase Inhibitor Cocktail (Santa Cruz Biotechnologies), and 4) +PI+DI, with the addition of 1% (v/v) Phosphatase Inhibitor Cocktail 3 and 1% Deacetylase Inhibitor Cocktail. Following incubation with saponin, rinses and respiration measurements were conducted identically between treatments.

3.2.4 Isolation of Mitochondria

The remainder of the liver (approximately 4 g) was used immediately for mitochondrial isolation and purification as described in Chapter 2.2.2. Following isolation, mitochondria were used immediately for assessment of mitochondrial respiration.

3.2.5 Respirometry

The wet mass of permeabilized liver slices was determined, following blotting on filter paper, using a microbalance (MX5, Mettler Toledo). Liver tissue slices were then transferred to chambers of an Oxygraph-2K high-resolution respirometer (Oroboros Instruments, Austria) containing 2 ml of mitochondrial respiration medium under constant stirring (750 rpm) at 37 °C. As in other permeabilized tissue preparations (Kuznetsov et al., 2008), the medium was rendered slightly hyperoxic (approximately 350 nmol/ml, 1.8-fold air saturation) to ensure adequate oxygen supply over the relatively large diffusion distances of tissue slices, compared with isolated mitochondria. Hyperoxygenation was achieved by injecting gaseous oxygen into the gas space above the medium within the chambers while stirring before the lids were closed, rendering the chambers airtight. Oxygen was replenished in the medium whenever the concentration

fell below approximately 200 nmol/ml to ensure that respiration was not limited by oxygen availability (Pesta and Gnaiger, 2012).

Separate slices of tissue from the same liver were used to assess respiration with pyruvate (10 mM), glutamate (30 mM; both with 4 mM malate) and succinate (30 mM, with 0.5 μ M rotenone in ethanol) as oxidative substrates. Succinate (30 mM with 0.5 μ M rotenone in ethanol) was used as an oxidative substrate to assess the effect of phosphatase and deacetylase inhibitors during permeabilization. These concentrations are similar to those used with other saponin-permeabilized tissue preparations (e.g., Benani et al., 2009) and yielded maximal rates in preliminary trials. Once a stable state 2 respiration was reached following substrate addition, ADP and Mg^{2+} (both 5 mM) were added to stimulate state 3 respiration. This high concentration of ADP is required to maximize state 3 over the relatively large diffusion distances of permeabilized tissue preparations (Kuznetsov et al., 2008). Such high ADP concentrations, along with the presence of ATPases in the permeabilized tissue preparations, preclude tissues from reaching true state 4 respiration; therefore, state 4 was estimated by the addition of oligomycin (160 μ g/ml in 95% ethanol). Liver slice respiration rates were expressed relative to wet weight.

Respiration of isolated liver mitochondria was determined at 37 °C in 2 ml of the mitochondrial respiration medium under constant stirring. The respiration medium was equilibrated with room air (approximately 190 nmol/ml) without hyperoxygenation. Respiration rates were determined with pyruvate (1 mM), glutamate (5 mM, both with 1 mM malate) and succinate (6 mM, with 0.5 μ M rotenone). State 3 was stimulated with 0.2 mM ADP. State 4 was approximated by addition of oligomycin. Unless stated otherwise, all added compounds were dissolved in mitochondrial respiration buffer. Examples of respiration measurements in both isolated mitochondria and permeabilized liver tissue are shown in Figure 3-1.

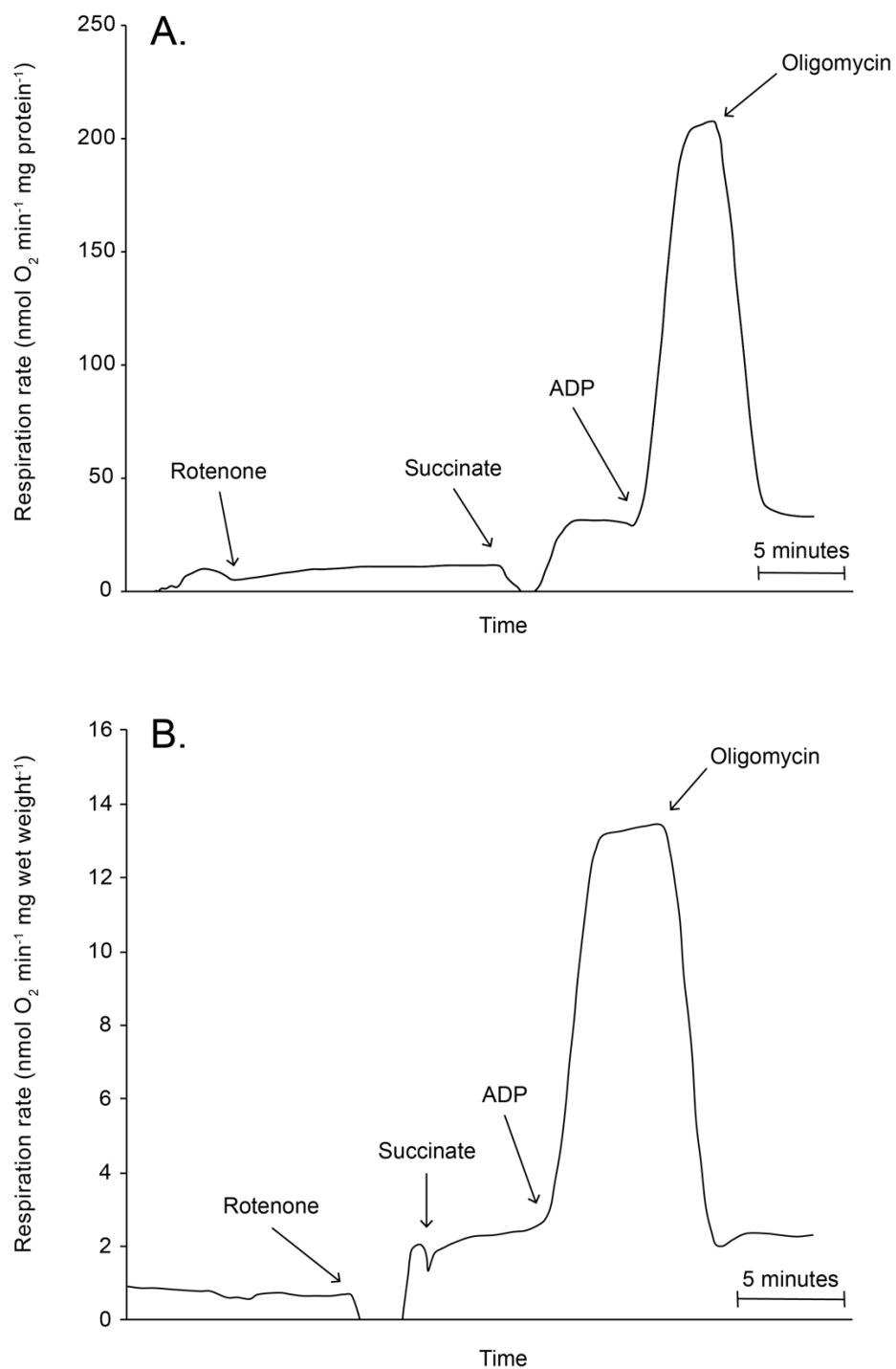


Figure 3-1. Representative traces showing succinate oxidation in isolated liver mitochondria (A) and permeabilized liver tissue (B) from the same animal. After stable basal rates were established, rotenone (0.5 μM) and succinate (30 μM) were injected, causing brief injection artifacts. After steady state 2 respiration rates were established, ADP (5 μM) was added to stimulate state 3 respiration. Oligomycin (160 $\mu\text{g/ml}$) was then added to estimate state 4 respiration.

3.2.8 Statistical analysis

All statistical analyses were conducted using R. For both isolated mitochondria and permeabilized tissue, one-tailed, unpaired t-tests were used to compare protein- and wet weight-standardized respiration rates, respectively, between torpor and IBE. Two-way ANOVA was used to compare respiration rates following phosphatase and deacetylase incubations between torpor and IBE. Since there was a significant effect of hibernation state on state 3 respiration rates in the phosphatase and deacetylation incubation experiment, one-tailed, unpaired t-tests were used to compare torpor and IBE within each treatment group. Differences were considered significant for p-values ≤ 0.05 .

3.3 Results

Permeabilized tissue and mitochondria isolated from IBE animals showed strong respiratory control, increasing respiration rate up to 6-fold upon addition of ADP when succinate was used as an oxidative substrate (Figure 3-1). The mass of tissue slices treated with saponin ranged from 4.0-12.1 mg, but mass-specific state 3 respiration rate was independent of tissue slice mass (Figure 3-2), indicating that the saponin treatment yielded similar effects across this mass range.

Succinate-fueled state 3 respiration of isolated mitochondria in torpor was suppressed by 65% when compared with IBE. This metabolic suppression was not reflected in saponin-permeabilized tissue taken from the livers of the same animals (Figure 3-3). State 3 respiration did not differ significantly between IBE and torpor in either permeabilized liver or isolated mitochondria when either glutamate or pyruvate was supplied as substrate (Table 3-1). There were no significant differences between state 4 rates during torpor and IBE for any of the substrates in either isolated mitochondria or permeabilized tissue (Table 3-1 and Figure 3-3).

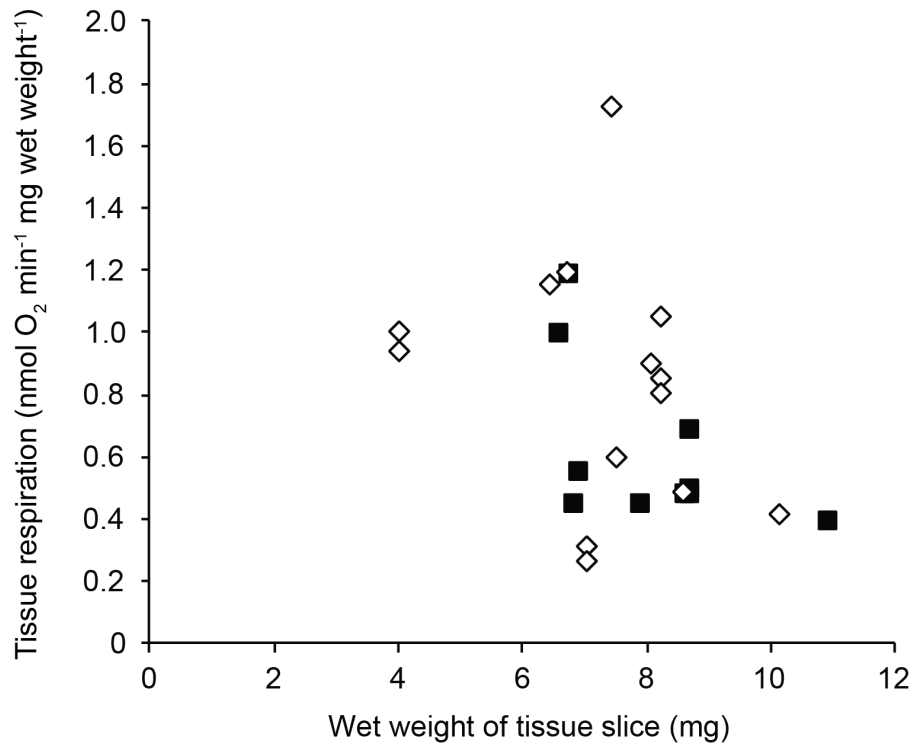


Figure 3-2. Succinate oxidation of permeabilized liver slices is independent of slice wet weight. Open diamonds represent samples from IBE squirrels (n=14) and filled squares indicate samples from torpid squirrels (n=10).

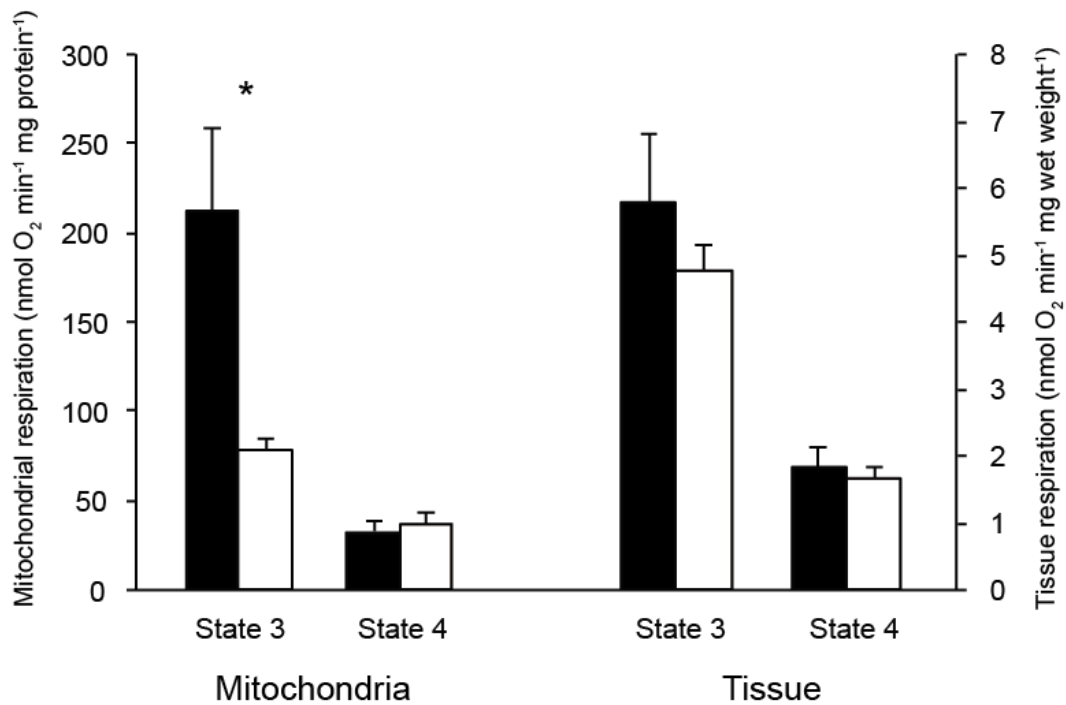


Figure 3-3. Succinate oxidation by isolated liver mitochondria and permeabilized liver tissue. Liver was taken from squirrels during IBE (black bars) and torpor (white bars). Both state 3 and state 4 rates are shown. Respiration rates of isolated mitochondria were standardized to protein concentration, and for permeabilized tissue respiration were standardized to wet weight. Values represent means \pm SE. Sample sizes for tissue slices are 5 (IBE) and 4 (torpor). Sample sizes for mitochondria are 5 (IBE) and 5 (torpor). Asterisk represents significant difference ($p \leq 0.05$).

Table 3-1. State 3 respiration rates of isolated mitochondria and permeabilized liver tissue. Respiration rates were measured in liver mitochondria and tissue from the same animals sampled during torpor and IBE. Rates were measured with glutamate and pyruvate as oxidative substrates, and were standardized to protein concentration (mitochondria) and wet weight (tissue). Data are presented as mean \pm SE. Sample sizes for tissue slices are 5 (IBE) and 4 (torpor). Sample sizes for mitochondria are 5 (IBE) and 5 (torpor).

		State 3 respiration		State 4 respiration	
		IBE	T	IBE	T
Mitochondria (nmol O ₂ min ⁻¹ mg protein ⁻¹)	Glutamate	28.84 \pm 6.73	22.87 \pm 6.06	9.31 \pm 2.43	16.67 \pm 3.58
	Pyruvate	19.52 \pm 4.23	15.24 \pm 3.80	10.10 \pm 2.52	16.63 \pm 13.93
Tissue (nmol O ₂ min ⁻¹ mg wet weight ⁻¹)	Glutamate	1.55 \pm 0.15	1.08 \pm 0.13	0.93 \pm 0.05	0.91 \pm 0.11
	Pyruvate	1.37 \pm 0.20	0.98 \pm 0.10	0.96 \pm 0.08	0.86 \pm 0.08

To further investigate the effect of the permeabilization process on respiration, I compared respiration between tissue permeabilized in the presence and absence of phosphatase inhibitors and deacetylase inhibitors, either alone or in combination. While there was no difference in the succinate-fueled state 3 rate between torpor and IBE without these inhibitors, the respiration rates were significantly lower during torpor when tissue was incubated with phosphatase inhibitors ($p=0.02$) and phosphatase and deacetylase inhibitors together ($p=0.05$; Figure 3-4). The difference between respiration rates for torpor and IBE tissue incubated with deacetylase inhibitors alone was not statistically significant ($p=0.08$).

3.4 Discussion

This study provides novel evidence that phosphorylation is critical for suppression of mitochondrial metabolism during torpor and that this phosphorylation and its suppressive effects can be rapidly reversed during permeabilization.

The first goal of this study was to assess how suitable saponin permeabilization is for studying mitochondrial metabolism in mammalian liver. In comparison with an earlier study using mechanically permeabilized pig liver (Kuznetsov et al., 2002), ground squirrel liver yielded state 3 respiration rates fueled by succinate that were slightly higher and respiratory control ratios (state 3/state 4) that were slightly lower. When supplied with oxidative substrates – especially succinate – permeabilized ground squirrel liver tissue displayed robust respiratory control, with rapid and substantial increases in oxygen consumption upon addition of ADP that were virtually eliminated upon addition of oligomycin (Figure 3-1B). I conclude, therefore, that permeabilization of liver tissue yields similar respiratory characteristics to isolated liver mitochondria.

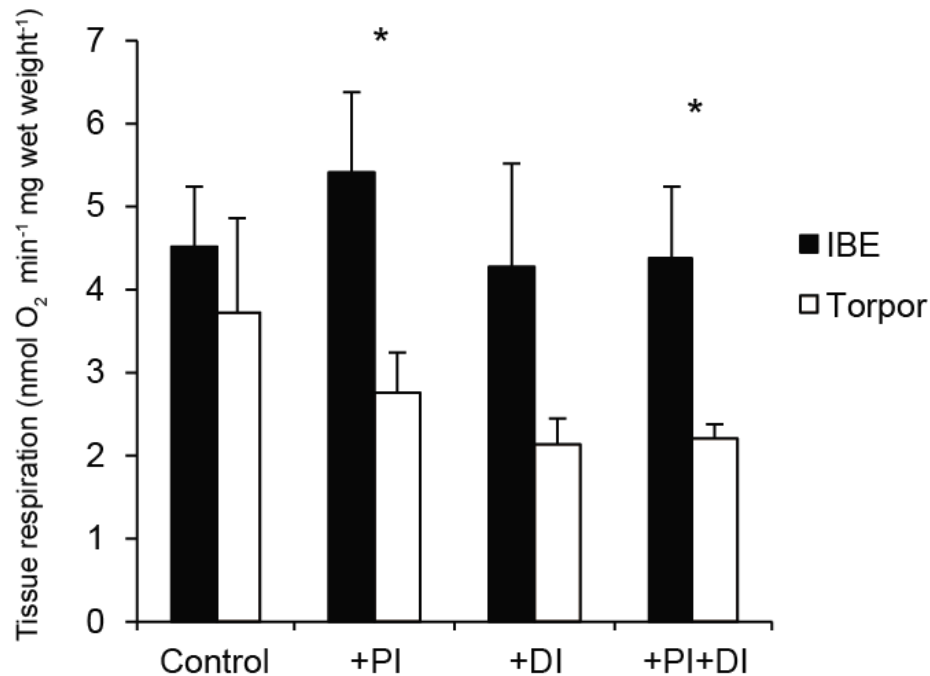


Figure 3-4. State 3 respiration rates with succinate in permeabilized liver tissue incubated with phosphatase and deacetylase inhibitors. Liver slices from ground squirrels sampled during IBE (n=5) and torpor (n=5) were permeabilized using saponin. During permeabilization samples of liver from the same animals were incubated without added inhibitors (control), with phosphatase inhibitors (+PI), with deacetylase inhibitors (+DI), and with both phosphatase and deacetylase inhibitors (+PI+DI). Bars represent means \pm SE. Within each treatment, asterisks indicate a significant difference ($p \leq 0.05$) between torpor and IBE.

The second goal of this study was to assess the utility of saponin permeabilization for evaluating mitochondrial metabolism in metabolic states that are known to change the metabolism of isolated mitochondria. Tissue permeabilization has previously been employed in rat brain tissue to assess mitochondrial function in relation to physiological conditions that affect whole-animal metabolism, such as fasting (Benani et al., 2009). In the current study, state 3 respiration rates, fueled by succinate, were 65% lower in mitochondria isolated from torpid animals compared with IBE. In permeabilized liver tissue from the same animal, there was no difference in respiration rate between torpor and IBE (Figure 3-3).

It is possible that these observed differences between isolated mitochondria and permeabilized tissue are due to changes that occur to mitochondria during the isolation process. A study comparing respiration between isolated mitochondria and permeabilized myofibers found that mitochondrial isolation causes dramatic changes in mitochondrial morphology and respiratory characteristics (Picard et al., 2011). Compared to permeabilized myofibers, isolated mitochondria showed a significantly higher respiration rates when complex IV was stimulated directly, suggesting that mitochondrial isolation leads to a loss of regulatory control of complex IV. When flux through complexes I-IV and II-IV was measured, however, maximal respiration rates were similar between the two methods. Since there is no evidence that mitochondrial isolation affects complex I and II activity, potential changes in mitochondrial morphology and regulatory properties during the isolation process are unlikely to explain the differences between isolated mitochondria and permeabilized tissue observed in the present study. Further, any morphological changes that may occur during mitochondrial isolation would likely have the same effect on mitochondria from torpid and IBE animals.

It is possible that that the observed differences between isolated mitochondria and permeabilized tissue were due to a reversal of regulatory mechanisms during the permeabilization process. Specifically, the lack of difference between torpor and IBE in permeabilized tissue may be due to a reversal of regulatory post-translational modifications. Post-translational modification (PTM) of proteins can be a powerful

regulator of mitochondrial metabolism (Hofer and Wenz, 2014), though its role in regulating mitochondrial metabolism during hibernation remains largely unexplored. My previous work suggests that PTMs may regulate changes in mitochondrial metabolism as ground squirrels transition between torpor and IBE, since the activities of complexes I and II rapidly change with no corresponding changes in protein content (Chapter 2).

To test the possibility that regulatory PTMs are reversed during the permeabilization process, I repeated the experiment, including treatments with phosphatase and deacetylase inhibitors during permeabilization in an attempt to preserve the phosphorylation and acetylation state of the mitochondrial proteins in question. In contrast to the treatment with no added inhibitors where there was no difference in state 3 respiration between torpor and IBE, permeabilization in the presence of phosphatase inhibitors yielded significant suppression during torpor compared to IBE (Figure 3-4), though to a slightly lesser degree (50% vs. 65%). The lower suppression in the permeabilized tissue may be due to kinases that were active during permeabilization, phosphorylating previously unphosphorylated proteins. It is also possible that regulatory mechanisms other than phosphorylation and acetylation are necessary for preserving the metabolic suppression in mitochondria from torpid animals.

These results suggest that phosphorylation is critical for the suppression of liver mitochondrial metabolism during torpor. It appears that during the standard permeabilization protocol, phosphorylation in mitochondria from torpid animals is reversed, diminishing the metabolic differences between torpor and IBE. In isolated mitochondria, these effects were observed when succinate was used a respiratory fuel, suggesting that the point of regulation is likely at ETS complex II, confirming results reported in Chapter 2. In human cells treated with phosphatases, complex II activity increased following the dephosphorylation of the flavoprotein subunit (Tomitsuka et al., 2009). Treatment with kinases caused phosphorylation of the flavoprotein subunit and a decrease in complex II activity, with evidence that the phosphorylated form of the enzyme catalyzes the reverse reaction (converting fumarate to succinate) (Tomitsuka et al., 2009). Given that phosphorylation of complex II is associated with suppression of its

activity, phosphorylation is a potential mechanism for regulating metabolic suppression during torpor.

It is possible that during the permeabilization process, since the mitochondria remain in a mostly intact cellular environment, extramitochondrial proteins and signaling pathways may influence changes in the phosphorylation state of mitochondrial proteins. Although mitochondrial isolation is a longer process than tissue permeabilization overall, mitochondria are quickly separated from other cellular components early in the process by homogenization and centrifugation. Since the regulation of mitochondrial phosphatases is not well understood, it is difficult to speculate how mitochondrial proteins may have been dephosphorylated in the permeabilized tissue from torpid animals. However, it is possible that the redox status would differ between isolated mitochondria and permeabilized tissue, a mechanism by which some phosphatases are regulated. For example, pyruvate dehydrogenase phosphatase is inhibited by high NADH/NAD⁺ ratios (Pettit et al., 1975). Other cytosolic changes, such as ATP/ADP ratios, free calcium, and pH, could feasibly change during the permeabilization process and influence the activity of mitochondrial phosphatases.

3.5 Summary

In summary, I found that saponin permeabilization of liver slices can result in preparations with robust mitochondrial respiratory control. On the other hand, when standard protocols are used, the metabolic suppression during torpor, seen in isolated liver mitochondria, is reversed during the permeabilization process. It is possible to preserve this suppression phenotype by including phosphatase inhibitors during permeabilization. I advise caution to researchers considering the use of tissue permeabilization for assessment of mitochondrial function, as my data show that appropriate inhibitors are necessary to preserve metabolic state when post-translational modifications are involved in regulation. This study has given unique insight into the regulatory mechanisms of liver mitochondrial suppression during hibernation, and in the next chapters, I will examine PTMs in liver mitochondria and their metabolic effects.

3.6 References

- Augereau, O., Claverol, S., Boudes, N., Basurko, M.-J., Bonneu, M., Rossignol, R., Mazat, J.-P., Letellier, T. and Dachary-Prigent, J. (2005) Identification of tyrosine-phosphorylated proteins of the mitochondrial oxidative phosphorylation machinery. *Cellular and Molecular Life Sciences*, 62(13) 1478–1488.
- Benani, A., Barquissau, V., Carnerio, L., Salin, B., Colombani, A.-L., Leloup, C., Casteilla, L., Rigoulet, M. and Pénicaud, L. (2009) Method for functional study of mitochondria in rat hypothalamus. *Journal of Neuroscience Methods*, 178 301–307.
- Brands, M., Hoeks, J., Sauerwein, H.P., Ackermans, M.T., Ouwens, M., Lammers, N.M., van der Plas, M.N., Schrauwen, P., Groen, A.K. and Serlie, M.J. (2011) Short-term increase of plasma free fatty acids does not interfere with intrinsic mitochondrial function in healthy young men. *Metabolism: Clinical and Experimental*, 60(10) 1398–1405.
- Brown, J.C.L., Chung, D.J., Belgrave, K.R. and Staples, J.F. (2012) Mitochondrial metabolic suppression and reactive oxygen species production in liver and skeletal muscle of hibernating thirteen-lined ground squirrels. *American Journal of Physiology - Regulatory, Integrative and Comparative Physiology*, 302(1) R15-28.
- Casas, F., Pessemeuse, L., Grandemange, S., Seyer, P., Gueguen, N., Baris, O., Lepourry, L., Cabello, G. and Wrutniak-Cabello, C. (2008) Overexpression of the mitochondrial T3 receptor p43 induces a shift in skeletal muscle fiber types. *PLoS One*, 3(6) e2501.
- Chance, B. and Williams, G. (1955) Respiratory enzymes in oxidative phosphorylation. *The Journal of Biological Chemistry*, 217 395–408.
- Clerc, P. and Polster, B.M. (2012) Investigation of mitochondrial dysfunction by sequential microplate-based respiration measurements from intact and permeabilized neurons. *PLoS One*, 7(4) e34465.
- Galli, G.L.J. and Richards, J.G. (2012) The effect of temperature on mitochondrial respiration in permeabilized cardiac fibres from the freshwater turtle, *Trachemys scripta*. *Journal of Thermal Biology*, 37 195–200.
- Gruno, M., Peet, N., Tein, A., Salupere, R., Sirotkina, M., Valle, J., Peetsalu, A. and Seppet, E.K. (2008) Atrophic gastritis: deficient complex I of the respiratory chain in the mitochondria of corpus mucosal cells. *Journal of Gastroenterology*, 43(10) 780–788.
- Hofer, A. and Wenz, T. (2014) Post-translational modification of mitochondria as a novel mode of regulation. *Experimental Gerontology*, 56 202–220.

- Krähenbühl, L., Ledermann, M., Lang, C. and Krähenbühl, S. (2000) Relationship between hepatic mitochondrial functions in vivo and in vitro in rats with carbon tetrachloride-induced liver cirrhosis. *Journal of Hepatology*, 33(2) 216–223.
- Krieger, D.A., Tate, C.A., McMillin-Wood, J. and Booth, F.W. (1980) Populations of rat skeletal muscle mitochondria after exercise and immobilization. *Journal of Applied Physiology: Respiratory, Environmental and Exercise Physiology*, 48(1) 23–28.
- Kunz, W.S., Kuznetsov, A. V., Schulze, W., Eichhorn, K., Schild, L., Striggow, F., Bohnensack, R., Neuhof, S., Grasshoff, H., Neumann, H.W. and Gellerich, F.N. (1993) Functional characterization of mitochondrial oxidative phosphorylation in saponin-skinned human muscle fibers. *Biochimica et Biophysica Acta*, 1144 46–53.
- Kuznetsov, A. V., Strobl, D., Ruttman, E., Königsrainer, A., Margreiter, R. and Gnaiger, E. (2002) Evaluation of mitochondrial respiratory function in small biopsies of liver. *Analytical Biochemistry*, 305 186–194.
- Kuznetsov, A.V., Veksler, V., Gellerich, F.N., Saks, V., Margreiter, R. and Kunz, W.S. (2008) Analysis of mitochondrial function in situ in permeabilized muscle fibers, tissues and cells. *Nature Protocols*, 3(6) 965–976.
- Meffert, G., Gellerich, F.N., Margreiter, R. and Wyss, M. (2005) Elevated creatine kinase activity in primary hepatocellular carcinoma. *BMC Gastroenterology*, 5 9.
- Nath, A.K., Ryu, J.H., Jin, Y.N., Roberts, L.D., Dejam, A., Gerszten, R.E. and Peterson, R.T. (2015) PTPMT1 inhibition lowers glucose through phosphorylation of SDH. *Cell Reports*, 10(5) 694–701.
- Ogura, M., Nakamura, Y., Tanaka, D., Zhuang, X., Fujita, Y., Obara, A., Hamasaki, A., Hosokawa, M. and Inagaki, N. (2010) Overexpression of SIRT5 confirms its involvement in deacetylation and activation of carbamoyl phosphate synthetase 1. *Biochemical and Biophysical Research Communications*, 393(1) 73–78.
- Pagliarini, D.J., Wiley, S.E., Kimple, M.E., Dixon, J.R., Kelly, P., Worby, C.A., Casey, P.J. and Dixon, J.E. (2005) Involvement of a mitochondrial phosphatase in the regulation of ATP production and insulin secretion in pancreatic β cells. *Molecular Cell*, 19(2) 197–207.
- Pesta, D. and Gnaiger, E. (2012) High-resolution respirometry: OXPHOS protocols for human cells and permeabilized fibers from small biopsies of human muscle. *Methods in Molecular Biology*, 810 25–58.
- Petit, P.X., O'Connor, J.E., Grunwald, D. and Brown, S.C. (1990) Analysis of the membrane potential of rat- and mouse-liver mitochondria by flow cytometry and possible applications. *European Journal of Biochemistry*, 194(2) 389–397.

- Pettit, F.H., Pelley, J.W. and Reed, L.J. (1975) Regulation of pyruvate dehydrogenase kinase and phosphatase by acetyl-CoA/CoA and NADH/NAD ratios. *Biochemical and Biophysical Research Communications*, 65(2) 575–582.
- Phillips, D., Covian, R., Aponte, A.M., Glancy, B., Taylor, J.F., Chess, D. and Balaban, R.S. (2012) Regulation of oxidative phosphorylation complex activity: effects of tissue-specific metabolic stress within an allometric series and acute changes in workload. *American Journal of Physiology - Regulatory, Integrative and Comparative Physiology*, 302(9) R1034-1048.
- Picard, M., Taivassalo, T., Ritchie, D., Wright, K.J., Thomas, M.M., Romestaing, C. and Hepple, R.T. (2011) Mitochondrial structure and function Are disrupted by standard isolation methods. *PLoS One*, 6(3) e18317.
- Pichaud, N., Hébert-Chatelain, E., Ballard, J.W.O., Tanguay, R., Morrow, G. and Blier, P.U. (2010) Thermal sensitivity of mitochondrial metabolism in two distinct mitotypes of *Drosophila simulans*: evaluation of mitochondrial plasticity. *Journal of Experimental Biology*, 213 1665–1675.
- Salvi, M., Brunati, A.M. and Toninello, A. (2005) Tyrosine phosphorylation in mitochondria: A new frontier in mitochondrial signaling. *Free Radical Biology and Medicine*, 38(10) 1267–1277.
- Tomitsuka, E., Kita, K. and Esumi, H. (2009) Regulation of succinate-ubiquinone reductase and fumarate reductase activities in human complex II by phosphorylation of its flavoprotein subunit. *Proceedings of the Japan Academy, Series B*, 85(7) 258–265.
- Yao, J., Irwin, R.W., Zhao, L., Nilsen, J., Hamilton, R.T. and Brinton, R.D. (2009) Mitochondrial bioenergetic deficit precedes Alzheimer's pathology in female mouse model of Alzheimer's disease. *Proceedings of the National Academy of Sciences of the United States of America*, 106(34) 14670–14675.
- Yeagle, P.L. (1985) Cholesterol and the cell membrane. *Biochimica et Biophysica Acta*, 822(3–4) 267–287.

CHAPTER 4

4 Post-translational modification of liver mitochondrial proteins during hibernation

4.1 Introduction

During hibernation, an animal's body temperature and metabolic rate are actively suppressed to conserve energy from late autumn to spring, when cold ambient temperatures and low food availability present a potential metabolic stress. In animals such as the 13-lined ground squirrel (*Ictidomys tridecemlineatus*), hibernation is characterized by a cycle between torpor and interbout euthermia (IBE; described in detail in section 1.2.2). Much of the whole-animal metabolic suppression involves reducing thermogenic metabolism through a decrease in the lower level of the thermoneutral zone (Snapp and Heller, 1981). Metabolism in non-thermogenic tissues (e.g. liver) is also suppressed actively, rather than through passive thermal effects, and whole-animal metabolism declines before body temperature falls during entrance into torpor. The mechanisms underlying this suppression are not fully understood, but the speed at which the transitions between torpor and IBE occur (4-6 hours), the large change in body temperature between the two states (approximately 4 °C and 37 °C, respectively), and the pattern of change in mitochondrial metabolism in relation to body temperature offers some clues.

Mitochondria are key for understanding metabolic suppression as they are responsible for the majority of aerobic ATP generation. In 13-lined ground squirrels, respiration in liver mitochondria (phosphorylating “state 3” respiration measured at 37 °C with succinate as a substrate) has consistently been shown to be suppressed by up to 70% during torpor (Muleme et al., 2006; Armstrong and Staples, 2010; Brown et al., 2012). This effect is also seen in other hibernating ground squirrels (Barger et al., 2003) as well as hamsters

(*Mesocricetus auratus*) (Roberts and Chaffee, 1972). In 13-lined ground squirrels, maximal suppression of liver mitochondrial respiration occurs before body temperature decreases as squirrels enter torpor (Chung et al., 2011). In Chapter 2, I demonstrated that suppression of liver mitochondrial metabolism corresponds with suppression of flux through ETS complexes I-IV and II-IV, as well as a reduction in the maximal activity of both complexes I and II. That these changes occur when body temperature is fairly high and are independent of changes in protein content suggests that enzyme-catalyzed post-translational modification is a likely a regulatory factor. In Chapter 3 I provided evidence that phosphorylation is important for maintaining metabolic suppression during torpor.

Protein phosphorylation mediates important metabolic changes associated with hibernation, especially regulating a shift of fuel use away from carbohydrate and toward lipid. For example, phosphorylation of pyruvate dehydrogenase during hibernation renders the enzyme 96% inactive, a likely mechanism for reducing the rate of glycolysis (Brooks and Storey, 1992). Little is known about post-translation modification of other mitochondrial proteins in hibernators. Several types of post-translational modification, including phosphorylation, acetylation, and succinylation, can play a complex role in regulating mitochondrial metabolism (reviewed by Hofer and Wenz, 2014). For example, several phosphorylation sites have been identified on complex I; some are associated with increased activity of the enzyme (Papa et al., 1996; Augereau et al., 2005; Ogura et al., 2012), whereas other sites are associated with decreased activity (Hébert-Chatelain et al., 2011). Though many seasonal differences have been documented, the role of post-translational modification in regulating the metabolic changes between torpor and IBE has only recently been explored.

A large-scale study of the liver proteome in 13-lined ground squirrels found few differences in levels of metabolic proteins and minimal differences in phosphorylation and acetylation between torpor and IBE (Hindle et al., 2014). This study examined the proteome of the whole liver tissue however, so it is possible that the proteomics methods lacked the resolution required to detect subtle changes in mitochondrial proteins that account for only a small fraction of total liver protein. In rat hepatocytes, mitochondria

account for only 7-19% of total cell volume (Quinlan et al., 1983), though, to my knowledge the proportion of cellular protein accounted for by mitochondrial proteins is not known

In this Chapter I investigated changes in the liver mitochondrial proteome between torpor and IBE to identify possible sites of metabolic regulation. I used two-dimensional differential gel electrophoresis (2D-DiGE), a powerful technique that allows the identification of proteins that differ in abundance or isoelectric point (an indicator of PTM) between two conditions. I used subsequent staining and immunoblots to identify proteins that differed in phosphorylation or acetylation state between torpor and IBE. I also used Blue-Native polyacrylamide gel electrophoresis (BN-PAGE), to examine ETS proteins that differed in phosphorylation or acetylation state between torpor and IBE.

4.2 Materials and Methods

4.2.1 Animals

13-lined ground squirrels were live-trapped, housed, and euthanized as described in Chapter 2.2.1. For this study, animals were sampled either during torpor (a stable body temperature of ~ 5 °C for 3-5 days) or during IBE (a stable body temperature of ~ 37 °C for 4-6 hours following spontaneous arousal).

4.2.2 Mitochondrial isolation

Liver mitochondria were isolated by differential centrifugation and purified via Percoll gradient centrifugation as described in Chapter 2.2.2. Following isolation, mitochondrial protein was quantified for each preparation via Bradford assay using BSA dissolved in homogenization buffer as standards. Aliquots containing 0.5 mg mitochondrial protein were centrifuged at 10,000 g for 10 min and stored at -80 °C until used in gel electrophoresis.

4.2.3 Purification and solubilization of mitochondrial proteins

Mitochondrial protein was precipitated via a trichloroacetic acid (TCA)/acetone cleanup protocol to remove contaminants such as salts, nucleic acids, and lipids, which can interfere with 2D electrophoresis (Jiang et al., 2004). Mitochondrial pellets (0.5 mg protein) were solubilized in 500 μ l lysis buffer (7 M urea, 2 M thiourea, 30 mM Tris, 4% (w/v) CHAPS). One volume (500 μ l) of 40% (v/v) TCA was added and samples were incubated at -20 °C for 30 min. Samples were centrifuged at 10,000 g for 10 min at 4 °C. Following centrifugation, the supernatant was discarded, and pellets were resuspended in 750 μ l ice-cold acetone. The centrifugation and acetone wash step was repeated two more times to remove residual TCA from protein samples. Acetone was then removed by aspiration and protein pellets were air-dried at room temperature for 3 min. Lysis buffer (100 μ l) was added to each protein pellet, and samples were incubated on ice for 10 min following vortexing. Samples were centrifuged at 13,000 g for 10 min, and the supernatant (containing solubilized protein) was collected. Protein was quantified using a detergent compatible (DC) protein assay (Bio-Rad) using BSA dissolved in lysis buffer as protein standards and, following quantification, samples were diluted to a concentration of 2 mg/ml in lysis buffer for use in two-dimensional electrophoresis.

4.2.4 Two-dimensional differential gel electrophoresis (2D DiGE)

Two-dimensional electrophoresis (2DE) involves separating proteins first by isoelectric point (the first dimension), then by molecular mass (the second dimension). This allows better separation of individual peptides than traditional SDS-PAGE, which separates proteins solely by molecular mass. In 2D differential gel electrophoresis (DiGE), lysine groups on proteins are labeled with covalently linked cyanine fluorescent dyes (Cy dyes) prior to 2D electrophoresis. From the two experimental conditions being compared equal amounts of protein are labeled with Cy3 and Cy5 dyes, which fluoresce at excitation/emission wavelengths of 550/570 and 650/670 nm, respectively. A separate dye, Cy2, which fluoresces at 492/510 nm, is used to label an internal standard consisting of a pooled sample made of equal amounts of protein from all experimental animals. The

three labeled protein samples are then electrophoresed together on one gel. Including the same internal standard in each gel allows quantitative comparisons of all proteins within a single gel as well as comparisons of individual proteins among gels. A summary of the methods used for 2D DiGE experiments and subsequent protein identification is shown in Figure 4-1.

4.2.4.1 Labelling with CyDyes

Solubilized liver mitochondrial protein (as described in section 4.2.3) were labeled with CyDye DiGE Fluor minimal dyes according to manufacturer specifications (GE Healthcare). Torpor and IBE protein samples were randomly selected and paired for each DiGE gel. Subsequently, 50 µg of each protein sample was labeled separately with 200 pmol of CyDye (Cy3 or Cy5) dissolved in 99.8% dimethylformamide and incubated at 0 °C in the dark for 30 min. To preclude any possible dye binding bias, Cy3 and Cy5 were alternated between torpor and IBE protein samples. Internal standards, comprised of an equal mixture of all protein samples, were labelled with Cy2. The labelling reaction was stopped by the addition of 1 µl of 10 mM L-lysine and incubated on ice for 10 min. After labeling, equal amounts of protein from one torpor sample, one IBE sample, and the internal standard were combined, and 100 µg of total protein was electrophoresed together in a single 2D DiGE procedure.

4.2.4.2 Two-dimensional electrophoresis (2DE)

Combined mitochondrial samples labelled with CyDyes were added to rehydration buffer (7 M urea, 2 M thiourea, 2% (w/v) CHAPS, 0.002% (w/v) bromophenol blue), 2.5 µl dithiothreitol (DTT), 1.5 µl IPG ampholyte, and 1.5 µl DeStreak (GE Healthcare) to a volume of 125 µl and applied to immobilized pH gradient (IPG) strips (7 cm, pH 3-10, Bio-Rad). Strips were passively (i.e. with no electrical current) rehydrated at room temperature overnight before isoelectric focusing (IEF). IEF was performed using a GE Ettan IPGphor 3 system (GE Healthcare) at 20°C with the following protocol: 500 V for 1 hr, 1000 V for 1 hr, 6000 V for 2 hr, then 6000 V for 7700 Vhr. Following IEF, IPG strips were transferred to equilibration buffer (50 mM Tris, 6 M urea, 40% (v/v) glycerol, 2% (w/v) SDS, 0.001% bromophenol blue, pH 8.0) first with 10 mM DTT for 15 min

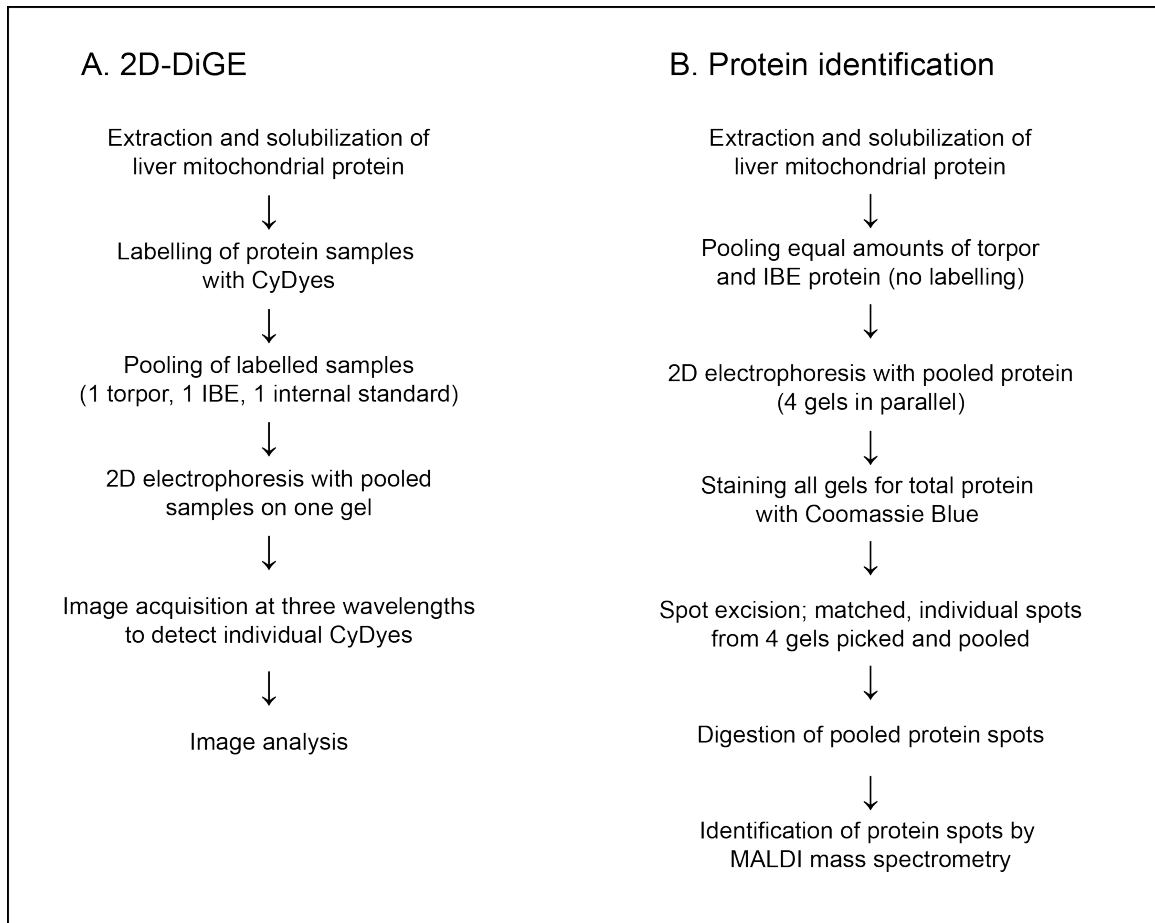


Figure 4-1. A summary of two-dimensional differential gel electrophoresis (2D DiGE) experimental methods. 2D DiGE was used to assess differences in the liver mitochondrial proteome between torpor and IBE (A), and subsequently, proteins that differed between the two states were identified by MALDI mass spectrometry (B).

then with 55 mM iodoacetamide for a further 15 min at room temperature. Strips were then placed horizontally on top of a 10% polyacrylamide resolving gel and sealed into place using warm agarose (1% wt/vol). Gels were electrophoresed at 100V for 2 hr in SDS-PAGE running buffer (25 mM Tris, 192 mM glycine, 0.1% (w/v) SDS).

4.2.4.3 Image acquisition and analysis

Following 2D electrophoresis, DiGE gels were immediately scanned using VersaDoc MP5000 Molecular Imager (Bio-Rad). Each gel gave three images, one corresponding to each CyDye. Cy2 images were collected using a Blue LED light source with a 530BP28 filter and excitation/emission wavelengths of 492/510 nm. Cy3 images were collected using Green LED light source with a 605BP35 filter and excitation/emission wavelengths of 550/570 nm. Cy5 images were collected using a Red LED light source with a 695BP55 filter and excitation/emission wavelengths of 650/670 nm. Images were exported for subsequent analysis with DeCyder Differential Analysis software (Amersham Biosciences, version 5.0). This software contains two modules: a differential in-gel analysis (DIA) module and a biological variance analysis (BVA) module. The DIA module is used to detect spots and calculate abundances for the three dyes (Cy2, Cy3, and Cy5) within one gel, and normalizes spots to the internal standard to allow comparison among gels. The BVA module aligns and matches spots across all gel images, which allows statistical analysis of changes in intensity of individual spots between samples. Protein spots localized at the same position in different gels were matched, and a total of 107 protein spots were matched across all gels, indicating that they were present in all samples. A two-tailed Student's t-test was used to compare average standardized intensity of each matched protein spot between torpor and IBE. Spots that showed significant differences were selected as spots of interest for protein identification if they differed by at least 1.4-fold. Other selected spots that showed visual reciprocal abundance patterns were also included for protein identification.

4.2.5 Spot excision and digestion

In parallel with each 2D DiGE gel, I also ran four identical preparative 2D gels for the purpose of spot excision for subsequent protein identification. For these gels, equal

amounts of liver mitochondrial protein from torpor and IBE individuals were pooled (100 µg total) and run together on each gel, using the same methods as described in section 4.2.4.2, but without labelling with CyDyes. Following electrophoresis, proteins within the gels were stained with Coomassie Blue R-250. Individual spots on these preparative gels were matched to the spots of interest identified from DiGE gels (section 4.2.4.3). Spots of interest were excised using an Ettan spot picker (GE Healthcare), with individual spots excised from each of the four preparative gels and pooled in order to maximize protein yield. In-gel digestion was performed as outlined by (Rosenfeld et al., 1992). Spot excision and in-gel digestion were performed at the UWO Functional Proteomics Facility (London, ON). I performed the spot picking myself, and the in-gel digestion was performed by the UWO Functional Proteomics Facility.

Gel pieces from picked protein spots were washed with 50% (v/v) acetonitrile and rehydrated with 100 mM NH₄HCO₃. Following washing, samples were treated with 50 mM DTT at 56 °C for 45 min in the dark to reduce cysteine residues, followed by treatment with 200 mM iodoacetamide at 25 °C for 30 min in the dark to alkylate proteins. Samples were washed again with 50% (v/v) acetonitrile and rehydrated with 100 mM NH₄HCO₃. Proteins were digested overnight at 37 °C with trypsin (12.5 ng/µl, Promega) in digestion buffer (25 mM NH₄HCO₃ pH 7.8, 2.5 mM NaCl₂). Following digestion, samples were washed first with 50% (v/v) acetonitrile, then 25 mM NH₄HCO₃, and finally a 50% (v/v) acetonitrile, 5% (v/v) formic acid solution, with extraction of supernatant following each wash. Prior to mass spectrometry, digested peptide samples were dissolved in a solution of 10% (v/v) acetonitrile and 0.1% (v/v) trifluoroacetic acid.

4.2.6 Protein identification by MALDI mass spectrometry

Following digestion, protein samples were submitted for matrix-assisted laser desorption/ionization-time of flight mass spectrometry (MALDI-TOF/TOF MS) analysis of peptide sequences by the UWO Functional Proteomics Lab (London, ON). Mass spectrometry was performed using a 4700 Proteomics Analyzer (Applied Biosystems) equipped with a 355 nm Nd:YAG laser with a laser rate of 200 Hz. Peptide sequences obtained from MALDI-TOF/TOF MS analysis were submitted to the NCBI

database from comparison with known protein sequences. For each peptide sequence, the alignment between sample peptides and known peptides was used to assign a protein score confidence interval, with a higher value indicating greater alignment.

4.2.7 Phosphoprotein staining of 2D gels

I also used 2D gels to identify any differences in phosphorylation of mitochondrial proteins between torpor and IBE. The fluorescent Pro-Q Diamond Phosphoprotein Gel Stain (ThermoFisher Scientific) binds to phosphate groups attached to serine, threonine, and tyrosine residues with a detection limit of 1-15 ng of phosphoprotein. A summary of the experimental methods used for determination of total phosphorylated protein is shown in Figure 4-2.

4.2.7.1 2D Electrophoresis

Following solubilization, samples of liver mitochondrial protein (100 µg) were used for 2D electrophoresis. In contrast to DiGE, in which protein samples from torpor and IBE individuals were labelled with CyDyes and run together on the same gel, only one sample was run per gel and protein was not labelled prior to electrophoresis. 2D electrophoresis was performed as described in section 4.2.4.2. As a positive control for phosphorylation, 7 µl of PeppermintStick phosphoprotein molecular weight standards (ThermoFisher Scientific), blotted on a small piece of filter paper, was included in the second dimension.

4.2.7.2 Phosphoprotein stain

Following 2D electrophoresis, gels were incubated overnight in a fixing solution (50% (v/v) methanol then washed with doubly distilled water three times for 10 min under gentle agitation. Gels were then stained with 60 ml Pro-Q Diamond Phosphoprotein Gel Stain (ThermoFisher Scientific) for exactly 90 minutes under gentle agitation in the dark. Following staining, gels were incubated with a destaining solution (20% acetonitrile, 50 mM sodium acetate, pH 4.0) for 90 mins. Gels were washed three times with doubly distilled water prior to imaging.

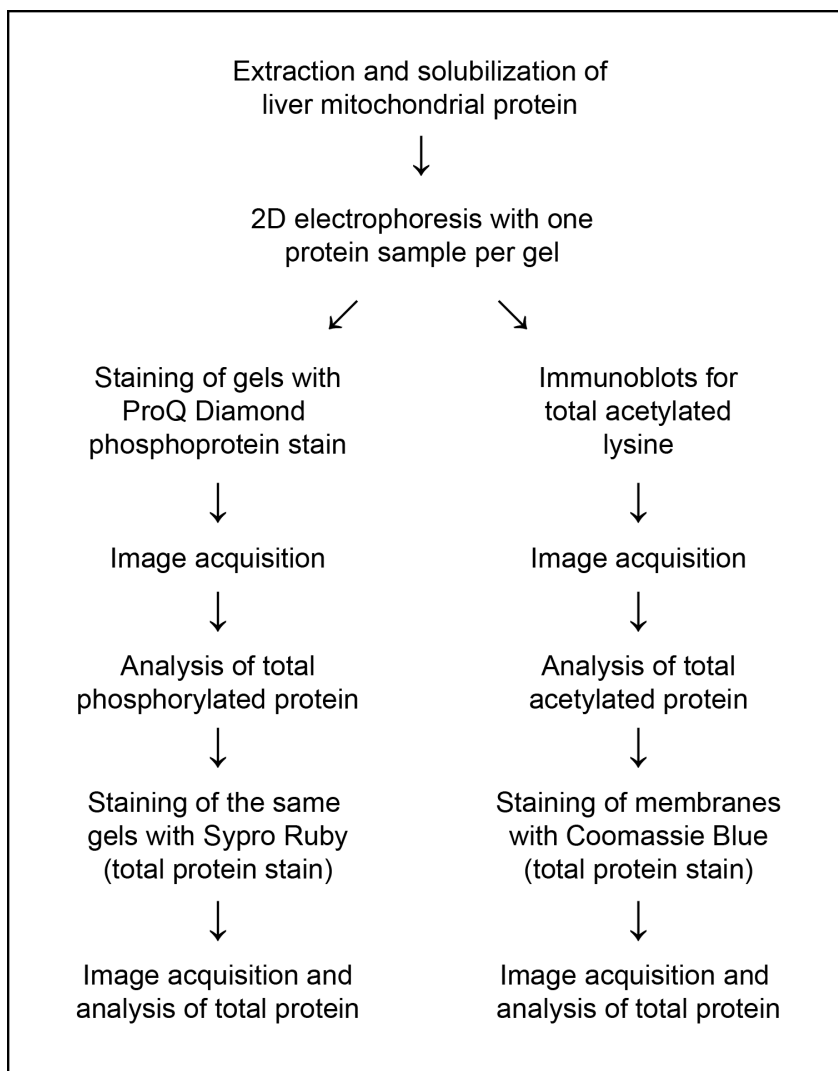


Figure 4-2. A summary of experimental methods used to determine total phosphorylation and acetylation of liver mitochondrial protein separated by 2D electrophoresis.

4.2.7.3 Sypro Ruby staining for total protein

Following phosphoprotein staining and imaging (described below), 2D gels were stained with Sypro Ruby Protein Gel Stain (ThermoFisher Scientific) to quantify total protein. Gels were incubated with 60 ml Sypro Ruby overnight under gentle agitation. Following staining, gels were incubating in a washing solution (10% methanol, 7% acetic acid) for 30 min and washed three times with doubly distilled water prior to imaging.

4.2.7.4 Image acquisition and analysis

Images of phosphopostained gels were acquired using a VersaDoc MP5000 imaging system. Images were scanned at the excitation and emission wavelengths for ProQ Diamond (530 and 575 nm, respectively) using green LED as a light source with a 605BP35 filter. Total loaded protein, as quantified by staining with Sypro Ruby (imaged using a trans UV light source with a 605BP35 filter at 302/470 nm), did not differ significantly ($p > 0.05$) among gels. Differences in phosphorylation of individual protein spots between torpor and IBE were analyzed using DeCyder software. The biological variance module (BVA) was used to align spots across all gel images and analyze changes in intensity of individual spots between samples. A two-tailed Student's t-test was used to compare average standardized intensity of each matched protein spot between torpor and IBE. Spots that showed significant differences were selected as spots of interest for protein identification if they differed by at least 1.4-fold.

4.2.8 Immunoblots for acetylated lysine

Immunoblots were conducted following 2D electrophoresis to assess any differences in acetylation of liver mitochondrial proteins between torpor and IBE. A summary of the experimental methods used for determination of total acetylated protein is shown in Figure 4-2.

4.2.8.1 2D Electrophoresis

2D electrophoresis was conducted as described in section 4.2.4.2 with one liver mitochondrial protein sample (100 µg) per gel. 7 µl of protein molecular weight standard (PrecisionPlus Protein Dual Color Standards, Bio-Rad) was added to a small piece of filter paper and included in the second dimension.

4.2.8.2 Protein transfer and immunodetection

Following 2D electrophoresis, proteins were transferred to polyvinylidene fluoride (PVDF) membranes (0.2 µm pore diameter, Bio-Rad) using a Mini-PROTEAN Tetra Cell system (Bio-Rad). Proteins were transferred under constant voltage (100V) at 4 °C for 1 hr in transfer buffer (25 mM Tris, 192 mM glycine, 20% (v/v) methanol). Following transfer, membranes were blocked for 2 hr with 5% (w/v) BSA in Tris-buffered saline with Tween 20 (TBST; 20 mM Tris, pH 7.5, 150 mM NaCl, 0.1% (v/v) Tween 20). Membranes were probed with Acetylated-Lysine primary antibody (Cell Signalling Technologies, #9441; rabbit) diluted to 1:1000 in TBST with 5% (w/v) BSA. Membranes were incubated with the primary antibody overnight at 4 °C on an orbital shaker at 300 rpm. After four 10 min washes with TBST, membranes were incubated with a goat anti-rabbit secondary antibody (Cell Signalling Technologies, #7074) diluted to 1:2000 in TBST. Membranes were incubated with the secondary antibody for 1 hr under constant agitation, and rinsed with TBST prior to image acquisition.

4.2.8.3 Image acquisition and analysis

2D immunoblots were visualized via Luminata Forte Western Horseradish Peroxidase (HRP) substrate (Millipore) using a VersaDoc MP5000 imaging system (Bio-Rad). Total loaded protein, as quantified by staining with Coomassie Blue, did not differ significantly ($p > 0.05$) among gels. Differences in protein acetylation between torpor and IBE were analyzed using DeCyder software. The biological variance module (BVA) was used to align spots across all gel images and analyze changes in intensity of individual spots between samples. A two-tailed Student's t-test was used to compare average standardized intensity of each matched protein spot between torpor and IBE. Spots that showed

significant differences were selected as spots of interest for protein identification if they differed by at least 1.4-fold.

4.2.9 2D Blue-native PAGE

While conventional 2D electrophoresis is suitable for resolving most mitochondrial proteins, it is poor at resolving membrane-bound proteins such as the mitochondrial ETS complexes. Since many of these proteins contain hydrophobic regions, they tend to aggregate and precipitate at the basic end of the IPG strip leading to poor resolution (Bailey et al., 2005). To overcome this technical constraint, I used Blue-Native PAGE to analyze the ETS subproteome within liver mitochondria from torpid and IBE ground squirrels. In this technique, first described by Schagger and von Jagow (1991), Coomassie Blue dye is used as a charge-shift molecule instead of SDS, which allows separation of protein complexes in their native state. Following native separation, proteins can be further resolved in a second denaturing dimension, separating individual peptides based on molecular weight. A summary of the Blue-Native PAGE experimental methods is shown in Figure 4-3.

4.2.9.1 Protein solubilization

Mitochondrial pellets (0.5 mg) were solubilized in 50 μ l mitochondrial extraction buffer (0.75 M aminocaproic acid, 50 mM bis-tris, pH 7.0) with 25 μ l 10% (w/v) lauryl maltoside and incubated on ice under gentle shaking for 30 min. Samples were then centrifuged at 21,000 *g* for 20 min at 4 °C and combined with BN-PAGE sample buffer (200 mM bis-tris, 40% (v/v) glycerol, 200 mM NaCl, pH 7.2) and 12.6 μ l Coomassie brilliant blue G-250 (5% (w/v) in 0.75 M aminocaproic acid).

4.2.9.2 Native electrophoresis and SDS-PAGE

Mitochondrial protein (150 μ g) was loaded into a 4-16% (w/v) bis-acrylamide precast gradient gel (Invitrogen, Carlsbad CA) beside 7 μ l of NativeMark unstained protein standard. Electrophoresis was performed using an XCell Surelock Mini-Cell (Invitrogen, Carlsbad CA) at 4 °C under a constant current of 12 mA for 2 hr. The buffer system

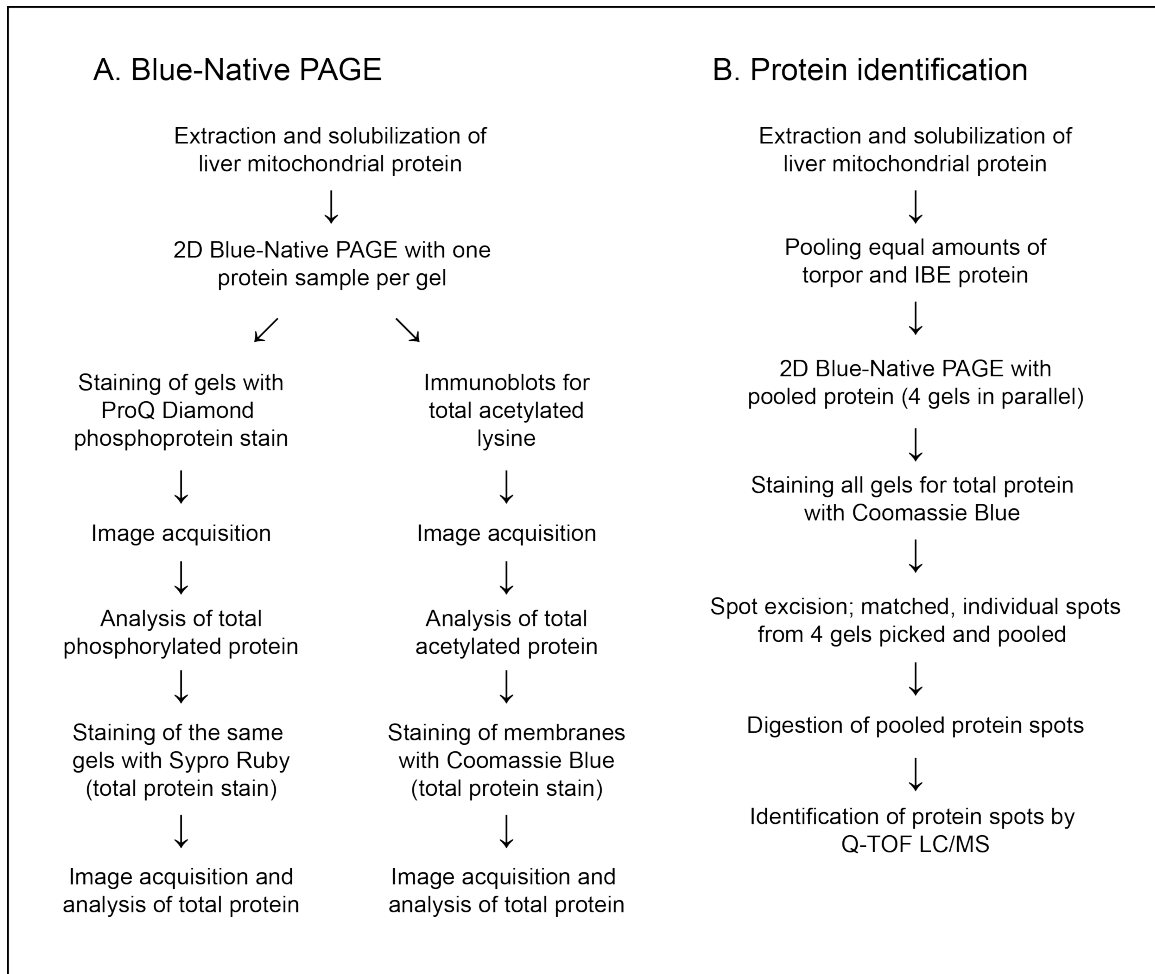


Figure 4-3. A summary of Blue-Native (BN) PAGE experimental methods. BN-PAGE was used to assess differences in liver electron transport system proteins between torpor and IBE, with subsequent analysis of differences in phosphorylation and acetylation of these proteins between the two hibernation states (A). Proteins that differed in phosphorylation or acetylation between the two states were identified by MALDI mass spectrometry (B).

consisted of an anode buffer (50 mM bis-tris, 50 mM tricine, pH 7.0) and a cathode buffer (50 mM bis-tris, 50 mM tricine, 0.002% (w/v) Coomassie brilliant blue G-250). Following electrophoresis, vertical lanes corresponding with separated native protein complexes from individual mitochondrial samples were excised and incubated in a denaturing solution (1% (v/v) β -mercaptoethanol, 1% (w/v) SDS) for 15 min at 25 °C and for 3 min at 50 °C. Strips were rinsed with SDS-PAGE running buffer and laid horizontally on 10% polyacrylamide resolving gels. Gels were electrophoresed at 100 V for 2 hr in SDS-PAGE running buffer.

4.2.9.3 Confirming the presence of ETC complexes following 2D BN-PAGE

In order to confirm that all ETS complexes were present following 2D BN-PAGE, I performed immunoblots of gels using the MitoProfile antibody cocktail (which contains antibodies for one subunit of each ETS complex) as described in Chapter 2.2.5. Figure 4-4 shows a representative immunoblot image.

4.2.9.4 Phosphoprotein staining of BN-PAGE gels

Following 2D BN-PAGE, gels were stained with ProQ diamond phosphoprotein stain using the same methods described in section 4.2.7.2. Gels images were acquired and analyzed using the same methods described in section 4.2.7.4. Total loaded protein, as quantified by staining with Sypro Ruby (as described in section 4.2.7.3) did not differ significantly ($p > 0.05$) among gels. Protein spots that differed significantly in phosphorylation between torpor and IBE were selected for identification by quadruple time-of-flight (Q-TOF) liquid chromatography-mass spectrometry (LC/MS; see section 4.2.10).

4.2.9.5 Acetylation immunoblots from BN-PAGE gels

Following 2D BN-PAGE, immunoblots for total acetylated lysine were performed using the same methods described in section 4.2.8.2. Gel images were acquired and analyzed using the same methods described in section 4.2.8.3. Total loaded protein, as quantified by staining with Coomassie Blue, did not differ significantly ($p > 0.05$) among gels.

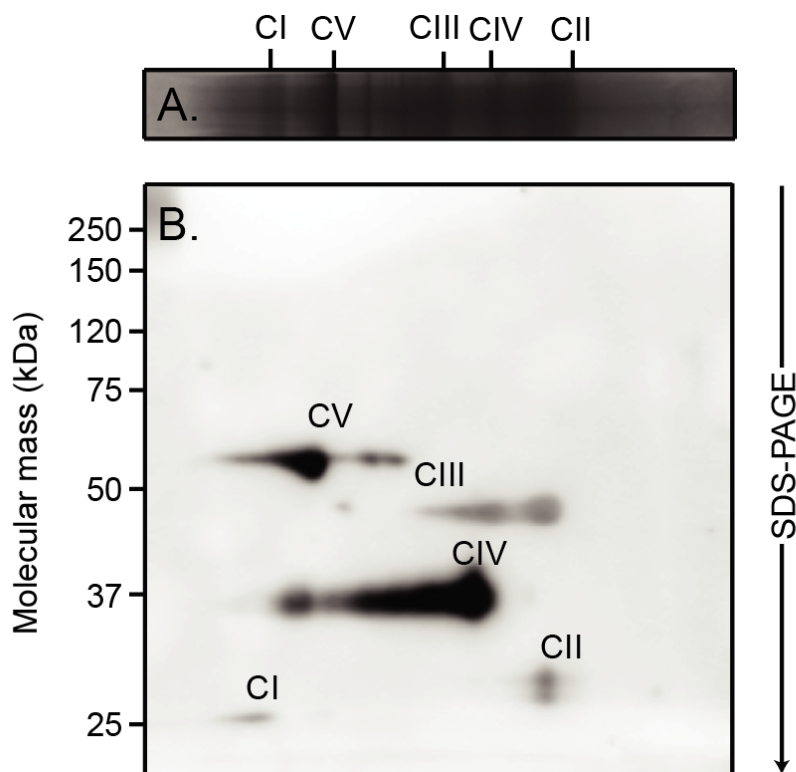


Figure 4-4. Immunoblot of five ETS subunits in liver mitochondrial protein separated by BN-PAGE. Liver mitochondria protein was isolated from one 13-lined ground squirrel. Protein was separated in the first dimension by molecular mass (A; horizontal) under non-denaturing conditions. Protein was then separated by molecular mass again in a second dimension under denaturing conditions (vertical) using SDS-PAGE (B). Immunoblots using the rodent Mitoprofile antibody cocktail confirm the presence of the following ETS subunits: Complex I (CI), NDUFB8 (22 kDa); Complex II (CII), Iron-sulfur protein subunit (30 kDa); Complex III (CIII), core protein II (48 kDa); Complex IV (CIV), subunit I (40 kDa); Complex V (CV), alpha subunit (55 kDa).

Protein spots that differed significantly in acetylation between torpor and IBE were selected for identification by Q-TOF LC/MS.

4.2.10 Q-TOF LC/MS

Four preparative BN-PAGE gels were run for both torpor and IBE and stained with Coomassie R-250 for spot picking. Spots were excised by myself at the UWO Functional Proteomics Lab (London, ON) and digested as described in Section 4.2.5. Following digestion, protein samples were submitted Q-TOF LC/MS for analysis of peptide sequence at the UWO Biological Mass Spectrometry Lab (London, ON). Mass spectrometry was performed on a QToF Ultima Global mass spectrometer (Waters) equipped with a Z-spray source and run in positive ion mode with an Agilent 1100 HPLC used for LC gradient diversity. Peptide sequences obtained from MALDI –TOF/TOF MS analysis were submitted to the NCBI database for comparison with known protein sequences. For each peptide sequence, the alignment between sample peptides and known peptides was used to assign a protein score confidence interval, with a higher value indicating greater alignment.

4.3 Results

4.3.1 2D-DiGE analysis of liver mitochondrial proteins in torpor and IBE

I used two-dimensional differential gel electrophoresis (2D-DiGE) to assess global changes in liver mitochondrial proteins between torpor and IBE. Equal amounts of liver mitochondrial protein from animals sampled during torpor and IBE were labeled with cyanine dyes and electrophoresed together with an internal protein standard. Within the representative gel image (Figure 4-5), protein spots that appear yellow fully overlap between the two hibernation states and therefore do not differ in abundance. Single protein spots that are visibly red or green are more abundant in either IBE or torpor, respectively. A pair of red and green spots in close proximity at the same molecular weight (a reciprocal abundance pattern) indicates a shift in isoelectric point between torpor and IBE.

The normalized ratio of the expression relative to the internal standard was quantified for each spot. Preliminary analysis identified 14 spots of interest that appeared to differ, but subsequent analysis revealed that there were only 7 significantly different spots ($p \leq 0.05$) between torpor and IBE (Table 4-1). Among these were proteins involved in the TCA cycle (succinyl-CoA ligase; spots 5 and 6, fumarase; spot 12), leucine catabolism (isovaleryl-CoA dehydrogenase; spots 9 and 10), β -oxidation ($\Delta(3,5)$ - $\Delta(2,4)$ -dienoyl-CoA isomerase; spot 14), and ROS detoxification (catalase; spots 3 and 4). All proteins but fumarase showed distinct patterns of reciprocal abundance, indicating a shift in isoelectric point of each protein between torpor and IBE rather than a change in abundance.

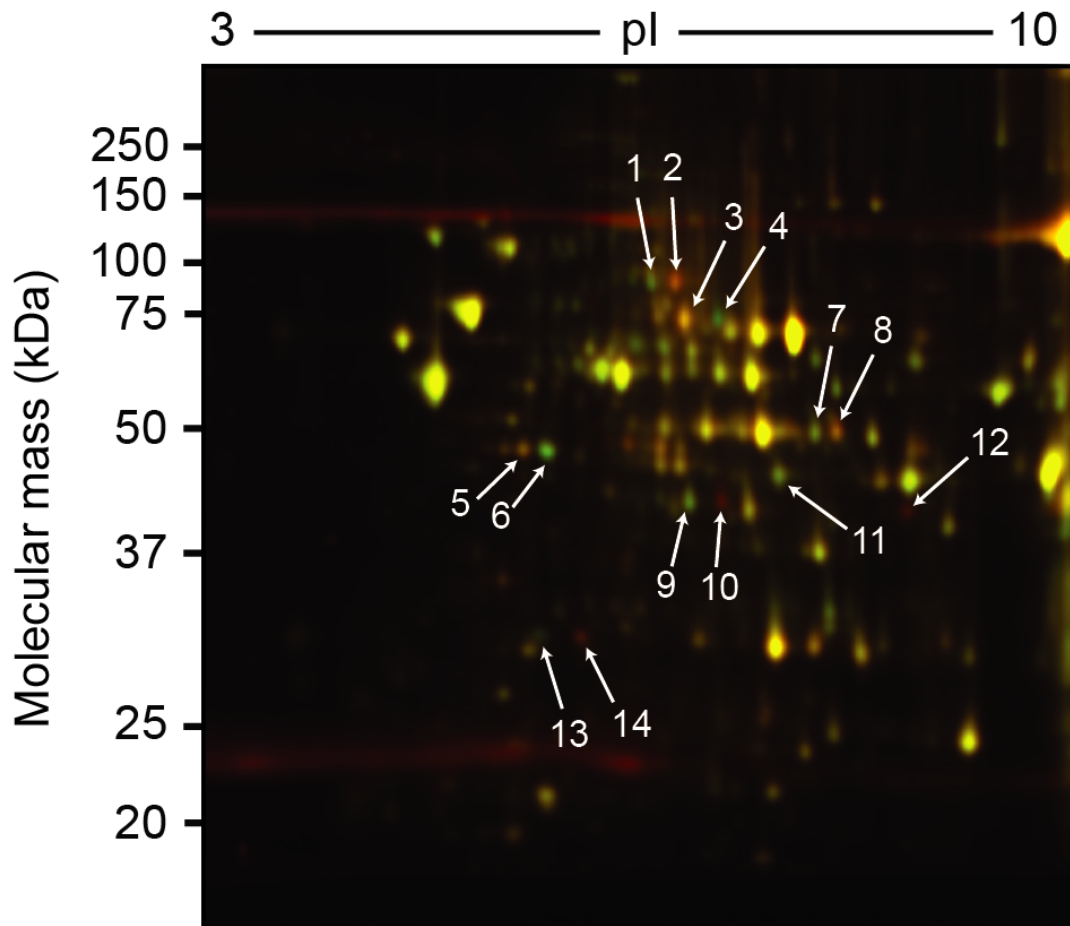


Figure 4-5. Ground squirrel liver mitochondrial proteins compared between torpor and IBE by 2D-DiGE. This representative image shows liver mitochondrial protein spots from one torpid (Cy3, labelled green) and one IBE (Cy5, labelled red) animal. Proteins were separated by isoelectric point (pI; horizontal dimension), then by molecular mass (vertical dimension). Arrows indicate proteins of interest, summarized in Table 4-1.

Table 4-1. Proteins identified by MALDI mass spectrometry from spots of interest in 2D-DiGE analysis comparing IBE and torpor.

Spot numbers correspond with spots shown in Figure 4-5. Protein score, which indicates alignment between sample peptides and known peptide, is $-10 \cdot \log(P)$, where P is the probability that the protein match is random. Protein scores greater than 72 are considered significant ($p \leq 0.05$). Fold change from torpor to IBE and associated p-value were calculated from quantitative analysis of spot density ($n=5$), and a significant difference between torpor and IBE is denoted by an asterisk.

Spot number	Protein ID	Protein score	Pathway	Fold change in IBE	p-value
1	Phosphoenolpyruvate carboxykinase [GTP], mitochondrial	176	Gluconeogenesis		0.469
2	Phosphoenolpyruvate carboxykinase [GTP], mitochondrial	208	Gluconeogenesis		0.345
3	Catalase	250	ROS detoxification	+1.4	0.039*
4	Catalase	83	ROS detoxification	-1.3	0.033*
5	Succinyl-CoA ligase [GDP-forming] subunit beta, mitochondrial	91	TCA cycle	+1.5	0.010*
6	Succinyl-CoA ligase [GDP-forming] subunit beta, mitochondrial	100	TCA cycle	-1.7	0.050*
7	Peroxisomal acyl-coenzyme A oxidase 1 isoform X2	90	β -Oxidation		0.342
8	Peroxisomal acyl-coenzyme A oxidase 1 isoform X2	97	β -Oxidation		0.367
9	Isovaleryl-CoA dehydrogenase	127	Leucine catabolism	+2.6	<0.001*
10	Isovaleryl-CoA dehydrogenase	103	Leucine catabolism	-1.8	0.004*
11	Short-chain specific acyl-CoA dehydrogenase	107	β -Oxidation		0.435
12	Fumarase	79	TCA cycle	+1.7	0.047*
13	Delta(3,5)-Delta(2,4)-dienoyl-CoA isomerase, mitochondrial	77	β -Oxidation	-1.1	0.035*
14	Delta(3,5)-Delta(2,4)-dienoyl-CoA isomerase, mitochondrial	72	β -Oxidation	+1.6	0.040*

4.3.2 Phosphorylation and acetylation of liver mitochondrial proteins during torpor and IBE

The patterns of reciprocal abundance indicated by DiGE analysis for four liver mitochondrial proteins indicates a difference in isoelectric point between torpor and IBE, which is likely a consequence of differential post-translational modification. I conducted 2D electrophoresis with subsequent phosphoprotein staining to determine whether any of the proteins identified by DiGE as differing in isoelectric point between torpor and IBE were differentially phosphorylated (representative gels from IBE and torpor shown in Figure 4-6). Using densitometry analysis, I measured the intensity of ProQ staining of individual protein spots, which corresponds with protein phosphorylation. Three protein spots differed significantly between torpor and IBE (summarized in Table 4-2). Two of these spots aligned with spots 5 and 6 in Figure 4-5 and were identified as succinyl-CoA ligase [GDP-forming], each spot corresponding with a different isoelectric point. These spots showed significantly greater phosphorylation in IBE than torpor. A third spot (17) with a molecular weight of approximately 50 kDa did not align with any protein from 2D DiGE gels, but showed more phosphorylation during torpor. These patterns were found in each of the four 2D gels analyzed for each of torpor and IBE.

Using immunoblots following 2D electrophoresis of liver mitochondrial protein, I found 3 spots that differed significantly in degree of total acetylated lysine between torpor and IBE (Figure 4-7). One of these spots (spot 19) aligned with succinyl-CoA ligase [GDP-forming], from Figure 4-5, and showed less acetylation during IBE compared with torpor. Two other protein spots (18 and 20) showed significantly lower acetylation during IBE, but these proteins do not correspond with any of the spots identified from DiGE gels, and so remain unidentified. The molecular weights of these unknown proteins are approximately 60 kDa and 40 kDa, respectively. These patterns of differential acetylation were found in all four gels used for each of torpor and IBE.

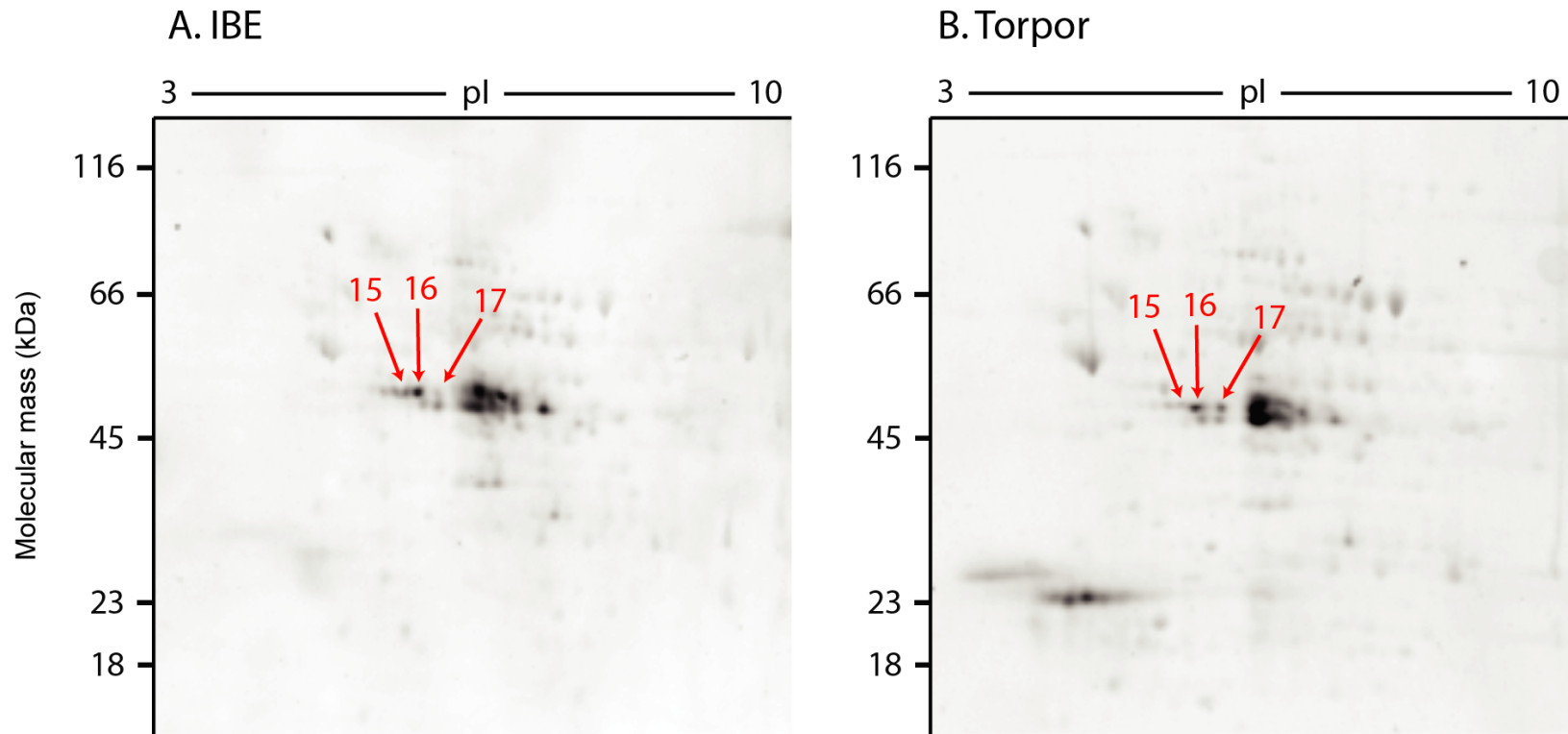


Figure 4-6. Total phosphorylation of liver mitochondrial protein from IBE and torpid ground squirrels. Representative gels from one IBE animal (A) and one torpid animal (B). In each gel proteins were separated by 2D electrophoresis and stained with ProQ Diamond Phosphoprotein Stain. Arrows indicate proteins that differed in phosphorylation between torpor and IBE (torpor: n=4; IBE: n=4), with corresponding spots indicated by the same number on each gel. Data for all gels are summarized in Table 4-2.

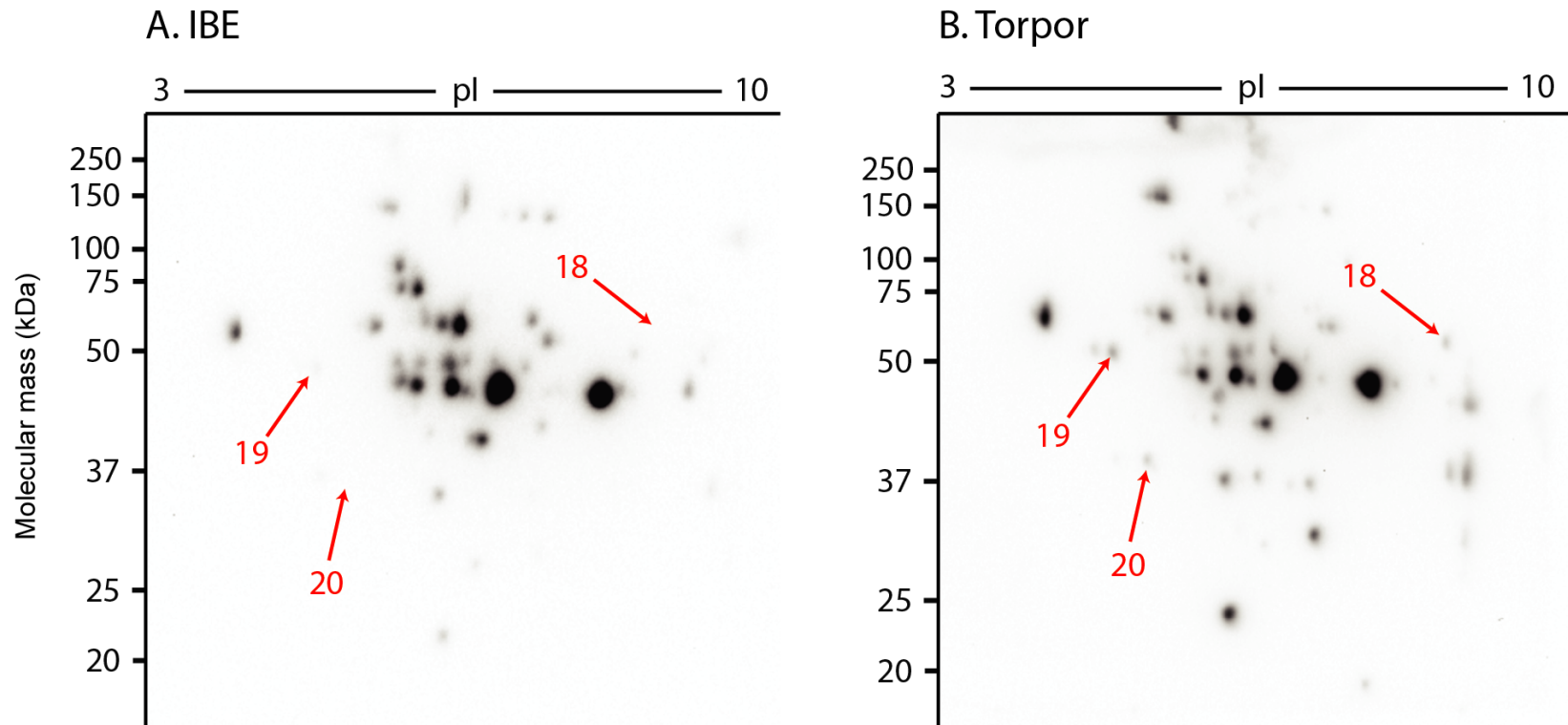


Figure 4-7. Total lysine acetylation in liver mitochondrial protein from IBE (A) and torpid (B) ground squirrels. Representative gels from one IBE animal (A) and one torpid animal (B). Proteins were separated by 2D electrophoresis and immunoblotted for total acetylated lysine. Arrows indicate proteins that differed in amount of acetylation between torpor and IBE (torpor: n=4; IBE: n=4), with corresponding spots indicated by the same number on each gel. Data from all gels are summarized in Table 4-2.

Table 4-2. Liver mitochondrial proteins, resolved by 2D electrophoresis, differing in phosphorylation and acetylation between IBE and torpor. Spot numbers correspond with spots shown in Figure 4-6 and Figure 4-7. Fold change and associated p-value were calculated from quantitative analysis of spot density, and a significant difference between torpor and IBE is denoted by an asterisk.

Spot	Modification	Fold change in IBE	p-value	Protein ID
15	Phosphorylation	+2.3	0.03*	Succinyl-CoA ligase [GDP-forming] subunit beta, mitochondrial
16	Phosphorylation	+3.4	<0.001*	Succinyl-CoA ligase [GDP-forming] subunit beta, mitochondrial
17	Phosphorylation	-2.5	0.05*	Protein unknown
18	Acetylation	-3.9	0.05*	Protein unknown
19	Acetylation	-2.8	0.03*	Succinyl-CoA ligase [GDP-forming] subunit beta, mitochondrial
20	Acetylation	-4.7	0.002*	Protein unknown

4.3.3 Analysis of ETS proteins by BN-PAGE

I used blue-native polyacrylamide gel electrophoresis (BN-PAGE) to examine liver mitochondrial ETS complexes specifically. In this technique, the five ETS complexes are separated first by molecular mass in their native state (i.e. under non-denaturing conditions). Each complex is then further separated into individual polypeptides, again based on molecular mass but under denaturing conditions (a representative gel image is shown in Figure 4-8).

Following BN-PAGE with liver mitochondrial protein, I used a phosphoprotein stain to assess differences in phosphorylation of ETS complex proteins between torpor and IBE (Figure 4-9). Densitometry analysis revealed a consistent pattern in all gels, with two spots that differed significantly in phosphorylation (summarized in Table 4-3). I excised these spots and used Q-TOF LC/MS to identify them. A protein identified as the 75 kDa subunit of complex I (37 matched peptides with 63% sequence coverage) showed a 1.5-fold increase in phosphorylation during torpor (spot 21; $p=0.011$). A protein identified as the flavoprotein subunit of complex II (6 matched peptides with 9% sequence coverage) showed a 4.6-fold increase in phosphorylation during IBE relative to torpor (spot 22; $p<0.001$).

I conducted immunoblots for total acetylated lysine following BN-PAGE to assess change in acetylation of ETS proteins between torpor and IBE (Figure 4-10). One protein consistently showed a significant difference in acetylation (summarized in Table 4-3): it was identified as subunit 1 of complex IV (32 matched peptides with 29% sequence coverage) showed 2.4-fold more acetylation during torpor compared to IBE ($p=0.050$, spot 23).

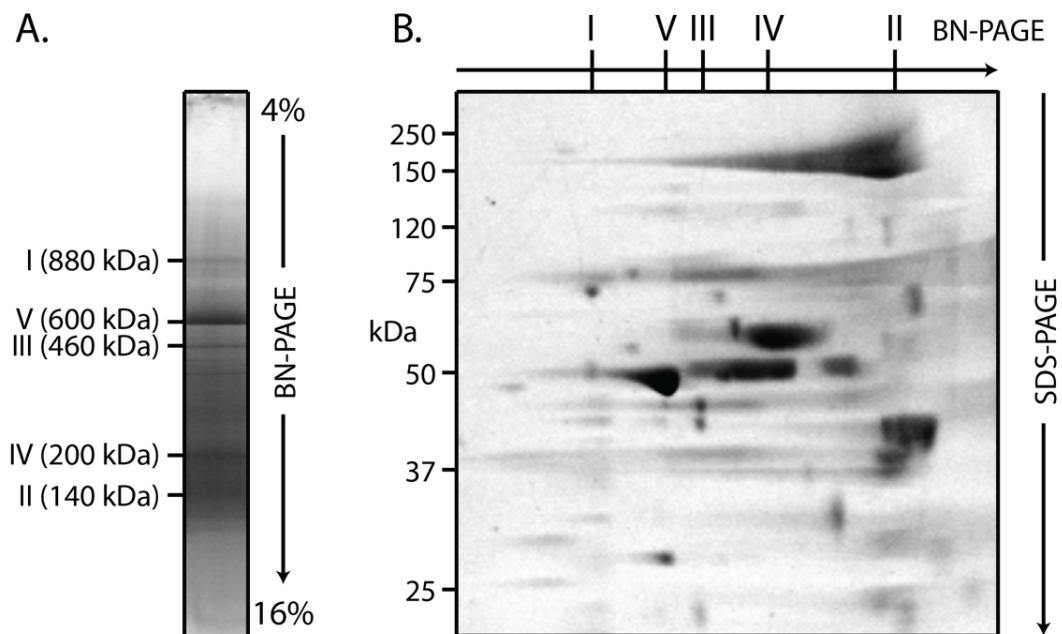


Figure 4-8. 2D Blue-Native PAGE of liver mitochondrial protein from a ground squirrel in IBE. Intact ETS complexes were separated under non-denaturing conditions and were identified by molecular mass on a 4-16% gradient gel following Coomassie staining (A). Subunits of the native complexes were denatured and separated by SDS-PAGE on a 10% (w/v) polyacrylamide gel (B).

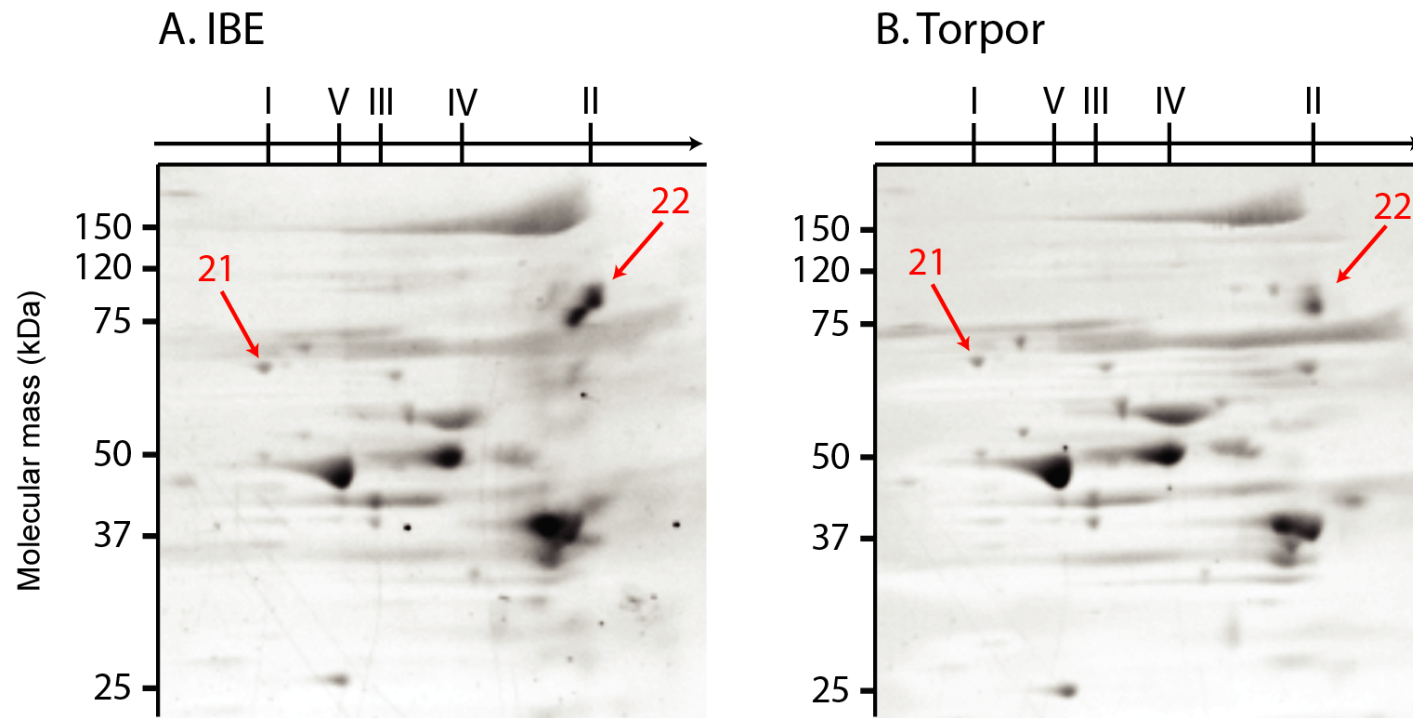


Figure 4-9. Total protein phosphorylation in liver mitochondria from IBE (A) and torpid (B) ground squirrels following separation by 2D BN-PAGE. Representative gels from one IBE animal (A) and one torpid animal (B). Arrows indicate proteins that differed significantly in phosphorylation between torpor and IBE (torpor: n=4; IBE: n=4), with corresponding spots indicated by the same number on each gel. Spot 22, present in IBE (A) is absent from torpor (B), with an arrow indicating where the spot would be if present. Data from all gels are summarized in Table 4-3.

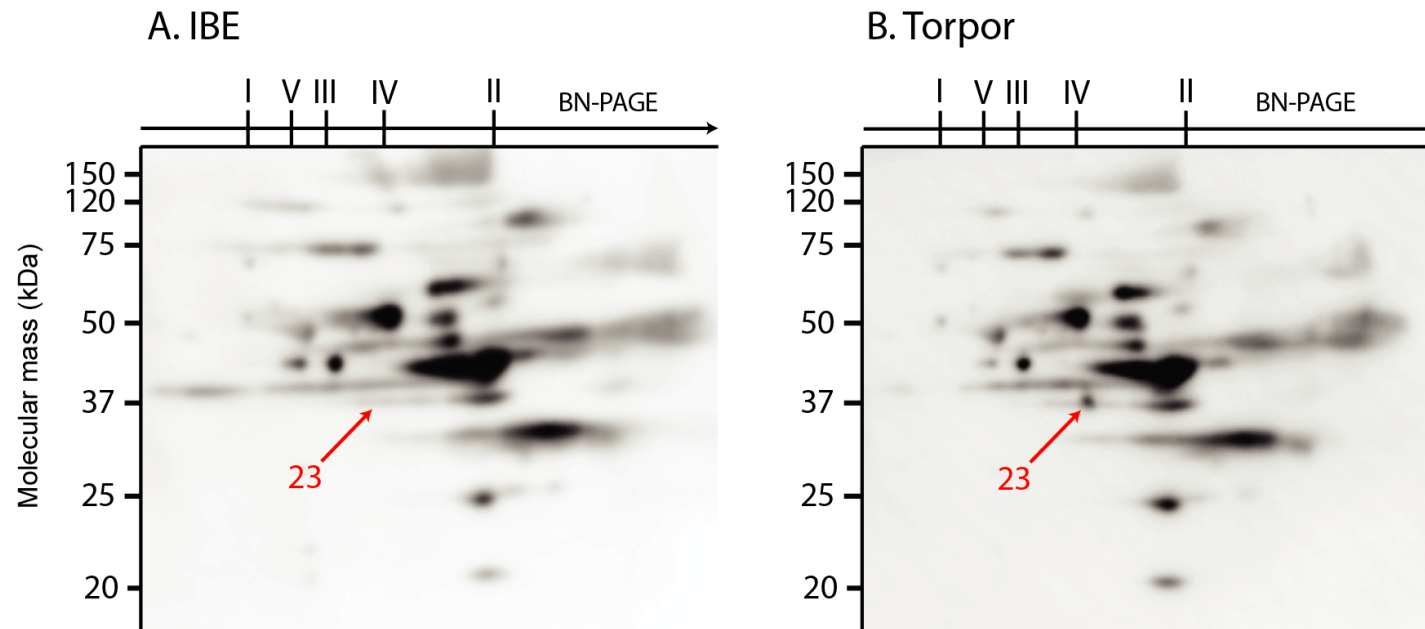


Figure 4-10. Total protein acetylation in liver mitochondria from IBE (A) and torpid (B) ground squirrels following separation by 2D BN-PAGE. Representative gels from one IBE animal (A) and one torpid animal (B). Arrows indicate proteins that differ significantly in acetylation between torpor and IBE (torpor: n=4; IBE: n=4), with corresponding spots indicated each gel. Data from all gels are summarized in Table 4-3.

Table 4-3. Electron transport system proteins, resolved by BN-PAGE, differing in phosphorylation and acetylation between IBE and torpor.

Spot numbers correspond with spots shown in Figure 4-9 and Figure 4-10. Fold change and associated p-value were calculated from quantitative analysis of spot density, and a significant difference between torpor and IBE is denoted by an asterisk. Protein score, which indicates alignment between sample peptides and known peptide, is $-10 \cdot \log(P)$, where P is the probability that the protein match is random. Protein scores greater than 72 are considered significant ($p \leq 0.05$).

Spot	Modification	Fold change in IBE	p-value	Protein ID	Protein score
21	Phosphorylation	-1.5	0.011	NADH dehydrogenase, 75 kDa subunit	275.64
22	Phosphorylation	+4.6	<0.001	Succinate dehydrogenase, flavoprotein subunit	110.76
23	Acetylation	-2.4	0.050	Cytochrome c oxidase, subunit 1	197.31

4.4 Discussion

In this study I found convincing, consistent evidence of several liver mitochondrial proteins that show differential post-translational modification within a torpor-arousal cycle. Most significant among these findings is that ETS complexes I and II are differentially phosphorylated between torpor and IBE, providing a potential mechanism for the metabolic changes that occur during hibernation.

4.4.1 Differences in liver mitochondrial proteins between torpor and IBE identified following 2D-DiGE

The use of 2D-DiGE allowed me to directly compare all liver mitochondrial proteins between torpor and IBE. When linking functional changes to mechanisms, the proteome is, arguably, the most relevant level of biological organization to investigate as it represents the culmination of changes in transcription, translation, and regulation. 2D electrophoresis is an especially useful technique as it can identify proteins that differ not only in expression between two conditions, but also shifts in isoelectric point, indicative of post-translational modification (PTM) or isoform switching. I identified five liver mitochondrial proteins with significantly altered abundance between torpor and IBE. Four of these proteins presented distinct reciprocal abundance patterns, indicating shifts in PTM or protein isoform between the two hibernation states rather than up- or down-regulation within one state.

Two enzymes involved in the tricarboxylic acid (TCA) cycle showed differences between torpor and IBE. Succinyl-CoA ligase (SCL; Figure 4-5, spots 5 and 6) presented as a pair of spots with reciprocal abundance in torpor and IBE. This shift in isoelectric point corresponds with increased phosphorylation of SCL during IBE (Figure 4-6, spots 15-16) and increased acetylation during torpor (Figure 4-7, spot 19). Succinyl-CoA ligase (SCL) catalyzes the conversion of succinyl-CoA to succinate, coupling the reaction with the formation of either GTP or ATP. SCL is the only mitochondrial enzyme capable of

producing ATP (or GTP) by substrate-level phosphorylation in the absence of oxygen (Kaufman et al., 1953). As a critical step in the TCA cycle, SCL is a potential site of mitochondrial metabolic regulation. In pig heart mitochondria, the activity of SCL increases more than 2-fold when phosphorylated (Phillips et al., 2009). This phosphorylation is not enzyme-catalyzed and apparently involves non-covalent bonds, which may represent a way by which mitochondrial metabolism can be regulated in response to intramitochondrial energy status since free phosphate levels increase as ATP is consumed. Since SCL is less phosphorylated (and therefore likely to have lower activity) during torpor, dephosphorylation of this enzyme during torpor could be an important regulatory mechanism for limiting flux through the TCA cycle as animals enter torpor. I also found that SCL showed greater acetylation in torpor compared to IBE. No known acetylation sites have been documented on SCL, so the functional consequences of this modification remain unknown. Acetylation during torpor could contribute to inhibition of SCL activity which would be a novel mechanism of regulation. Protein levels of fumarase (Figure 4-5, spot 12), which catalyzes the conversion of fumarate to malate in the TCA cycle, decreased by 1.7-fold in torpor compared to IBE with no apparent change in isoelectric point. Together, decreased protein levels of fumarase and decreased activity of SCL by dephosphorylation could contribute to the suppression of mitochondrial metabolism during torpor by limiting the amount of reducing equivalents (NADH, FADH₂) available to enter the ETS.

Delta(3,5)-Delta(2,4)-dienoyl-CoA isomerase (ECH1; Figure 4-5, spots 13-14), involved in β -oxidation, also showed a shift in isoelectric point between torpor and IBE. This shift does not correspond with any changes in phosphorylation or acetylation of ECH1, so it is likely that another PTM differs between the two hibernation states. For example, modifications such as succinylation, S-nitrosylation, and O-GlcNAcylation have all been shown to alter the activity of mitochondrial proteins (Stram and Payne, 2016). It is possible that a yet unknown PTM inhibits ECH1 during torpor, which could contribute to overall mitochondrial suppression by limiting the supply of acetyl-CoA to the TCA cycle. Indeed, fatty acid-fueled state 3 respiration rates in isolated liver mitochondria are reduced by 50% in torpor compared to IBE (Mathers and Staples, unpublished data).

Since hibernators rely primarily on lipid metabolism during the hibernation season (reviewed by Dark, 2005) beta-oxidation represents another important site of metabolic regulation. Together, suppression of both β -oxidation and the TCA cycle likely contribute to the suppression of respiration that occurs in liver mitochondria. Isovaleryl-CoA dehydrogenase (Figure 4-5, spots 9-10) is involved in leucine catabolism, also shows a shift in isoelectric point between torpor and IBE. I know of no PTMs that regulate activity of this enzyme, nor are there data about how leucine catabolism might differ among phases of a torpor bout.

Catalase facilitates the conversion of hydrogen peroxide to water and oxygen, and as such plays an important role in mitigating oxidative damage. I found that catalase undergoes a shift in isoelectric point between torpor and IBE (Figure 4-5, spots 3-4), which likely indicates differential PTM between the two hibernation states. Though catalase is regulated by phosphorylation (Cao et al., 2003), the shift in PTM that I found does not correspond with differential phosphorylation or acetylation as measured by phosphoprotein staining and immunoblots. It is possible that catalase is modified by a yet unknown PTM that alters its activity to mitigate oxidative damage that occurs during torpor or IBE. Hibernators may upregulate antioxidant defences to protect tissues from potential ischemia-reperfusion injury (IRI) during transitions between torpor and IBE (Carey et al., 2003). IRI occurs when blood flow returns to a tissue after a period of restriction, a condition that may be especially important for hibernators, who experience rapid changes in heart rate and therefore the amount of oxygenated blood that reaches tissues. Reperfusion is associated with oxidative damage, as reintroduction of oxygen causes greater production of reactive oxygen species (ROS) including hydrogen peroxide (Slezak et al., 1995). Hibernators do show some enhanced resistance to oxidative stress in tissues such as liver (Lindell et al., 2005), however other evidence suggests that hibernators experience increased oxidative damage during torpor. In 13-lined ground squirrels, free radical release from liver mitochondria is higher in torpor than IBE (Brown et al., 2012) and in intestinal mucosa lipid peroxide metabolites are higher during early torpor than IBE (Carey et al., 2000). Catalase activity in liver is lower during torpor

compared to summer (Page et al., 2009), but a comparison between torpor and IBE has not yet been made, to my knowledge.

4.4.2 Differences in ETS proteins in liver mitochondria between torpor and IBE identified following BN-PAGE

I used Blue-Native PAGE to analyze the ETS subproteome within liver mitochondria from torpid and IBE ground squirrels, and used phosphostaining and immunoblots to identify any differences in phosphorylation and acetylation in ETS proteins between torpor and IBE.

The flavoprotein subunit of complex II showed greater phosphorylation in IBE, increasing by 4.6-fold compared with torpor (Figure 4-9, spot 22). This observation is quite significant since the patterns of phosphorylation parallel the suppression of complex II activity during torpor as well suppression of mitochondrial respiration with fuels enter the ETS at complex II (Chapter 2). It is possible, therefore, that this phosphorylation mediates the observed changes in enzyme activity and mitochondrial metabolism over a torpor-IBE cycle. Phosphorylation of the flavoprotein subunit of complex II has been previously demonstrated, with phosphorylation of the tyrosine 604 residue by Fgr kinase associated with increased enzyme activity (Acín-Pérez et al. 2014). Complex II is also the target for phosphorylation by cAMP-dependent protein kinase A (PKA), with phosphorylation of an as yet unidentified serine or threonine residue on the flavoprotein subunit associated with a decrease in enzyme activity (Tomitsuka et al., 1999). It is clear that phosphorylation of different sites can have dramatically different effects on the activity of complex II, so future work should characterize the specific residues that are differentially phosphorylated between torpor and IBE.

The 75 kDa subunit of complex I showed significantly increased phosphorylation in torpor relative to IBE (Figure 4-9, spot 21). This change in phosphorylation corresponds with a change in protein activity, with complex I showing both a reduction in V_{\max} and contributing to a reduction in flux through the ETS (Chapter 2). Phosphorylation of

complex I has been described in mammals, with several phosphorylation sites identified, including on the 39kDa subunit (Augereau et al., 2005). To my knowledge, no phosphorylation sites have yet been identified on the 75 kDa subunit, so my finding is completely novel. Though the functional consequences of phosphorylation at specific sites remain largely unknown, the stimulation of phosphorylation pathways has led to some opposing results. For example, phosphorylation of complex I by PKA activates the enzyme (Papa et al., 1996), but phosphorylation by an Src kinase led to a decrease in enzyme activity (Hébert-Chatelain et al., 2010).

A previous study using similar techniques found no differences in phosphorylation of any ETS proteins between torpor and IBE (Chung et al., 2013). It is unclear why these studies have conflicting results. In the present study I used a phosphostain, which binds to any phosphorylated residues, whereas the previous study (Chung et al., 2013) used separate immunoblots for phosphorylation of tyrosine, threonine, and serine residues. It is also possible that multiple residues are phosphorylated on these proteins, and that my technique could detect such changes. It is also possible that the 2D-BN-PAGE methods I used allowed greater resolution of individual ETS subunits.

Complex IV, as the terminal step of the ETS, is an important regulatory site of oxidative phosphorylation. Immunoblots of ETS complexes separated by BN-PAGE revealed differential acetylation of the COX-1 subunit, with 2.4-fold more acetylation in torpor compared to IBE (Figure 4-10, spot 23). This difference in acetylation does not correspond with functional changes in liver mitochondria, as I previously found no difference in flux through complex IV in intact mitochondria, as well as no difference in maximal activity of complex IV in isolated liver mitochondria or in homogenized liver tissue (Chapter 2). It is possible that acetylation does in fact change enzyme's function, but that the fluxes and V_{\max} values measured in isolated mitochondria and homogenized tissue do not accurately represent the enzyme's *in vivo* function.

Since acetylation of mitochondrial proteins is usually associated with decreased enzyme activity (Baeza et al., 2016), complex IV acetylation could contribute to suppression of

mitochondrial metabolism during torpor. The acetylation state of many mitochondrial proteins is regulated by Sirtuin 3 (Sirt3), a NAD-dependent deacetylase, which regulates mitochondrial metabolism by deacetylating proteins when NAD⁺ levels are high. A knockdown of Sirt3 in mice led to increased acetylation of ETS proteins and a corresponding 50% decrease in liver ATP content (Ahn et al., 2008). In 13-lined ground squirrels, there is significantly less liver Sirt3 protein during the winter hibernation season compared to the summer. This change corresponds with higher overall protein acetylation in the winter (Hindle et al., 2014). Since NAD⁺ activates Sirtuins, changes in tissue NAD⁺ levels can facilitate deacetylation and activation of mitochondrial proteins. If changes in NAD⁺ mediate the observed changes in acetylation of complex IV between torpor and IBE, I predict that NAD⁺ levels in the liver would increase immediately before arousal. While liver metabolites have been measured in hibernators, with higher NAD⁺ during entrance into torpor compared to late torpor (Epperson et al., 2011), a comparison has not been made with early arousal or IBE. Moreover whole-tissue metabolomics data may not accurately represent changes in intramitochondrial metabolites. Future work should investigate NAD⁺ levels at all stages of a torpor-arousal cycle, especially in mitochondria, as it is a very plausible mechanism for triggering changes in acetylation and thus mitochondrial protein function.

4.5 Summary

This study identified several proteins likely involved in regulating the metabolic changes that occur in liver mitochondria between torpor and IBE. I identified differences in PTMs of two key mitochondrial ETS proteins which correspond with suppression of their maximal activities, a potentially novel mechanism for metabolic suppression. In the next chapter I attempt to manipulate liver mitochondrial metabolism in hibernators by altering the phosphorylation state of mitochondrial proteins.

4.6 References

- Acín-Pérez, R., Carrascoso, I., Baixauli, F., Roche-Molina, M., Latorre-Pellicer, A., Fernández-Silva, P., Mittelbrunn, M., Sanchez-Madrid, F., Pérez-Martos, A., Lowell, C.A., Manfredi, G. and Enríquez, J.A. (2014) ROS-triggered phosphorylation of complex II by Fgr kinase regulates cellular adaptation to fuel use. *Cell Metabolism*, 19(6) 1020–1033.
- Ahn, B.-H., Kim, H.-S., Song, S., Lee, I.H., Liu, J., Vassilopoulos, A., Deng, C.-X. and Finkel, T. (2008) A role for the mitochondrial deacetylase Sirt3 in regulating energy homeostasis. *Proceedings of the National Academy of Sciences*, 105(38) 14447–14452.
- Armstrong, C. and Staples, J.F. (2010) The role of succinate dehydrogenase and oxaloacetate in metabolic suppression during hibernation and arousal. *Journal of Comparative Physiology B - Biochemical, Systems, and Environmental Physiology*, 180(5) 775–783.
- Augereau, O., Claverol, S., Boudes, N., Basurko, M.-J., Bonneu, M., Rossignol, R., Mazat, J.-P., Letellier, T. and Dachary-Prigent, J. (2005) Identification of tyrosine-phosphorylated proteins of the mitochondrial oxidative phosphorylation machinery. *Cellular and Molecular Life Sciences*, 62(13) 1478–1488.
- Baeza, J., Smallegan, M.J. and Denu, J.M. (2016) Mechanisms and dynamics of protein acetylation in mitochondria. *Trends in Biochemical Sciences*, 41(3) 231–244.
- Bailey, S.M., Landar, A. and Darley-Usmar, V. (2005) Mitochondrial proteomics in free radical research. *Free Radical Biology and Medicine*, 38(2) 175–188.
- Barger, J.L., Brand, M.D., Barnes, B.M. and Boyer, B.B. (2003) Tissue-specific depression of mitochondrial proton leak and substrate oxidation in hibernating arctic ground squirrels. *American Journal of Physiology - Regulatory, Integrative and Comparative Physiology*, 284(5) R1306-1313.
- Brooks, S.P.J. and Storey, K.B. (1992) Mechanisms of glycolytic control during hibernation in the ground squirrel *Spermophilus lateralis*. *Journal of Comparative Physiology B - Biochemical, Systems, and Environmental Physiology*, 162(1) 23–28.
- Brown, J.C.L., Chung, D.J., Belgrave, K.R. and Staples, J.F. (2012) Mitochondrial metabolic suppression and reactive oxygen species production in liver and skeletal muscle of hibernating thirteen-lined ground squirrels. *American Journal of Physiology - Regulatory, Integrative and Comparative Physiology*, 302(1) R15-28.

- Cao, C., Leng, Y. and Kufe, D. (2003) Catalase activity is regulated by c-Abl and Arg in the oxidative stress response. *Journal of Biological Chemistry*, 278(32) 29667–29675.
- Carey, H.V., Andrews, M.T. and Martin, S.L. (2003) Mammalian hibernation: cellular and molecular responses to depressed metabolism and low temperature. *Physiological Reviews*, 83(4) 1153–1181.
- Carey, H.V., Frank, C.L. and Seifert, J.P. (2000) Hibernation induces oxidative stress and activation of NK-kappaB in ground squirrel intestine. *Journal of Comparative Physiology B - Biochemical, Systemic, and Environmental Physiology*, 170(7) 551–559.
- Chung, D., Lloyd, G.P., Thomas, R.H., Guglielmo, C.G. and Staples, J.F. (2011) Mitochondrial respiration and succinate dehydrogenase are suppressed early during entrance into a hibernation bout, but membrane remodeling is only transient. *Journal of Comparative Physiology B - Biochemical, Systems, and Environmental Physiology*, 181(5) 699–711.
- Chung, D.J., Szyszka, B., Brown, J.C.L., Hüner, N.P.A. and Staples, J.F. (2013) Changes in the mitochondrial phosphoproteome during mammalian hibernation. *Physiological Genomics*, 45(10) 389–399.
- Dark, J. (2005) Annual lipid cycles in hibernators: integration of physiology and behavior. *Annual Review of Nutrition*, 25 469–497.
- Epperson, L.E., Karimpour-Fard, A., Hunter, L.E. and Martin, S.L. (2011) Metabolic cycles in a circannual hibernator. *Physiological Genomics*, 43(13) 799–807.
- Hébert-Chatelain, E., Dupuy, J.-W., Letellier, T. and Dachary-Prigent, J. (2011) Functional impact of PTP1B-mediated Src regulation on oxidative phosphorylation in rat brain mitochondria. *Cellular and Molecular Life Sciences*, 68(15) 2603–2613.
- Hébert-Chatelain, E.H., Dupuy, J.-W., Letellier, T. and Dachary-Prigent, J. (2010) Functional impact of PTP1B-mediated Src regulation on oxidative phosphorylation in rat brain mitochondria. *Cellular and Molecular Life Sciences*, 68(15) 2603–2613.
- Hindle, A.G., Grabek, K.R., Epperson, L.E., Karimpour-Fard, A. and Martin, S.L. (2014) Metabolic changes associated with the long winter fast dominate the liver proteome in 13-lined ground squirrels. *Physiological Genomics*, 46(10) 348–361.
- Hofer, A. and Wenz, T. (2014) Post-translational modification of mitochondria as a novel mode of regulation. *Experimental Gerontology*, 56 202–220.

- Kaufman, S., Gilvarg, C., Cori, O. and Ochoa, S. (1953) Enzymatic oxidation of alpha-ketoglutarate and coupled phosphorylation. *The Journal of Biological Chemistry*, 203(2) 869–888.
- Jiang, L., He, L. and Fountoulakis, M. (2004) Comparison of protein precipitation methods for sample preparation prior to proteomic analysis. *Journal of Chromatography A*, 1023(2) 317–320.
- Liko, I., Degiacomi, M.T., Mohammed, S., Yoshikawa, S., Schmidt, C. and Robinson, C.V. (2016) Dimer interface of bovine cytochrome c oxidase is influenced by local posttranslational modifications and lipid binding. *Proceedings of the National Academy of Sciences*, 113(29) 8230–8235.
- Lindell, S.L., Klahn, S.L., Piazza, T.M., Mangino, M.J., Torrealba, J.R., Southard, J.H. and Carey, H.V. (2005) Natural resistance to liver cold ischemia-reperfusion injury associated with the hibernation phenotype. *American Journal of Physiology. Gastrointestinal and Liver Physiology*, 288(3) G473–480.
- Muleme, H.M., Walpole, A.C. and Staples, J.F. (2006) Mitochondrial metabolism in hibernation: Metabolic suppression, temperature effects, and substrate preferences. *Physiological and Biochemical Zoology*, 79(3) 474–483.
- Ogura, M., Yamaki, J., Homma, M.K. and Homma, Y. (2012) Mitochondrial c-Src regulates cell survival through phosphorylation of respiratory chain components. *The Biochemical Journal*, 447(2) 281–289.
- Page, M., W. Peters, C., F. Staples, J. and Stuart, J. (2009) Intracellular antioxidant enzymes are not globally upregulated during hibernation in the major oxidative tissues of the 13-lined ground squirrel *Spermophilus tridecemlineatus*. *Comparative Biochemistry and Physiology A - Molecular and Integrative Physiology*, 152(1) 115–122.
- Papa, S., Sardanelli, A.M., Cocco, T., Speranza, F., Scacco, S.C. and Technikova-Dobrova, Z. (1996) The nuclear-encoded 18 kDa (IP) AQDQ subunit of bovine heart complex I is phosphorylated by the mitochondrial cAMP-dependent protein kinase. *FEBS Letters*, 379(3) 299–301.
- Phillips, D., Aponte, A.M., French, S.A., Chess, D.J. and Balaban, R.S. (2009) Succinyl-CoA synthetase is a phosphate target for the activation of mitochondrial metabolism. *Biochemistry*, 48(30) 7140–7149.
- Picard, M., Taivassalo, T., Ritchie, D., Wright, K.J., Thomas, M.M., Romestaing, C. and Hepple, R.T. (2011) Mitochondrial structure and function are disrupted by standard isolation methods. *PLoS One*, 6(3) e18317.
- Quinlan, P.T., Thomas, A.P., Armston, A.E. and Halestrap, A.P. (1983) Measurement of the intramitochondrial volume in hepatocytes without cell disruption and its elevation by hormones and valinomycin. *Biochemical Journal*, 214(2) 395–404.

- Roberts, J.C. and Chaffee, R.R. (1972) Suppression of mitochondrial respiration in hibernation and its reversal in arousal. In: R.E. Smith, J.C. Shields, P.P. Hannon, B.A. Horwitz (eds.) *Proceedings of the International Symposium on Environmental Physiology: Bioenergetics and Temperature Regulation*. FASAB. Bethesda: 101–107.
- Rosenfeld, J., Capdevielle, J., Guillemot, J.C. and Ferrara, P. (1992) In-gel digestion of proteins for internal sequence analysis after one- or two-dimensional gel electrophoresis. *Analytical Biochemistry*, 203(1) 173–179.
- Schägger, H. and von Jagow, G. (1991) Blue native electrophoresis for isolation of membrane protein complexes in enzymatically active form. *Analytical Biochemistry*, 199(2) 223–231.
- Slezak, J., Tribulova, N., Pristacova, J., Uhrík, B., Thomas, T., Khaper, N., Kaul, N. and Singal, P.K. (1995) Hydrogen peroxide changes in ischemic and reperfused heart. Cytochemistry and biochemical and X-ray microanalysis. *The American Journal of Pathology*, 147(3) 772–781.
- Snapp, B.D. and Heller, H.C. (1981) Suppression of metabolism during hibernation in ground squirrels (*Citellus lateralis*). *Physiological Zoology*, 54(3) 297–307.
- Stram, A.R. and Payne, R.M. (2016) Post-translational modifications in mitochondria: protein signaling in the powerhouse. *Cellular and Molecular Life Sciences*, 1–11.
- Tomitsuka, E., Kita, K. and Esumi, H. (2009) Regulation of succinate-ubiquinone reductase and fumarate reductase activities in human complex II by phosphorylation of its flavoprotein subunit. *Proceedings of the Japan Academy, Series B*, 85(7) 258–265.

CHAPTER 5

5 Manipulating metabolism in liver mitochondria of hibernators

5.1 Introduction

Hibernation, characterized by a seasonal suppression of metabolic rate and body temperature, is an excellent natural model of metabolic suppression. Small mammals such as the 13-lined ground squirrel spend most of the hibernation season in torpor, during which body temperature and metabolic rate are actively suppressed by approximately 95% (reviewed in Chapter 1.2.2). Bouts of torpor, lasting up to 2 weeks, are periodically interrupted by spontaneous arousal into interbout euthermia (IBE), during which body temperature and metabolic rate rapidly increase to euthermic levels and are maintained for 8-12 hours. Despite experiencing an extreme reduction in body temperature, metabolism, and blood flow followed by rapid rewarming, hibernators appear to suffer no damage to organs and tissues (e.g., Zancanaro et al., 1999), an intriguing phenomenon for both biological and medical research.

The ability to induce metabolic suppression in non-hibernators (including humans) would have diverse medical applications, such as limiting organ damage during organ transplantation, cardiac arrest, and surgery. At the whole animal level several pharmacological compounds, including hydrogen sulfide, 5'-adenosine monophosphate, and thyroid hormones, have been investigated for their potential in inducing a torpor-like state in non-hibernators (reviewed by Bouma et al., 2012). Some of these compounds appear to reduce metabolic rate and body temperature in some mammals, but not in others (see section 1.7). Further, the functional significance of these compounds is unclear since the underlying mechanisms responsible for metabolic suppression during hibernation are largely unknown.

Mitochondria, responsible for the vast majority of aerobic ATP generation, are critical to a mechanistic understanding of the rapid metabolic changes that occur during hibernation. In 13-lined ground squirrels, isolated liver mitochondrial metabolism is suppressed by as much as 70% during torpor, with maximal suppression occurring early during entrance into a torpor bout, prior to large decreases in body temperature (Chung et al., 2011). This suppression corresponds with a reduction in flux through electron transport system (ETS) complexes I and II in intact mitochondria, as well as a reduction in the maximal enzymatic activity of both complexes (Chapter 2). In addition, the suppression in the activity of complexes I and II is paralleled by changes in their phosphorylation state between torpor and IBE; phosphorylation of the 75 kDa subunit of complex I increases during torpor, compared with IBE, whereas phosphorylation of the complex II flavoprotein subunit decreases (Chapter 4). In this study, I investigate the hypothesis that phosphorylation mediates the regulation of these enzymes and mitochondrial respiration during torpor-IBE cycles.

Phosphorylation of mitochondrial proteins is an active area of research, and is proposed to be a critical regulator of mitochondrial metabolism (Thomson, 2002; Hopper et al., 2006; Pagliarini and Dixon, 2006), but little is known about mitochondrial kinases and phosphatases that likely regulate these modifications. The mitochondrial cyclic AMP-dependent protein kinase (PKA) has been well studied recently as a regulator of acute changes to mitochondrial metabolism, but its role is controversial. Acín-Pérez et al. first demonstrated a complete intra-mitochondrial PKA signaling cascade linking nutrient sensing with functional changes in mitochondrial metabolism (Acín-Pérez et al., 2009). In this pathway, bicarbonate (HCO_3^-), derived from the TCA cycle, activates intramitochondrial soluble adenylylase (sAC) which generates cyclic AMP, in turn activating PKA. The authors manipulated this pathway in rat liver by incubating isolated mitochondria with 8Br-cAMP (a membrane-permeable cAMP analog) and HCO_3^- . Both treatments increased State 3 respiration rate, and the effect was interpreted as an increase in ETS complex activity following phosphorylation by PKA. These functional changes were indeed paralleled by changes in the phosphorylation state of several ETS complex proteins, including subunits 1 and 4-2 of complex IV.

Following evidence from Acín-Pérez et al. (2009) that stimulation of the mitochondrial PKA pathway increases mitochondrial respiration, subsequent studies have found contradictory results. In permeabilized rat heart fibers, addition of a membrane-permeable cAMP analog actually decreased mitochondrial respiration (Rosca et al., 2011). A study investigating the PKA pathway found no effect of 8Br-cAMP on pig heart mitochondrial respiration, and furthermore, no effect of 8Br-cAMP nor H89 (a specific inhibitor of PKA) on any post-translational modifications of mitochondrial proteins (Covian et al., 2014). These contradictory results were found using heart tissue, however, which likely undergoes differential mitochondrial regulation than liver, the tissue in which PKA pathway activation was initially demonstrated. Given the acute changes in liver mitochondrial metabolism between torpor and IBE, ground squirrel liver mitochondria are an excellent model in which to investigate the potential roles of the PKA pathway and post-translational modifications for mediating metabolic changes.

The first objective of this study was to alter respiration in intact isolated mitochondria by manipulating the PKA pathway. If PKA-mediated phosphorylation of mitochondrial proteins is responsible for the changes in liver mitochondria metabolism between torpor and IBE, then activators of the PKA pathway would have different effects on mitochondria from torpid and IBE animals. Since complex II is dephosphorylated during torpor, I predicted that activation of the PKA pathway would increase state 3 respiration in mitochondrial isolated from animals in torpor.

The second goal of this study was to manipulate the phosphorylation state of complexes I and II directly (i.e. not in intact mitochondria) and compare the effects on maximal activity between torpor and IBE. If phosphorylation of complex I is responsible for suppression of its maximal activity during torpor, I predicted that removal of phosphate groups (via treatment with phosphatases) should increase the V_{\max} of complex I of from mitochondria of torpid animals. Likewise, phosphorylation of complex I (via treatment with ATP and kinases) should reduce V_{\max} in mitochondria from IBE animals. If phosphorylation of complex II regulates the increase in its activity during IBE, phosphatase treatment should decrease its V_{\max} in mitochondria from IBE animals, and

phosphorylation should increase its V_{\max} in mitochondria from torpid animals. I tested these hypotheses using the same mitochondria used for respiration and proteomics experiments presented in Chapters 3 and 4.

5.2 Materials and Methods

5.2.1 Animals

Ground squirrels were live trapped in Carman, MB, Canada and housed as described in Chapter 2 (Section 2.2.1). This study compared ground squirrels sampled during torpor (a stable body temperature near 5 °C for 3-5 days) and IBE (A stable body temperature near 37°C for 3-4 hours following spontaneous arousal).

5.2.2 Mitochondrial isolation

Liver tissue was dissected from ground squirrels immediately following euthanasia. Liver mitochondria were isolated via differential centrifugation and purified via Percoll gradient as described in Chapter 2 (Section 2.2.2). Purified mitochondria were suspended in 1 ml of homogenization buffer (250 mM sucrose, 10 mM HEPES, 1 mM EGTA, pH 7.4) and used immediately for assessment of mitochondrial respiration. The protein content of each mitochondrial sample was determined with protein assay dye (Bio-Rad) using BSA dissolved in homogenization buffer as protein standards. Aliquots containing 0.5 mg protein were centrifuged for 10 min at 10,000 g, and the resulting mitochondrial pellets were flash frozen and stored at -80°C for subsequent enzyme assays.

5.2.3 Mitochondrial respiration

Mitochondrial oxygen consumption was measured using an Oxygraph-2K high-resolution respirometer (Oroboros Instruments, Austria) as described in Chapter 2 (Section 2.2.3). Mitochondria (10 μ l, ~150 μ g protein) were transferred to respiration chambers containing 2 ml of mitochondrial respiration medium (0.5 mM EGTA, 3 mM MgCl₂, 60

mM L-lactobionate, 20 mM taurine, 10 mM KH_2PO_4 , 20 mM HEPES, 110 mM sucrose, 1 g/l fatty acid free BSA, pH 7.1; (Kuznetsov et al., 2008) under constant stirring (750 rpm) at 37 °C.

Various activators of the PKA pathway were added in attempts to stimulate endogenous PKA, and the resulting respiration rates were compared between torpor and IBE. For each treatment, parallel respiration measurements were conducted with and without the addition of 1 μM H89, an inhibitor of PKA. The following treatments were used: 1) Control (no addition of activators), 2) addition of 1 mM 8-Bromoadenosine 3',5'-cyclic monophosphate (8Br-cAMP), 3) addition of 0.8 mM CaCl_2 (corresponding with 0.95 μM free Ca^{2+}), and 4) addition of 1 mM 8Br-cAMP and 0.95 μM Ca^{2+} together. After a 10 min incubation with each treatment, 6 mM succinate and 0.5 μM rotenone were added to the respiratory chambers, followed 5 min later by 0.2 mM ADP to induce State 3. Respiration rates were expressed relative to total mitochondrial protein.

5.2.4 Treatment of mitochondrial homogenates with exogenous kinases and phosphatases

Mitochondrial homogenates were prepared by thawing mitochondrial pellets on ice and resuspended in either Protein Kinase Buffer (50 mM Tris, 10 mM MgCl_2 , 0.1 mM EDTA, 2 mM DTT, 0.01% (w/v) Brij 35, pH 7.5) or Protein Phosphatase Buffer (50 mM HEPES, 1 mM MnCl_2 , 100 mM NaCl, 2 mM DTT, 0.01% (w/v) Brij 35, pH 7.5).

Mitochondrial homogenates were prepared from previously frozen mitochondrial pellets. These samples were subjected to three cycles of freezing in liquid nitrogen and thawing on ice prior to incubation with kinases/phosphatases. Separate buffers were used for kinase and phosphatase treatments, following manufacturer specifications, to provide optimal reaction conditions for each enzyme.

For treatment with a protein kinase, mitochondrial homogenates (0.25 mg protein in Protein Kinase Buffer) were incubated with 2500 U cAMP-dependent Protein Kinase, Catalytic Subunit (PKA; New England BioLabs) and 200 μM ATP at 37 °C for 30 min. I

also conducted parallel incubations with no additions, to serve as a negative control. For treatment with a protein phosphatase, mitochondrial homogenates (0.25 mg in Protein Phosphatase Buffer) were incubated with 400 U Lambda Protein Phosphatase (LPP; New England BioLabs) at 37 °C for 30 min. I conducted a control incubation in parallel without any additions.

5.2.4 Enzyme assays

Following the incubations described above, I performed assays for maximal activity of both complex I and II, as described by (Kirby et al., 2007), using a Spectromax plate spectrophotometer (Molecular Devices, Sunnyvale, CA) at 37 °C. For each sample from an individual animal, assays were run in triplicate, and V_{max} values were calculated from the mean of triplicates. Complex I activity was measured following the addition of 5 μ l of mitochondrial homogenate (corresponding to 5 μ g protein) to 295 μ l of assay mixture containing 25 mM K_2HPO_4 (pH 7.4), 2 μ g/ml antimycin A, 2 mM KCN, 2.5 mg/ml BSA, and 0.2 mM NADH. Absorbance values (340 nm) were collected for 3-5 mins. Complex II activity was measured following the addition of 2.5 μ l of mitochondrial homogenate (corresponding to 2.5 μ g protein) to 296.5 μ l of assay mixture containing 25 mM K_2HPO_4 (pH 7.4), 2 μ g/ml rotenone, 2 μ g/ml antimycin A, 2 mM KCN, 20 mM succinate, and 50 μ M dichlorophenolindophenol (DCPIP). The reaction was started with 1 μ l of 10 μ M ubiquinone₁, and absorbance values (600 nm) were collected for 3-5 min.

5.2.6 Statistical analysis

All statistical analyses were conducted using R. The effects of treatment with PKA activators and H89 on respiration in isolated mitochondria were assessed using repeated measures two-factor ANOVA and Student-Newman-Keuls post-hoc tests, with hibernation state (torpor or IBE) as the first factor and PKA activator/inhibitor treatment as the second factor. The effects of kinases and phosphatase treatment on maximal activity of both ETS complexes I and II were assessed using two-factor repeated measures ANOVA and Student-Newman-Keuls post-hoc tests, with hibernation state

(torpor or IBE) as the first factor and treatment (Control or kinase/phosphatase) as the second factor. Differences were considered significant for p -values ≤ 0.05 .

5.3 Results

I compared respiration rates in isolated liver mitochondria from torpid and IBE ground squirrels following incubation with various activators and an inhibitor of the mitochondrial PKA pathway. Under control conditions (no activators or inhibitors), succinate-fueled state 3 respiration was suppressed by 70% during torpor relative to IBE ($p < 0.001$), consistent with previous results from our lab (Muleme et al., 2006; Chung et al., 2011; Brown et al., 2012). Incubation with H89, a specific inhibitor of PKA, had no effect on respiration in mitochondria from IBE ($p = 0.994$) or torpid ($p = 0.726$) animals (Figure 5-1).

While assessing the effects of PKA activators on mitochondrial respiration, I conducted parallel respiratory measurements with and without the addition of H89 as a control for the effect of PKA activation since H89 is a specific inhibitor of PKA. I predicted a greater proportional change in torpor than IBE so I expressed respiration rates relative to control state 3 rates (measured with no additions) for each mitochondrial sample. This analysis allows assessment of any differences between hibernation states in the degree that respiration changes relative to a common baseline. Absolute values for these measurements are presented in Table 5-1.

I used two-factor repeated measures ANOVA to analyze of the effects of hibernation state (torpor or IBE) and the effects of H89 inclusion for each PKA pathway activator. When mitochondria were incubated with 8Br-cAMP, there was no effect of hibernation state or inclusion of H89 on the relative respiration rate ($p = 0.867$ and $p = 0.793$, respectively; Figure 5-2A), and no interaction between the two factors ($p = 0.764$). Upon incubation with Ca^{2+} there was also no effect of hibernation state or H89 inclusion on relative respiration rate ($p = 0.148$ and $p = 0.723$, respectively; Figure 5-2B), and no

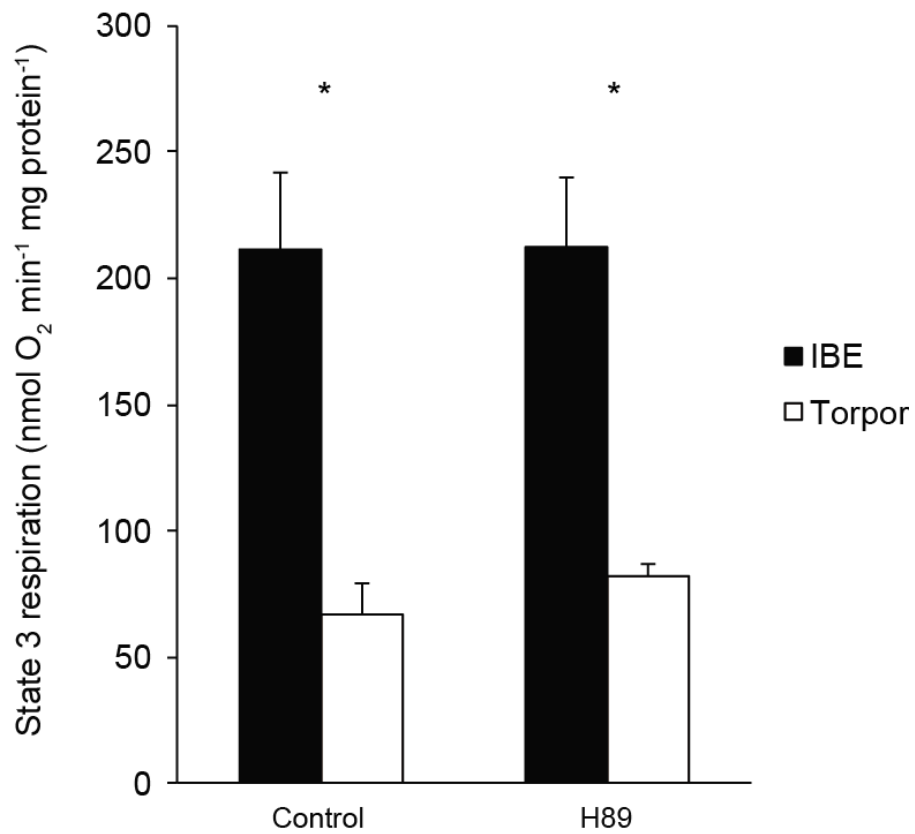


Figure 5-1. Succinate-fueled state 3 respiration in liver mitochondria in control conditions and following incubation with H89. Respiration was measured at 37 °C in mitochondria isolated from ground squirrels sampled during IBE (n=5) and torpor (n=5). Bars represent mean + SE. Asterisks indicate a significant difference between torpor and IBE within each treatment ($p \leq 0.05$).

Table 5-1. Succinate-fueled respiration in liver mitochondrial following incubation with activators of the PKA pathway.

Respiration rates ($\text{nmol O}_2 \text{ min}^{-1} \text{ mg protein}^{-1}$) were measured in liver mitochondria isolated from 13-lined ground squirrels in torpor ($n=5$) or IBE ($n=5$). An asterisk indicates a significant difference between torpor and IBE within a particular treatment.

		Control	H89	8Br-cAMP	8Br-cAMP+H89	Ca^{2+}	Ca^{2+} +H89	8Br-cAMP+ Ca^{2+}	8Br-cAMP+ Ca^{2+} +H89
IBE	Mean	211.63*	211.93*	199.57*	223.96*	327.26*	310.97*	284.47*	227.35*
	SE	30.29	28.25	36.99	30.54	48.67	45.58	45.82	43.13
Torpor	Mean	66.91	81.98	63.94	58.03	71.99	73.83	52.75	63.24
	SE	12.71	5.23	14.01	13.35	15.21	19.75	2.74	14.20

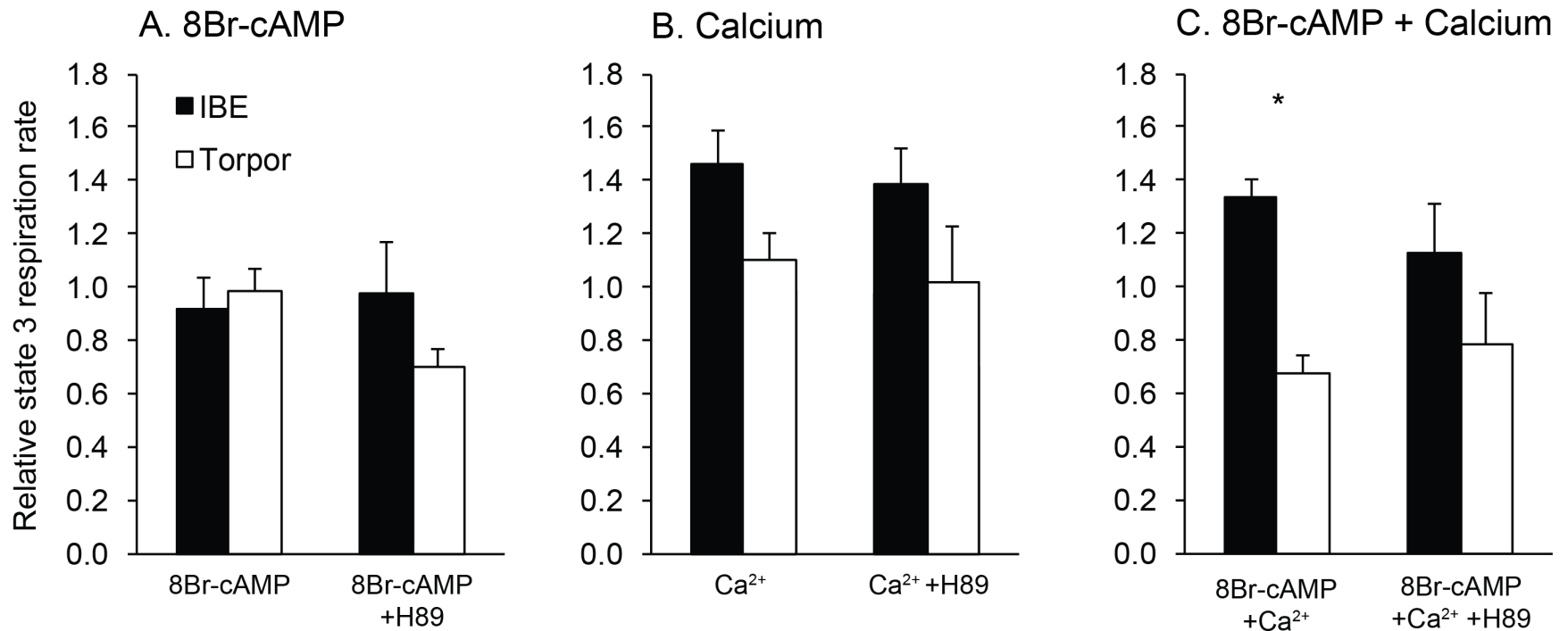


Figure 5-2. Relative succinate-fueled respiration in liver mitochondrial following incubation with activators of the PKA pathway. Mitochondria were isolated from animals sampled during IBE (n=5) and torpor (n=5). Respiration rates are expressed relative to the control state 3 rate for each treatment. Bars represent mean + SE. Asterisk indicate a significant difference between torpor and IBE within a treatment (p≤0.05).

interaction between the two factors ($p=0.327$). Following the addition of 8Br-cAMP and calcium together, there was a significant effect of hibernation state ($p=0.011$), with IBE showing a 30% increase relative to control and torpor showing a 30% decrease (Figure 5-2C). There was no significant effect of H89 inclusion overall ($p=0.142$), but a significant interaction between hibernation state and H89 inclusion. Post-hoc pairwise comparisons revealed a significant difference in response between torpor and IBE without H89 ($p=0.006$), but no difference between torpor and IBE with H89 inclusion ($p=0.151$).

I measured the maximal activities of ETS complexes I and II in homogenized liver mitochondria following incubation with exogenous kinases and phosphatases, and compared rates between torpor and IBE. I used two-factor repeated measures ANOVA to assess the effects of hibernation state and incubation of PKA or LPP on the maximal activities of each complex.

There was no significant effect of hibernation state nor PKA incubation on the V_{\max} of complex I ($p=0.150$ and $p=0.225$, respectively; Figure 5-3A), and no significant interaction between hibernation state and PKA incubation ($p=0.340$). Following LPP incubation, there was a significant interaction effect between hibernation state and incubation on the V_{\max} of complex I ($p=0.003$). In the control treatment (no addition of LPP), complex I V_{\max} was 20% higher in IBE compared to torpor ($p=0.038$; Figure 5-3B). Incubation with LPP significantly increased the V_{\max} of complex I in mitochondria from torpid animals ($p=0.009$), but had no effect on the complex I from IBE animals ($p=0.247$). Following LPP incubation, there was no difference in V_{\max} of complex I between IBE and torpor ($p=0.919$).

There was a significant interaction effect between hibernation state and PKA incubation on the V_{\max} of complex II ($p=0.042$). Within the control treatment, the V_{\max} of complex II was 60% higher in liver mitochondrial from IBE animals compared to torpor ($p<0.001$; Figure 5-4A). There was no significant effect of PKA incubation on complex II V_{\max} in the torpor or IBE group ($p=0.096$ and $p=0.344$, respectively). Following incubation with PKA, the difference in V_{\max} between torpor and IBE was diminished, but still

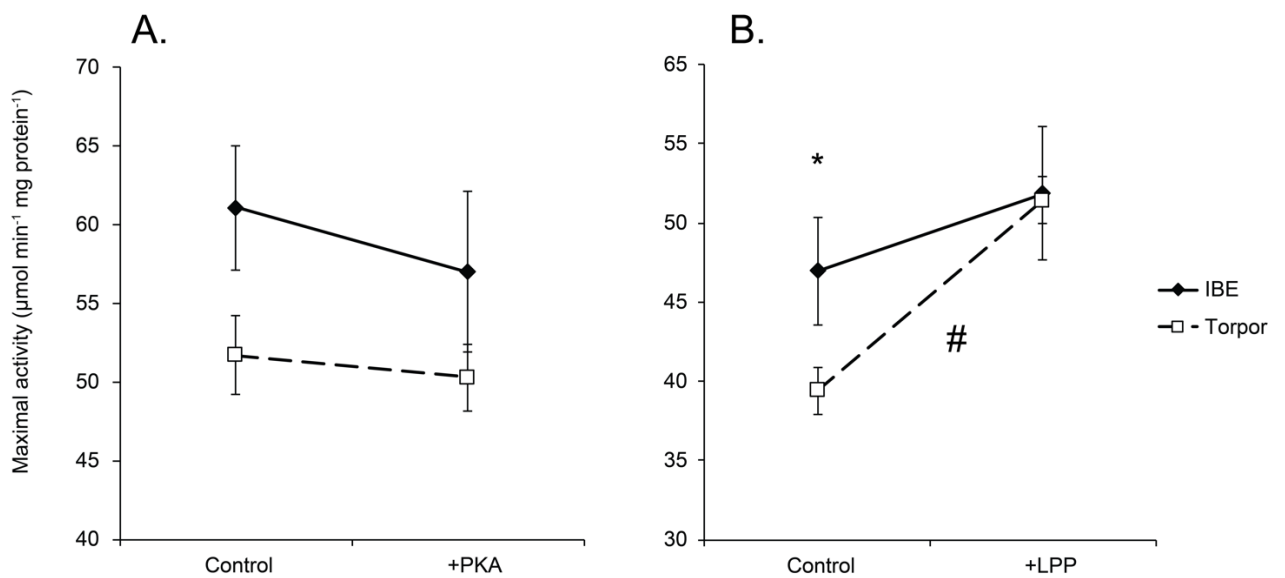


Figure 5-3. Maximal activity of ETS Complex I in isolated liver mitochondria following incubation with protein kinase A (PKA; Panel A) and protein phosphatase (PP; Panel B). Homogenates were prepared from mitochondria isolated from animals sampled during torpor (n=6) and IBE (n=6). A separate control is included for each treatment since the incubations were conducted in different buffers. Asterisks indicate a significant difference between torpor and IBE within a treatment, and a significant effect of treatment within either torpor or IBE is indicated by “#” (p≤0.05).

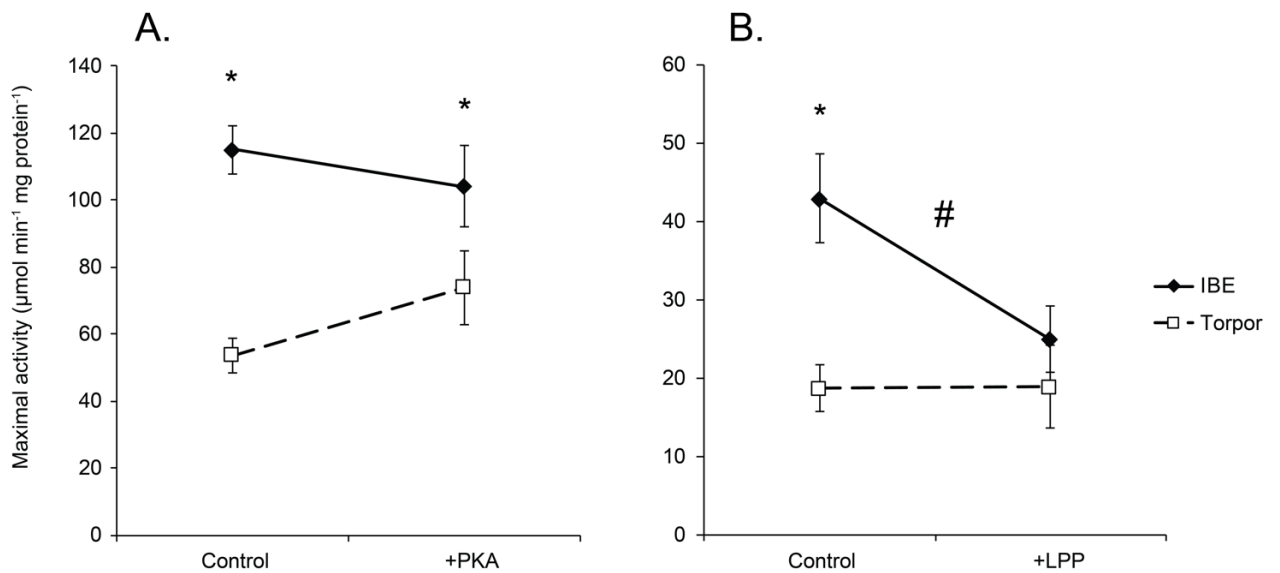


Figure 5-4. Maximal activity of ETS Complex II in isolated liver mitochondria following incubation with protein kinase A (PKA; Panel A) and protein phosphatase (PP; Panel B). Homogenates were prepared from mitochondria isolated from animals sampled during torpor (n=6) and IBE (n=6). A separate control is included for each treatment since the incubations were conducted in different buffers. Asterisks indicate a significant difference between torpor and IBE within a treatment, and a significant effect of treatment within either torpor or IBE is indicated by “#” ($p \leq 0.05$).

significantly different ($p=0.012$). There was also a significant interaction effect between hibernation state and LPP incubation on the V_{\max} of complex II ($p=0.033$). Incubation with LPP significantly decreased the V_{\max} of complex II in mitochondria from IBE animals ($p=0.015$; Figure 5-4B), but had no effect on complex II from torpid animals (0.983). Following LPP incubation, there was no difference in the V_{\max} of complex II between IBE and torpor ($p=0.256$).

5.4 Discussion

This study demonstrates that post-translational modification by phosphorylation is likely involved in regulating the activity of complexes I and II during hibernation. I successfully manipulated the maximal activity of both complexes I and II by incubating liver mitochondrial homogenates with exogenous kinases and phosphatases, which suggests the role of phosphorylation in regulating the activity of these enzymes.

I first attempted to manipulate the endogenous PKA pathway in liver mitochondria isolated from ground squirrels. I predicted that successful activation of PKA would cause a greater increase in respiration in mitochondria isolated from torpid animals, with PKA-mediated phosphorylation activating complex II. A possible corollary of this prediction is that inhibition of PKA, using the specific inhibitor H89, would decrease complex II phosphorylation in IBE, resulting in a suppression of liver mitochondrial respiration. Indeed, recent research with rat liver mitochondria found a 50% suppression in state 3 respiration following H89 incubation (Acín-Pérez et al., 2009). In my experiment, however, incubation with H89 had no effect on respiration in mitochondria from either torpid or IBE squirrels (Figure 5-1), indicating either that there is no immediate effect of inhibiting the PKA pathway in either hibernation state, or that in my experiments, H89 was not able to enter the mitochondrial matrix.

I subsequently attempted to activate intramitochondrial PKA directly by incubating intact isolated mitochondria with 8Br-cAMP, a cAMP analog that has been shown to activate

the PKA pathway in rat liver mitochondria (Acín-Pérez et al., 2009). In my experiments, incubation with 8Br-cAMP had no effect on respiration in either hibernation state (Figure 5-2A), which suggests that either 8Br-cAMP was not able to enter the mitochondria, or that subsequent PKA activation has no effect on mitochondrial respiration. In addition to the 30 min incubations with 1 mM 8Br-cAMP, I also performed preliminary experiments using an incubation time of up to 60 minutes, conditions in which 8Br-cAMP has been shown to reach the mitochondrial matrix in cardiomyocytes (Di Benedetto et al., 2013). Even with such extended incubations, respiration rates were not affected (data not shown). Covian et al. (2014) found a similar insensitivity of isolated pig heart mitochondria to 8Br-cAMP, and in addition found no effect of db-cAMP, a cAMP analog that is 10-fold more lipophilic. From these results I conclude that liver mitochondria of 13-lined ground squirrels are insensitive to 8Br-cAMP. It is unclear why ground squirrel mitochondria would be insensitive to conditions shown to increase respiration in rat liver, but perhaps the PKA pathway does not play an important regulatory role in liver mitochondria during hibernation.

I next attempted to stimulate PKA indirectly by incubating mitochondria with Ca^{2+} , which has been shown to activate mitochondrial sAC (Litvin et al., 2003). Calcium did appear to increase respiration relative to control, at least in IBE, but the difference in response between torpor and IBE was not significant. Moreover, inclusion of H89 did not change the effect of Ca^{2+} , which indicates that any Ca^{2+} effect is not mediated through PKA activation. Interestingly, incubation with 8Br-cAMP and calcium together had a different effect on mitochondria from torpor and IBE animals; in IBE, respiration increased by 40% relative to the control rate, and in torpor respiration decreased by 40% (Figure 5-2C). This suggests an effect of PKA pathway activation, as the parallel incubation with H89 led to no difference between torpor and IBE. It is unclear why 8Br-cAMP and calcium together affected mitochondrial respiration when either activator alone had no effect. This result is also contrary to my prediction that phosphorylation via PKA would lead to an increase in respiration in mitochondria from torpid animals. It is possible that my experimental treatments did not successfully activate the endogenous

mitochondrial PKA pathway, and it is also possible that the PKA pathway is not responsible for the changes in phosphorylation between torpor and IBE.

Following unsuccessful attempts to stimulate the PKA pathway within intact mitochondria, I investigated the effect of phosphorylation on ETS enzyme activity directly. I focused on complexes I and II since I have shown that their maximal activities are suppressed during torpor relative to IBE (Chapter 2) and both enzymes show differential phosphorylation between torpor and IBE (Chapter 4). I measured V_{\max} of each complex following incubation of mitochondrial homogenates with both exogenous PKA (with ATP) and an exogenous phosphatase to stimulate phosphorylation and dephosphorylation, respectively. Treatment with exogenous phosphatases significantly increased complex I activity in liver mitochondria from torpid animals but had no effect on mitochondria from IBE animals (Figure 5-4), suggesting that phosphorylation is necessary for the suppression of complex I during torpor, since removal of phosphate groups resulted in a complete reversal of suppression. These data fit with my previous findings that the 75 kDa subunit of complex I is phosphorylated to a greater degree during torpor compared to IBE (Chapter 4). Phosphorylation of complex I has been well described, though the underlying signaling mechanisms and the effects of phosphorylation on the activity of the enzyme are less understood. In rat brain, the 39 kDa subunit of complex I can be phosphorylated (Augereau et al., 2005), though to my knowledge, no phosphorylation sites have been identified on the 75 kDa subunit. In mitochondria isolated from bovine heart, phosphorylation of complex I by mitochondrial PKA is associated with activation of the enzyme (Papa et al., 1996). Other studies have demonstrated that complex I can be phosphorylated by Src kinases. Reports about the effects of phosphorylation of complex I by this pathway vary, however, with some showing decreased activity associated with loss of phosphorylation (Hébert-Chatelain et al., 2012; Ogura et al., 2012), but others showing that increased phosphorylation results in lower complex I, activity (Hébert-Chatelain et al., 2011).

Treatment with an exogenous phosphatase substantially reduced the V_{\max} of complex II in mitochondria from IBE animals but had no effect of mitochondria from torpid animals

(Figure 5-4B). These results provide strong evidence that dephosphorylation of complex II during entrance into torpor contributes to the suppression of mitochondrial respiration in torpor, which parallel the proteomics data from Chapter 4 in which I demonstrated that phosphorylation of the flavoprotein subunit of complex II is greater in IBE compared to torpor. Incubation with PKA had no significant effect on complex II activity in mitochondria from either torpor or IBE animals (Figure 5-4A), which suggests that the differences in phosphorylation between torpor and IBE are mediated by a kinase other than PKA. In support of this theory, a recent study found that phosphorylation of the flavoprotein subunit increased complex II activity (Acín-Pérez et al. 2014). The regulatory phosphorylation site was identified as Y604, phosphorylation of this site was mediated by Fgr kinase, a member of the Src kinase family.

PKA phosphorylates serine and threonine residues specifically, but LPP dephosphorylates any phosphorylated residue (serine, threonine, and tyrosine). Since there were significant effects of the phosphatase but not PKA, the regulatory phosphorylation sites are likely tyrosine residues. My data suggest that a pathway other than PKA may be responsible for the regulatory phosphorylation events during hibernation. Src kinases, which specifically phosphorylate tyrosine residues and have been well described in rat brain mitochondria (Salvi et al., 2002), are likely candidates for mediating this phosphorylation *in vivo*. Src kinases can be regulated directly by cellular conditions; for example, Fgr kinase activity is stimulated by increased H₂O₂ concentration, resulting in phosphorylation and increased activity of complex II (Acín-Pérez et al., 2014). Such a mechanism could underlie regulation of complexes I and II in hibernators, since there is evidence of changes in reactive oxygen species (ROS) production by liver mitochondria during hibernation (Brown et al., 2012). Src kinases are also regulated by their own phosphorylation state, which is in turn regulated by upstream kinases and phosphatases (Roskoski, 2005), though little is known about how these upstream kinases and phosphatases are regulated. Protein tyrosine phosphatase, mitochondrial 1 (PTPMT1) is a tyrosine-specific phosphatase that is involved in desphosphorylating mitochondrial Src kinases as well as other target proteins. PTPMT1 can also directly dephosphorylate complex II, and inhibition of PTPMT1 results in

increased complex II phosphorylation with a corresponding increase in its activity (Nath et al., 2015).

Future work should investigate the residues that are differentially phosphorylated on complexes I and II, since the phosphorylation sites themselves will offer clues about the mechanisms that underlie the differential phosphorylation. If the phosphorylation sites are tyrosine residues, then Src kinases are a likely regulatory mechanism. If Src kinases are responsible for differential phosphorylation, it would be useful to gain a better understanding of ROS production (using recently-developed techniques that can simultaneously measure O₂ consumption and ROS production) as well as redox status in liver mitochondria over a torpor-IBE cycle.

5.5 Summary

Phosphorylation is an important regulator of enzyme activity and, likely, mitochondrial metabolism during hibernation. Manipulation of phosphorylation state at the enzymatic level had significant effects on maximal activities of complexes I and II, that correspond at least partially with the pattern of respiration seen in intact mitochondria. However, my attempts to stimulate of an intramitochondrial kinase, PKA, did not significantly alter respiration rates. Future work investigating the endogenous regulatory pathways (e.g. kinases and phosphatases) responsible for these phosphorylation events is necessary for before manipulation of metabolism at higher biological levels can occur.

5.6 References

- Acín-Pérez, R., Salazar, E., Kamenetsky, M., Buck, J., Levin, L.R. and Manfredi, G. (2009) Cyclic AMP produced inside mitochondria regulates oxidative phosphorylation. *Cell Metabolism*, 9(3) 265–276.
- Acín-Pérez, R., Carrascoso, I., Baixauli, F., Roche-Molina, M., Latorre-Pellicer, A., Fernández-Silva, P., Mittelbrunn, M., Sanchez-Madrid, F., Pérez-Martos, A., Lowell, C.A., Manfredi, G. and Enríquez, J.A. (2014) ROS-triggered phosphorylation of complex II by Fgr kinase regulates cellular adaptation to fuel use. *Cell Metabolism*, 19(6) 1020–1033.
- Augereau, O., Claverol, S., Boudes, N., Basurko, M.-J., Bonneu, M., Rossignol, R., Mazat, J.-P., Letellier, T. and Dachary-Prigent, J. (2005) Identification of tyrosine-phosphorylated proteins of the mitochondrial oxidative phosphorylation machinery. *Cellular and Molecular Life Sciences*, 62(13) 1478–1488.
- Bouma, H.R., Verhaag, E.M., Otis, J.P., Heldmaier, G., Swoap, S.J., Strijkstra, A.M., Henning, R.H. and Carey, H.V. (2012) Induction of torpor: Mimicking natural metabolic suppression for biomedical applications. *Journal of Cellular Physiology*, 227(4) 1285–1290.
- Brown, J.C.L., Chung, D.J., Belgrave, K.R. and Staples, J.F. (2012) Mitochondrial metabolic suppression and reactive oxygen species production in liver and skeletal muscle of hibernating thirteen-lined ground squirrels. *American Journal of Physiology - Regulatory, Integrative and Comparative Physiology*, 302(1) R15–28.
- Chung, D., Lloyd, G.P., Thomas, R.H., Guglielmo, C.G. and Staples, J.F. (2011) Mitochondrial respiration and succinate dehydrogenase are suppressed early during entrance into a hibernation bout, but membrane remodeling is only transient. *Journal of Comparative Physiology B - Biochemical, Systems, and Environmental Physiology*, 181(5) 699–711.
- Covian, R., French, S., Kusnetz, H. and Balaban, R.S. (2014) Stimulation of oxidative phosphorylation by calcium in cardiac mitochondria is not influenced by cAMP and PKA activity. *Biochimica et Biophysica Acta*, 1837(12) 1913–1921.
- Di Benedetto, G., Scalzotto, E., Mongillo, M. and Pozzan, T. (2013) Mitochondrial Ca²⁺ uptake induces cyclic AMP generation in the matrix and modulates organelle ATP levels. *Cell Metabolism*, 17(6) 965–975.
- Hébert-Chatelain, E., Dupuy, J.-W., Letellier, T. and Dachary-Prigent, J. (2011) Functional impact of PTP1B-mediated Src regulation on oxidative phosphorylation in rat brain mitochondria. *Cellular and Molecular Life Sciences*, 68(15) 2603–2613.

- Hébert-Chatelain, E., Jose, C., Gutierrez Cortes, N., Dupuy, J.-W., Rocher, C., Dachary-Prigent, J. and Letellier, T. (2012) Preservation of NADH ubiquinone-oxidoreductase activity by Src kinase-mediated phosphorylation of NDUFB10. *Biochimica et Biophysica Acta*, 1817(5) 718–725.
- Hopper, R.K., Carroll, S., Aponte, A.M., Johnson, D.T., French, S., Shen, R.-F., Witzmann, F.A., Harris, R.A. and Balaban, R.S. (2006) Mitochondrial matrix phosphoproteome: effect of extra mitochondrial calcium. *Biochemistry*, 45(8) 2524–2536.
- Kirby, D.M., Thorburn, D.R., Turnbull, D.M. and Taylor, R.W. (2007) Biochemical assays of respiratory chain complex activity. *Methods in Cell Biology*, 80 93–119.
- Kuznetsov, A.V., Veksler, V., Gellerich, F.N., Saks, V., Margreiter, R. and Kunz, W.S. (2008) Analysis of mitochondrial function in situ in permeabilized muscle fibers, tissues and cells. *Nature Protocols*, 3(6) 965–976.
- Litvin, T.N., Kamenetsky, M., Zarifyan, A., Buck, J. and Levin, L.R. (2003) Kinetic properties of ‘soluble’ adenylyl cyclase. Synergism between calcium and bicarbonate. *The Journal of Biological Chemistry*, 278(18) 15922–15926.
- Muleme, H.M., Walpole, A.C. and Staples, J.F. (2006) Mitochondrial metabolism in hibernation: Metabolic suppression, temperature effects, and substrate preferences. *Physiological and Biochemical Zoology*, 79(3) 474–483.
- Nath, A.K., Ryu, J.H., Jin, Y.N., Roberts, L.D., Dejam, A., Gerszten, R.E. and Peterson, R.T. (2015) PTPMT1 inhibition lowers glucose through phosphorylation of SDH. *Cell Reports*, 10(5) 694–701.
- Ogura, M., Yamaki, J., Homma, M.K. and Homma, Y. (2012) Mitochondrial c-Src regulates cell survival through phosphorylation of respiratory chain components. *The Biochemical Journal*, 447(2) 281–289.
- Pagliarini, D.J. and Dixon, J.E. (2006) Mitochondrial modulation: reversible phosphorylation takes center stage? *Trends in Biochemical Sciences*, 31(1) 26–34.
- Papa, S., Sardanelli, A.M., Cocco, T., Speranza, F., Scacco, S.C. and Technikova-Dobrova, Z. (1996) The nuclear-encoded 18 kDa (IP) AQP subunit of bovine heart complex I is phosphorylated by the mitochondrial cAMP-dependent protein kinase. *FEBS Letters*, 379(3) 299–301.
- Rosca, M., Minkler, P. and Hoppel, C.L. (2011) Cardiac mitochondria in heart failure: normal cardiolipin profile and increased threonine phosphorylation of complex IV. *Biochimica et Biophysica Acta*, 1807(11) 1373–1382.
- Roskoski, R. (2005) Src kinase regulation by phosphorylation and dephosphorylation. *Biochemical and Biophysical Research Communications*, 331(1) 1–14.

- Salvi, M., Brunati, A.M., Bordin, L., La Rocca, N., Clari, G. and Toninello, A. (2002) Characterization and location of Src-dependent tyrosine phosphorylation in rat brain mitochondria. *Biochimica et Biophysica Acta*, 1589(2) 181–195.
- Thomson, M. (2002) Evidence of undiscovered cell regulatory mechanisms: phosphoproteins and protein kinases in mitochondria. *Cellular and Molecular Life Sciences*, 59(2) 213–219.
- Tomitsuka, E., Kita, K. and Esumi, H. (2009) Regulation of succinate-ubiquinone reductase and fumarate reductase activities in human complex II by phosphorylation of its flavoprotein subunit. *Proceedings of the Japan Academy, Series B*, 85(7) 258–265.
- Zancanaro, C., Malatesta, M., Mannello, F., Vogel, P. and Fakan, S. (1999) The kidney during hibernation and arousal from hibernation. A natural model of organ preservation during cold ischaemia and reperfusion. *Nephrology Dialysis Transplantation*, 14(8) 1982–1990.

CHAPTER 6

6 General Discussion

Metabolic suppression is a remarkable adaptation that allows animals to maintain energy homeostasis in conditions where the ability to obtain or transform energy from the environment is constrained. There has long been a search for the mechanisms that underlie the metabolic suppression that occurs during hibernation, and in particular, those related to the rapid transitions between torpor and interbout euthermia (IBE). In my thesis, I have demonstrated a mechanistic explanation for the reversible suppression of mitochondrial proteins during torpor that may underlie changes in mitochondrial metabolism between torpor and IBE. In this chapter I aim to integrate the results from the four experimental chapters in this thesis to propose a model by which mitochondrial metabolism is reversibly suppressed during torpor. I will also relate my results to a broader context of whole animal effects as well as describe how these findings will inform future directions for mechanistic research into metabolic suppression during hibernation.

6.1 A model for mitochondrial metabolic suppression during torpor

The most significant findings from my thesis work are that electron transport system (ETS) complexes I and II are differentially phosphorylated between torpor and IBE in liver mitochondria. These changes in phosphorylation parallel the suppression of liver mitochondrial metabolism that occurs during torpor along with suppression of the maximal enzymatic activity of complexes I and II.

With these novel results, I propose a model by which mitochondrial metabolism is reversibly suppressed during torpor. In this model, summarized in Figure 6-1, as 13-lined

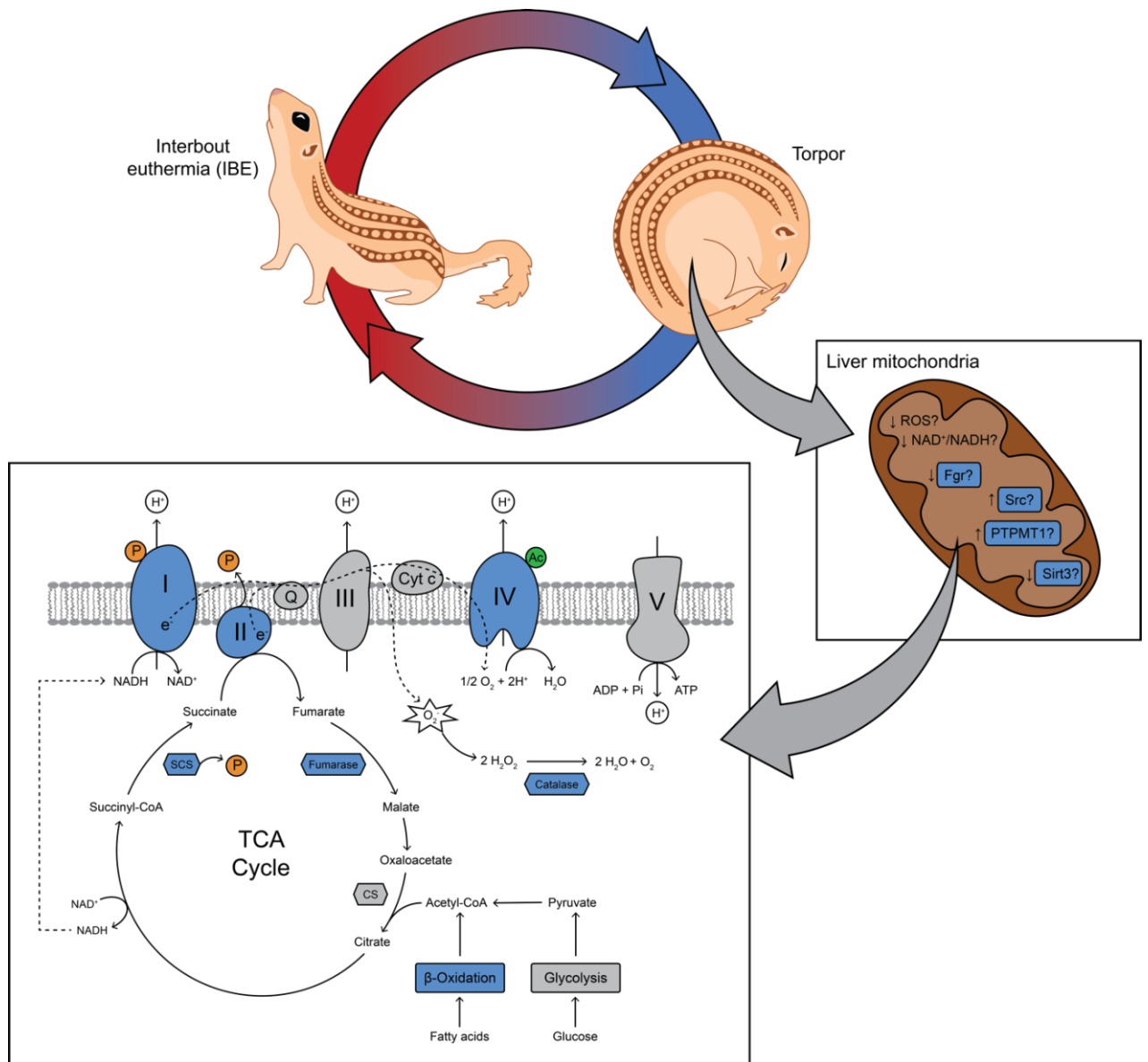


Figure 6-1. A model of potential mechanisms underlying reversible suppression of mitochondrial metabolism during entrance into torpor. This model integrates my findings to illustrate the significant changes to metabolic proteins that occur between torpor and IBE in liver mitochondria. In the TCA cycle, succinyl-CoA ligase (SCL) is dephosphorylated and fumarase protein content decreases. Complex II, involved in both the electron transport system and the TCA cycle, is desphosphorylated. In the electron transport system, complex I is phosphorylated (P) and complex IV is acetylated. These changes in phosphorylation are potentially mediated by tyrosine kinases (Fgr and Src) and phosphatases (PTPMT1) within liver mitochondria, which may respond to intramitochondrial signals such as reactive oxygen species (ROS). The activity of mitochondrial NAD-dependent deacetylase sirtuin-3 (Sirt3) potentially decreases to result in increased acetylation.

ground squirrels enter torpor, complex I undergoes increased phosphorylation, complex II undergoes increased dephosphorylation, and complex IV undergoes increased acetylation. Since my results indicate that the regulatory phosphorylation sites on complexes I and II are likely tyrosine residues, the changes in phosphorylation state of these enzymes are therefore likely mediated by mitochondrial tyrosine-specific kinase and phosphatases. Since overall phosphorylation appears to have contrasting effects on the activity of complexes I and II (with an inhibitory effect on complex I and an activating effect on complex II), the phosphorylation states of complexes I and II are likely mediated by different kinases and phosphatases (illustrated in detail in Figure 6-2). For the sake of simplicity I have designated these “kinase I” and “phosphatase I” for complex I, and “kinase II” and “phosphatase II” for complex II in my model. Figure 6-2 illustrates at a more detailed level how these kinase and phosphatases likely mediate changes in the phosphorylation states of complexes I and II in liver mitochondria as animals transition between torpor and IBE.

As suppression of complex I activity corresponds with increased phosphorylation during torpor, I propose that kinase I is activated and phosphatase I is inhibited during torpor. Possible candidate kinases are those within the Src kinase family, including Fyn, Src, Lyn, and Fgr kinases, which have been found within mitochondria (Salvi et al., 2002; Acín-Pérez et al., 2014). Activation of Src in particular corresponds with increased phosphorylation and decreased enzymatic activity of complex I (Hébert-Chatelain et al., 2011), so it is possible that Src kinase activation during torpor could underlie suppression of complex I activity in hibernators. Dephosphorylation of complex I during IBE may be mediated by a mitochondrial tyrosine-specific phosphatase. Several tyrosine phosphatases have been found within mitochondria, including PTPD1, PTP1B, and PTPMT1 (Lim et al., 2016), though no tyrosine phosphatases are currently known to directly dephosphorylate complex I.

As suppression of complex II activity corresponds with decreased phosphorylation during torpor, I propose that kinase II is inhibited and phosphatase II is activated during torpor.

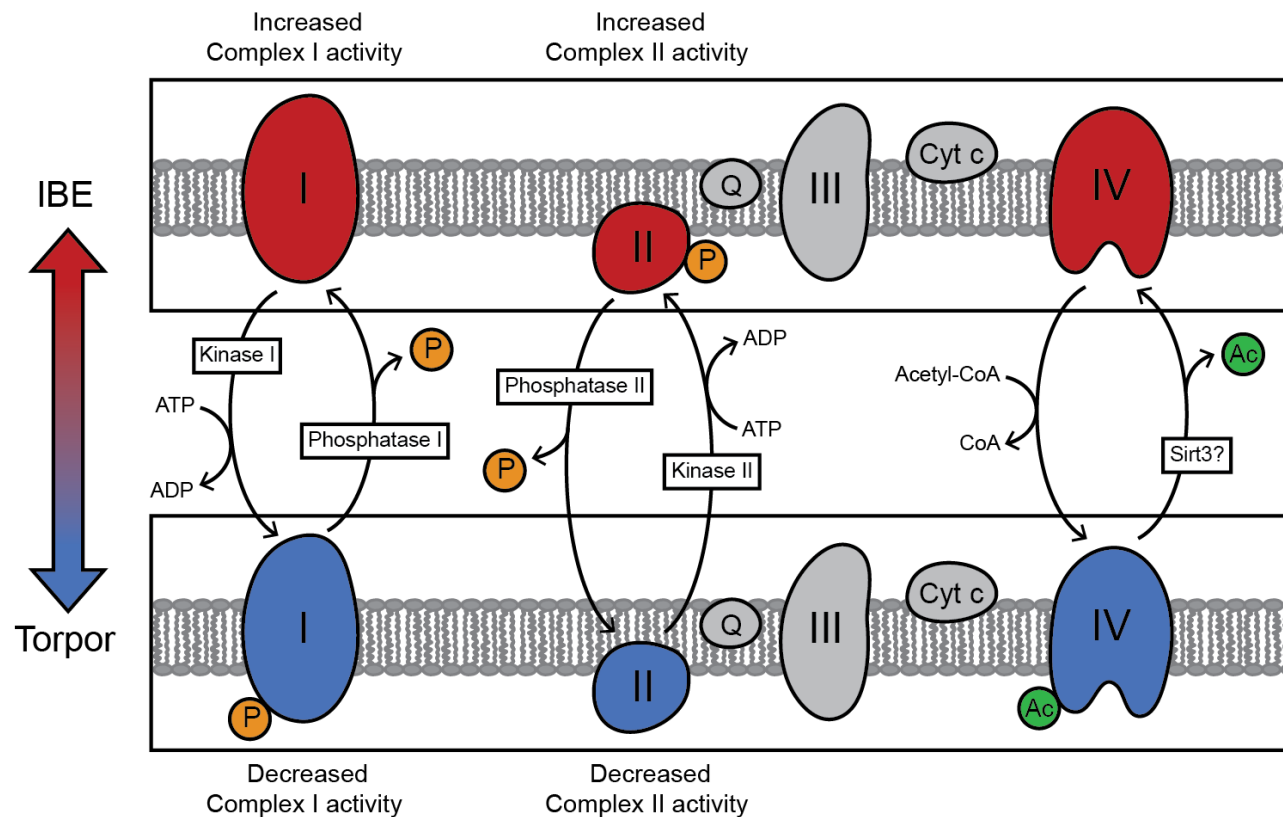


Figure 6-2. A model of potential changes in PTMs of mitochondrial electron transport system (ETS) proteins between IBE and torpor. During torpor, increased phosphorylation (P) of complex I by a potential “kinase I” corresponds with a decrease in enzymatic activity. Decreased phosphorylation of complex II, facilitated by a potential “phosphatase II” corresponds with a decrease in complex II activity. Increased acetylation (Ac) of complex IV potentially results from a decrease in the activity of NAD-dependent deacetylase sirtuin-3 (Sirt3).

Members of the Src kinase family are also potential candidates for the regulation of the phosphorylation state of complex II. Fgr kinase in particular is a potential regulator, since phosphorylation of complex II by Fgr kinase results in an increase in complex II activity (Acín-Pérez et al., 2014). Inhibition of such a kinase during torpor (and conversely, activation during IBE) could regulate the changes in phosphorylation state and activity of complex II that I demonstrated between torpor and IBE. Dephosphorylation of complex II during torpor may be mediated by a mitochondrial tyrosine-specific phosphatase. PTPMT1 is a likely candidate, since it has been shown to directly dephosphorylate complex II (Nath et al., 2015). Though little is known about regulation of PTPMT1 *in vivo*, pharmacological inhibition results in increased phosphorylation of complex II and a corresponding increase in complex II activity (Nath et al., 2015). It is possible, then, that PTPMT1 is activated during entrance into torpor, resulting in dephosphorylation of complex II and suppression of its activity.

Complex IV showed increased acetylation during torpor, though this did not correspond with any functional changes in enzyme activity. It is possible that, though no functional changes were apparent at the mitochondrial and tissue level, increased acetylation of complex IV during torpor contributes to mitochondrial metabolic suppression *in vivo*. Changes in acetylation of many mitochondrial proteins are regulated by Sirtuin 3 (Sirt3), which deacetylates proteins when intramitochondrial NAD⁺ concentration is high. Increased Sirt3 activity, mediated by and increased NAD⁺ concentration, could potentially regulate changes in acetylation of complex IV between torpor and IBE.

Decreased flux through the TCA cycle during torpor also likely contributes to liver mitochondrial metabolic suppression by limiting the availability of reducing equivalents to enter the ETS. Complex II, which is involved in both the ETS and the TCA cycle, is an important site of TCA cycle regulation. Succinyl-CoA ligase (SCL), which is significantly more phosphorylated in IBE than torpor, is another potential site of TCA cycle regulation. Increased phosphorylation of SCL is associated with increased activity; this phosphorylation occurs in a non-enzymatic manner, with increased phosphorylation resulting from increased free phosphate concentration (Phillips et al., 2009). Increased

phosphorylation of SCL during IBE could potentially result from an increase in matrix phosphate levels due to a decreased ATP/ADP ratio. Changes in phosphorylation could also result from increased dephosphorylation during torpor, potentially mediated by a mitochondrial phosphatase. There are currently no known phosphatases that target SCL however, and the regulatory phosphorylation sites are also unknown. Together, decreased SCL activity, decreased fumarase protein content, and decreased complex II activity could cause a substantial decrease in flux through the TCA cycle during torpor. Future work should investigate potential changes in enzymatic activity of SCL and fumarase between torpor and IBE to determine their contribution to mitochondrial suppression during torpor.

The signals that ultimately result in changes in PTMs of mitochondrial proteins may either originate within the mitochondria or involve secondary cellular messengers. It is possible that the mechanism responsible for activation and inhibition of regulatory kinases and phosphatases involves a yet unknown central signal; such a “hibernation induction trigger” originating in the blood could trigger the changes in regulatory PTMs that correspond with mitochondrial metabolic suppression. It is also possible that this signaling mechanism involves molecules originating within mitochondria. For example, Fgr kinase, which alters complex II activity by phosphorylation, is activated by increased mitochondrial H₂O₂ concentrations (Acín-Pérez et al., 2014). Since there is evidence of changes in ROS production by liver mitochondria during a torpor-IBE cycle (Brown et al., 2012), H₂O₂ could be a potential intramitochondrial signaling mechanism. For example, a potential increase in H₂O₂ concentration during arousal into IBE could activate Fgr kinase, leading to phosphorylation and subsequent activation of complex II.

6.2 The role of liver mitochondrial suppression in whole-animal metabolic suppression

Suppressing flux through complexes I and II likely represents an important mechanism for regulating metabolic changes *in vivo*. Since complexes I and II are the main sites

for reducing equivalents (NADH, FADH₂, respectively) to enter the ETS, suppression of their activities would greatly suppress the entire oxidative phosphorylation pathway and thus ATP production. Suppression of complex II in particular represents a significant site of regulation, since suppression of complex II activity would also contribute to reduced TCA cycle flux. After exploring regulatory mechanisms of liver mitochondrial suppression, it is worthwhile considering their role in the context of whole-animal metabolic suppression. While the 70% suppression that occurs in liver mitochondria during torpor may be largely explained by phosphorylation-mediated decreases in the enzymatic activities of ETS complexes I and II, whole-animal metabolism is suppressed by upwards of 95%. How much, then, can regulated suppression of mitochondrial metabolism contribute to the overall metabolic suppression that occurs during hibernation?

The metabolic suppression that occurs as an animal enters torpor is the summation of three separate components: 1) decreased thermogenic metabolism mediated by a shift in thermoregulatory set point, 2) active suppression of metabolism in non-thermogenic tissues, and 3) passive thermal effects. A large portion of the decrease in thermogenic metabolism is likely mediated by decreased thermogenesis in brown adipose tissue, as brown adipose tissue mitochondrial respiration is suppressed by up to 60% in torpor compared to IBE (McFarlane et al., 2017).

Active suppression of mitochondrial metabolism would be most important before body temperature decreases, and thus, along with adjusting the thermoregulatory set point, likely plays an important role in initiating the reduction in metabolic rate before passive thermal effects become significant. Liver is responsible for roughly 12% of basal metabolic rate (BMR) in small rodents (Martin and Fuhrman, 1955), and mitochondrial respiration has been estimated to account for as much as 90% of BMR (Rolfe and Brown, 1997). Active suppression in liver mitochondria alone can therefore explain roughly 7.5% of the total metabolic suppression that occurs in 13-lined ground squirrels, even with no change in body temperature. Active suppression of mitochondrial metabolism in other tissues can explain more of the whole animal metabolic suppression. Suppression of

skeletal muscle mitochondria can explain roughly 9% of whole-animal metabolic suppression, as skeletal muscle contributes approximately 34% of BMR (Martin and Fuhrman, 1955) and muscle mitochondria are suppressed by 30% in torpor (Brown et al., 2012). It would be useful to measure mitochondrial respiration in other metabolically active tissues such as the gut and kidneys, which make up an additional 20% of BMR and could thus contribute significantly to metabolic suppression.

Although the liver is a metabolically important organ, the suppression that occurs in liver mitochondria seems disproportionately high compared to other tissues. Recent work suggests that the liver may also be important to thermogenesis in 13-lined ground squirrels since uncoupling proteins UCP2 and UCP3 are upregulated in the winter (K.E. Mathers, L.I. Hayward and J.F. Staples, *in preparation*). If the liver is indeed involved in thermogenesis in hibernators, rapid suppression of mitochondrial metabolism during torpor (and reversal during IBE) could provide a much more significant contribution to the changes in body temperature that occur over a torpor-IBE cycle.




6.3 Conclusions

In my thesis, I have demonstrated that differential phosphorylation of ETS complexes I and II underlies significant changes in their activities as well as metabolism of intact mitochondria between torpor and IBE. It will be useful to characterize the exact sites of the proteins that are differentially phosphorylated, as such information will offer more insights into how these changes occur and suggest targets for manipulation. Src kinases and PTPMT1 may play an important role in regulating the changes in phosphorylation that occur between torpor and IBE. Future work should characterize these pathways and their targets in liver mitochondria of hibernators and attempt to manipulate them.

6.4 References

- Acín-Pérez, R., Carrascoso, I., Baixauli, F., Roche-Molina, M., Latorre-Pellicer, A., Fernández-Silva, P., Mittelbrunn, M., Sanchez-Madrid, F., Pérez-Martos, A., Lowell, C.A., Manfredi, G. and Enríquez, J.A. (2014) ROS-triggered phosphorylation of complex II by Fgr kinase regulates cellular adaptation to fuel use. *Cell Metabolism*, 19(6) 1020–1033.
- Brown, J.C.L., Chung, D.J., Belgrave, K.R. and Staples, J.F. (2012) Mitochondrial metabolic suppression and reactive oxygen species production in liver and skeletal muscle of hibernating thirteen-lined ground squirrels. *American Journal of Physiology - Regulatory, Integrative and Comparative Physiology*, 302(1) R15-28.
- Hébert-Chatelain, E., Dupuy, J.-W., Letellier, T. and Dachary-Prigent, J. (2011) Functional impact of PTP1B-mediated Src regulation on oxidative phosphorylation in rat brain mitochondria. *Cellular and Molecular Life Sciences*, 68(15) 2603–2613.
- Lim, S., Smith, K.R., Lim, S.-T.S., Tian, R., Lu, J. and Tan, M. (2016) Regulation of mitochondrial functions by protein phosphorylation and dephosphorylation. *Cell & Bioscience*, 6 25.
- Martin, A.W. and Fuhrman, F.A. (1955) The relationship between summated tissue respiration and metabolic rate in the mouse and dog. *Physiological Zoology*, 18–34.
- Nath, A.K., Ryu, J.H., Jin, Y.N., Roberts, L.D., Dejam, A., Gerszten, R.E. and Peterson, R.T. (2015) PTPMT1 inhibition lowers glucose through phosphorylation of SDH. *Cell Reports*, 10(5) 694–701.
- Phillips, D., Aponte, A.M., French, S.A., Chess, D.J. and Balaban, R.S. (2009) Succinyl-CoA synthetase is a phosphate target for the activation of mitochondrial metabolism. *Biochemistry*, 48(30) 7140–7149.
- Rolfe, D.F. and Brown, G.C. (1997) Cellular energy utilization and molecular origin of standard metabolic rate in mammals. *Physiological Reviews*, 77(3) 731–758.
- Salvi, M., Brunati, A.M., Bordin, L., La Rocca, N., Clari, G. and Toninello, A. (2002) Characterization and location of Src-dependent tyrosine phosphorylation in rat brain mitochondria. *Biochimica et Biophysica Acta*, 1589(2) 181–195.

APPENDIX A – 13-lined ground squirrel trapping permit

		WB11228 Valid 	WILDLIFE SCIENTIFIC PERMIT
Subject to the provisions of <i>The Wildlife Act</i> , the regulations made thereunder and the conditions set out in this permit:			
Permit Holder:		James F. Staples Department of Biology University of Western Ontario London ON N6A 5B9	
Is hereby authorised to conduct scientific research on the following wildlife or wildlife habitat:			
Species:		Thirteen-lined Ground Squirrels (<i>Spermophilus tridecemlineatus</i>)	
At, within or on the following location:			
Location:		University of Manitoba Carman Research Station	
Conditions:			
1	Research is limited to the activities described in the original application, proposal, or an amendment thereto that has been approved by the Director, Wildlife and Ecosystem Protection Branch, which form part of this permit. Where there is a difference between the application, proposal or amendment and this permit, this permit prevails.		
2	The authority granted by this permit is limited to (i) an employee or subcontractor of the permit holder while engaged in the duties approved or required by the permit holder, or (ii) an associate, or a person supervising or working under the supervision of the permit holder. The permit holder shall provide a person under subclause (ii), when working alone, with a counter-signed and dated photocopy of this permit.		
3	Prior to undertaking any field activity, the permit holder shall notify the local Natural Resource Officer.		
4	The permit holder may live trap, possess, and release the species identified herein for the purpose of conducting the research proposed.		
5	The permit holder may export from Manitoba to Ontario, for further study, up to 20 live specimens of wildlife, or parts thereof, per year, that are taken under this permit.		
6	The permit holder shall follow recognized protocols and Canadian Council of Animal Care (CCAC) guidelines during the collection, capture, possession, euthanizing or release of any species named herein.		
7	This permit is not valid a) in an ecological reserve, provincial park, special conservation area or a wildlife refuge unless otherwise approved in writing by the Director, Parks and Natural Areas Branch, or the Director, Wildlife and Ecosystem Protection Branch, respectively; b) on private land without permission of the owner or lawful occupant; or c) in a National Park without written authorization from Parks Canada.		
8	The permit holder will submit annually (no later than March 31) to the Director of Wildlife and Ecosystem Protection, a written report describing the activities carried out under authority of this permit, including the number, sex and use of specimens marked or collected and the origin by marking or collecting site, and the results or accomplishments achieved.		
9	The Government of Manitoba shall not be held responsible or liable for any damage, injury or loss sustained to the person or property of the permit holder or for any damage, injury or loss sustained by any other person or the property of any other person as a result of the exercise of a right or privilege granted herein.		
10	This permit may be cancelled or the conditions amended at any time.		
11	The exercise, by the permit holder, of a right or privilege granted herein shall be construed as acceptance of and agreement to comply with the conditions set out herein.		
Date Issued: June 14, 2010		Expiry Date: March 31, 2014	
Signature of Permit Holder: <div style="border: 1px solid black; width: 150px; height: 40px; margin-top: 5px;"></div>		Issued By: <div style="border: 1px solid black; width: 150px; height: 40px; margin-top: 5px;"></div>  For Minister of Conservation	

FORM REVISED: MAY 2004

Excerpts from *The Wildlife Act*:

A permit must be carried while exercising a right or privilege granted thereunder and must be produced upon the request of an officer.
 A permit and the rights and privileges thereunder are not transferable to another person.
 No wild animal or part thereof may be exported from Manitoba without first obtaining an export permit.

APPENDIX B – Animal Use Ethics Approval

eSirius3G-- 2012-016 Continuing Review Approved

Subject: eSirius3G -- 2012-016 Continuing Review Approved
From:
Date: 01/09/2017 1:02 PM
To:



2012-016:5:

AUP Number: 2012-016
AUP Title: Regulation of mitochondrial metabolism in mammalian hibernation and ageing.
Yearly Renewal Date: 08/05/2016

The YEARLY RENEWAL to Animal Use Protocol (AUP) 2012-016 has been approved by the Animal Care Committee (ACC), and will be approved for one year following the above review date.

Please, at this time review your AUP with your research team to ensure full understanding by everyone listed within this AUP.

As per your declaration within this approved AUP, you are obligated to ensure that:

- 1) Animals used in this research project will be cared for in alignment with:
 - a) Western's Senate MAPPs 7.12, 7.10, and 7.15
http://www.uwo.ca/ansp/policies_instruments/research.html
 - b) University Council on Animal Care Policies and related Animal Care Committee procedures
http://www.uwo.ca/ansp/policies_instruments/animal_care_and_use_policies.html
- 2) As per UCA's Animal Use Protocols Policy,
 - a) this AUP accurately represents intended animal use;
 - b) external approvals associated with this AUP, including permits and scientific/departmental peer approvals, are complete and accurate;
 - c) any divergence from this AUP will not be undertaken until the related Protocol Modification is approved by the ACC; and
 - d) AUP form submissions - Animal Protocol Renewals and Full AUP Renewals - will be submitted and attended to within timeframes outlined by the ACC. http://www.uwo.ca/research/services/animalethics/animal_use_protocols.html
- 3) As per MAPP 7.10 all individuals listed within this AUP as having any hands-on animal contact will
 - a) be made familiar with and have direct access to this AUP;
 - b) complete all required CAC mandatory training (ansp@uwo.ca); and
 - c) be overseen by me to ensure appropriate care and use of animals.
- 4) As per MAPP 7.15,
 - a) Practice will align with approved AUP elements;
 - b) Unrestricted access to all animal areas will be given to ACVS Veterinarians and ACC Leaders;
 - c) UCA's policies and related ACC procedures will be followed, including but not limited to:
 - i) Research Animal Procurement
 - ii) Animal Care and Use Records
 - iii) Sick Animal Response
 - iv) Continuing Care Visits
- 5) As per institutional OH&S policies, all individuals listed within this AUP who will be using or potentially exposed to hazardous materials will have completed in advance the appropriate institutional OH&S training, facility-level training, and reviewed related (M)SDS Sheets, <http://www.uwo.ca/hr/learning/required/index.html>

Submitted by: Copeman, Laura
on behalf of the Animal Care Committee
University Council on Animal Care

The University of Western Ontario
Animal Care Committee / University Council on Animal Care

ansp@uwo.ca <http://www.uwo.ca/research/services/animalethics/index.html>

--- THIS IS AN EMAIL NOTIFICATION ONLY PLEASE DO NOT REPLY ---

APPENDIX C – Permission to reprint published materials

Reprint permission for Chapter 2 from *Journal of Comparative Physiology B*

SPRINGER NATURE LICENSE TERMS AND CONDITIONS

Dec 19, 2017

This Agreement between Western University -- Katherine Mathers ("You") and Springer Nature ("Springer Nature") consists of your license details and the terms and conditions provided by Springer Nature and Copyright Clearance Center.

License Number	4252520728359
License date	Dec 19, 2017
Licensed Content Publisher	Springer Nature
Licensed Content Publication	Journal of Comparative Physiology B: Biochemical, Systemic, and Environmental Physiology
Licensed Content Title	Regulation of mitochondrial metabolism during hibernation by reversible suppression of electron transport system enzymes
Licensed Content Author	Katherine E. Mathers, Sarah V. McFarlane, Lin Zhao et al
Licensed Content Date	Jan 1, 2016
Licensed Content Volume	187
Licensed Content Issue	1
Type of Use	Thesis/Dissertation
Requestor type	non-commercial (non-profit)
Format	electronic
Portion	full article/chapter
Will you be translating?	no
Circulation/distribution	<501
Author of this Springer Nature content	yes
Title	Ms.
Instructor name	Katherine E. Mathers
Institution name	Western University
Expected presentation date	Jan 2018
Portions	Full article - Regulation of mitochondrial metabolism during hibernation by reversible suppression of electron transport system enzymes
Requestor Location	Western University 1151 Richmond St. London, ON N6A 5B7 Canada Attn: Kate Mathers
Billing Type	Invoice
Billing Address	Western University 1151 Richmond St. London, ON N6A 5B7 Canada Attn: Kate Mathers
Total	0.00 USD
Terms and Conditions	

Springer Nature Terms and Conditions for RightsLink Permissions

Springer Customer Service Centre GmbH (the Licensor) hereby grants you a non-exclusive, world-wide licence to reproduce the material and for the purpose and requirements specified in the attached copy of your order form, and for no other use, subject to the conditions below:

1. The Licensor warrants that it has, to the best of its knowledge, the rights to license reuse of this material. However, you should ensure that the material you are requesting is original to the Licensor and does not carry the copyright of another entity (as credited in the published version).

If the credit line on any part of the material you have requested indicates that it was reprinted or adapted with permission from another source, then you should also seek permission from that source to reuse the material.

2. Where **print only** permission has been granted for a fee, separate permission must be obtained for any additional electronic re-use.

3. Permission granted **free of charge** for material in print is also usually granted for any electronic version of that work, provided that the material is incidental to your work as a whole and that the electronic version is essentially equivalent to, or substitutes for, the print version.
4. A licence for 'post on a website' is valid for 12 months from the licence date. This licence does not cover use of full text articles on websites.
5. Where '**reuse in a dissertation/thesis**' has been selected the following terms apply: Print rights for up to 100 copies, electronic rights for use only on a personal website or institutional repository as defined by the Sherpa guideline (www.sherpa.ac.uk/romeo/).
6. Permission granted for books and journals is granted for the lifetime of the first edition and does not apply to second and subsequent editions (except where the first edition permission was granted free of charge or for signatories to the STM Permissions Guidelines <http://www.stm-assoc.org/copyright-legal-affairs/permissions/permissions-guidelines/>), and does not apply for editions in other languages unless additional translation rights have been granted separately in the licence.
7. Rights for additional components such as custom editions and derivatives require additional permission and may be subject to an additional fee. Please apply to Journalpermissions@springernature.com/bookpermissions@springernature.com for these rights.
8. The Licensor's permission must be acknowledged next to the licensed material in print. In electronic form, this acknowledgement must be visible at the same time as the figures/tables/illustrations or abstract, and must be hyperlinked to the journal/book's homepage. Our required acknowledgement format is in the Appendix below.
9. Use of the material for incidental promotional use, minor editing privileges (this does not include cropping, adapting, omitting material or any other changes that affect the meaning, intention or moral rights of the author) and copies for the disabled are permitted under this licence.
10. Minor adaptations of single figures (changes of format, colour and style) do not require the Licensor's approval. However, the adaptation should be credited as shown in Appendix below.

Biology Open

Open Access (rights and permissions)

Biology Open (Bio) is a fully (author-pays) Open Access journal. All articles are published under the [CC-BY license](#) and deposited into PMC for immediate release. We are also a member of CHORUS and will ensure that your article complies with US public access mandates. If you pay for Open Access publication and we fail to fulfil these Open Access commitments, an APC rebate is available – please contact the [editorial office](#).

Please see the table below for further details on what our Open Access policy means for you as an author.

	Gold Open Access
Author Information	
Fees	Article Processing Charge (APC): \$1495 (plus VAT if applicable).
License	CC-BY license
Copyright owner	The author
Preprint servers	This journal allows posting of the non-peer-reviewed version of primary research papers on preprint servers. Versions that have been revised following peer review at this journal should not be posted.
Content freely available on journal website	Immediately upon publication
Use in other articles created by the author	Allowed by CC-BY license
FREE deposition in PMC	FREE author service. Immediately upon publication. Final published PDF.
Self archiving	
Posting on author's website	Immediately upon publication of the final version. Any version, including final published PDF. Must attribute source e.g. by citing doi and linking to the published article on the journal website.
Inclusion in thesis	Immediately upon publication. Any version, including final published PDF. Must attribute source e.g. by citing doi and linking to the published article on the journal website.
Institutional repository, thesis repository or PMC Europe	Immediately upon publication. Any version, including final published PDF. Must attribute source e.g. by citing doi and linking to the published article on the journal website.
Use by parties other than the authors	
Teaching purposes	Allowed by CC-BY license
Commercial use	Allowed by CC-BY license
Third party article collections	Allowed by CC-BY license
Responsible text and	Allowed by CC-BY license

We use cookies to help us improve this website. [Learn more](#)

<http://bio.biologists.org/content/rights-permissions>

The Company of Biologists Open Access journals: *Disease Models & Mechanisms* and *Biology Open*

Open Access Rights and Permissions

Permission to use Material from Other Publications in The Company's Open Access Journals

Open Access Rights and Permissions for our Open Access Journals

BiO and DMM articles are published under the Open Access model. They are made freely available online via the Company's website immediately following publication, deposited in PMC for immediate release, and can be distributed under the terms of the Creative Commons Attribution (CC-BY) licence (the terms of which are set out at <http://creativecommons.org/licenses/by/3.0/>). Authors retain ownership of the copyright for their article, but undertake to allow anyone to download, reuse, reprint, modify, distribute, and/or copy articles, including for commercial purposes, provided that:

- (1) the original authorship is properly and fully attributed and the journal is attributed as the original place of publication with correct citation details given;
- (2) if an original work is subsequently reproduced or disseminated not in its entirety but only in part or as a derivative work this is clearly indicated.

No permission is required from the authors or the publishers under the CC-BY licence.

Authors are also permitted to post the final, published PDF of their article on a website, institutional repository or other free public server, immediately upon publication, provided a link is included between the web page containing the Article and the journal's website.

Disclaimer: Responsibility for (1) the accuracy of statements of fact; (2) the authenticity of scientific findings or observations; (3) expressions of scientific or other opinion; (4) any other material published in the journal rests solely with the author(s) of the article in which such statements, etc., appear. No responsibility for such matters is assumed by the Journal, its owners, publishers, referees or staff.

CURRICULUM VITAE

Katherine Mathers

EDUCATION

Ph.D. Biology	2013 – present
Supervisor: Dr. James Staples	
University of Western Ontario, London, ON, Canada	
M.Sc. Biology	2011 – 2013
Supervisor: Dr. Christopher Moyes	
B.Sc. (Honours) Biology	2007 – 2011
Queen's University, Kingston, ON, Canada	

SCHOLARSHIPS AND AWARDS

Malcolm Ferguson Award in Life Sciences	2017
Queen Elizabeth II Graduate Scholarship in Science and Technology	2016
Queen Elizabeth II Graduate Scholarship in Science and Technology	2015
Journal of Experimental Biology Traveling Fellowship	2014

PUBLICATIONS

MacCannell, A.D.V., Jackson, E.C., **Mathers, K.E.** and Staples, J.F. An improved method for detecting torpor entrance and arousal in a mammalian hibernator using heart rate data. *Journal of Experimental Biology*, in revision.

Little, A.G., Lau, G., **Mathers, K.E.**, Leary, S.E. and Moyes, C.D. Comparative biochemistry of cytochrome c oxidase in animals. *Comparative Physiology and Biochemistry*, in press.

McFarlane, S.V., **Mathers, K.E.** and Staples, J.F. (2017) Reversible temperature-dependent differences of brown adipose tissue mitochondrial respiration during torpor in a mammalian hibernator. *American Journal of Physiology – Regulatory, Integrative, and Comparative Physiology* 312:R432-R442.

Mathers, K.E., McFarlane, S.V., Zhao, L. and Staples, J.F. (2017) Regulation of mitochondrial metabolism during hibernation by reversible suppression of electron transport system enzymes. *Journal of Comparative Physiology B* 187:227-234.

Mathers, K.E. and Staples, J.F. (2014) Saponin-permeabilization is not a viable alternative to isolated mitochondria for assessing oxidative metabolism in hibernation. *Biology Open* 4:858-864.

Mathers K.E., Cox, J., Wang, Y. and Moyes, C.D. (2014) Exploring the consequences of mitochondrial differences arising through hybridization in sunfish. *Comparative Physiology and Biochemistry Part A: Molecular & Integrative Physiology* 178:1-6.

Davies, R.D.* , **Mathers, K.E.***, Hume, A.D., Bremer, K., Wang, Y. and Moyes, C.D. (2012) Hybridization in sunfish influences the muscle metabolic phenotype. *Physiological and Biochemical Zoology* 85(4):321-331.

* Denotes shared first authorship